

Lehrstuhl für  
Betriebswissenschaften und Montagetechnik  
der Technischen Universität München

**WORKSPACE SCALING AND HAPTIC FEEDBACK FOR INDUSTRIAL  
TELEPRESENCE AND TELEACTION SYSTEMS WITH HEAVY-DUTY  
TELEOPERATORS**

**Marwan Radi**

Vollständiger Abdruck der von der Fakultät für Maschinenwesen der  
Technischen Universität München zur Erlangung des akademischen Grades  
eines

Doktor-Ingenieurs (Dr.-Ing.)

genehmigten Dissertation.

Vorsitzender: Univ.-Prof. Dr.-Ing. Michael Zäh

Prüfer der Dissertation:

1. Univ.-Prof. Dr.-Ing. Gunther Reinhart
2. Univ.-Prof. Dr.phil.rer.soc.habil. Berthold Färber  
Universität der Bundeswehr München

Die Dissertation wurde am 02.11.2011 bei der Technischen Universität München  
eingereicht und durch die Fakultät für Maschinenwesen am 09.03.2012  
angenommen.



## Abstract / Zusammenfassung

The focus of this work was on the deployment of telepresence and teleaction technology for handling heavy parts in the industrial realm. To improve the industrial usability of telepresence systems, off-the-shelf components have been utilized, in particular due to their low construction and maintenance costs. Two of the challenges resulting out of utilizing such components were studied and analyzed in this work and several solutions were developed. The first challenge appears when the haptic device and the industrial robot are kinematically different. Several kinematic mapping and workspace scaling techniques have been developed and successfully implemented. The second challenge is the provision of haptic feedback in telepresence systems with heavy-duty teleoperators. A model-based force feedback has been developed to ensure stability of the system with high levels of transparency. In order to evaluate the developed techniques, two main psychophysical experiments have been designed and conducted. Furthermore, the work was accomplished by examining the operational and economic feasibility of the developed system.

Ziel dieser Arbeit ist der Einsatz von Telepräsenz- und Teleaktionstechnologien zur Handhabung schwerer Lasten vor allem im industriellen Bereich. Zur Verbesserung der industriellen Nutzbarkeit von Telepräsenzsystemen wurden Standardkomponenten, insbesondere aufgrund ihrer geringen Kosten, dem geringen Wartungsaufwand und der hohen Robustheit, verwendet. Zwei der daraus resultierenden Herausforderungen wurden untersucht und verschiedene Lösungen entwickelt. Die erste Herausforderung betrachtet die kinematische Unähnlichkeit zwischen dem haptischen Gerät und dem Industrieroboter. Verschiedene kinematische Mapping- und Skalierungsmethoden wurden entwickelt und erfolgreich umgesetzt. Die zweite betrachtete Herausforderung ist die Bereitstellung von haptischem Feedback in Telepräsenzsystemen mit Schwerlastteleoperatoren. Eine modellbasierte Krafterückkopplung wurde hierfür entwickelt, um die Stabilität des Systems mit einer hohen Transparenz zu gewährleisten. Zur Bewertung der technischen sowie wirtschaftlichen Realisierbarkeit der entwickelten Methoden wurden psychophysische Experimente konzipiert und durchgeführt.



## Acknowledgement

Foremost, I owe my deepest sincere gratitude, with all my due respects, to my supervisor Prof. Dr.-Ing. Gunther Reinhart. Without his expertise and guidance, this thesis would not have been written. I also would like to thank Prof. Dr.-Ing. Michael Zäh for his insightful comments and keen interest in the topic. I am also grateful to Prof. Dr. Berthold Färber for his willingness to be part of the examination committee and for the time and effort he invested.

I owe a lot to my colleagues at the Institute for Machine Tools and Industrial Management (*ivb*): Andrea Acker, Wolfgang Rösel, William Tekouo, Thomas Kirchmeier, Sherif Zaidan, and others, for their continuous support through the past years. I also thank my best friends: Abood Khalifeh, Ahmad Habbaba, Abdussalam Qaroush, Taiseer Aljazzar, Husain Aljazzar and Abdel Hakim Hassabou.

I would also like to express my great thanks to my parents, for supporting me spiritually throughout my life. I will never truly be able to express my sincere appreciation to both of you. Also I cordially thank my sisters for their moral support, prayers and patience during my long leave of absence to study in foreign countries. I also would like to thank my parents-in-law for their words of encouragement.

Last, but certainly not least, the biggest THANK YOU of all goes to my family, my wife Suzan and children Alhassan and Halla for their continuous help, unfailing love and patience.



*To my loving parents, Hassan and Nabila*



# Contents

<b>Abstract/Zusammenfassung</b>	<b>I</b>
<b>Acknowledgement</b>	<b>III</b>
<b>List of Abbreviations</b>	<b>XI</b>
<b>List of Symbols</b>	<b>XIII</b>
<b>List of Figures</b>	<b>XV</b>
<b>List of Tables</b>	<b>XIX</b>
<b>1 Introduction</b>	<b>1</b>
1.1 Industrial Robots as Handling Machines . . . . .	1
1.2 Human-Robot Interaction . . . . .	3
1.3 Recent Research in Human-Robot Interaction . . . . .	6
1.4 Thesis Structure . . . . .	11
<b>2 Telepresence and Teleaction Technology</b>	<b>15</b>
2.1 Definitions and Terminology . . . . .	15
2.2 Applications of TPTA-Systems . . . . .	19
2.2.1 Handling of Materials in Hazardous Environments . . . . .	19
2.2.2 Medicine . . . . .	20
2.2.3 Space Explorations and Maintenance . . . . .	21
2.2.4 Underwater Explorations and Maintenance . . . . .	21
2.2.5 Training, Education and Entertainment . . . . .	22
2.3 Lack of Industrial Applications . . . . .	22
2.4 On the Rationale for Industrial TPTA-Systems . . . . .	23
2.5 Problem Definition and Related Work . . . . .	24
2.5.1 Kinematic Mapping and Workspace Scaling . . . . .	25
2.5.2 Haptic Feedback and System Instability . . . . .	29
2.5.2.1 Time Delay . . . . .	30
2.5.2.2 Dynamic Masking . . . . .	32
2.6 Evaluation of Current Situation of Research . . . . .	33
2.7 Research Objectives . . . . .	34

<b>3 Mapping and Scaling Techniques</b>	<b>35</b>
3.1 Kinematic Mapping	35
3.1.1 Transformation	36
3.2 Scaling Techniques	38
3.2.1 Position Control	38
3.2.2 Rate Control	41
3.2.3 Human Intention-based Control (HIbC)	43
3.2.3.1 Single Zone	43
3.2.3.2 Double Zones	45
3.3 Conclusion	47
<b>4 Haptic Feedback</b>	<b>49</b>
4.1 The Nature of Haptic Feedback	49
4.2 Direct Force Feedback	50
4.3 Model-based Force Feedback	56
4.3.1 Vibration-based Force Feedback (VbFF)	57
4.3.2 Impedance-based Force Feedback (IbFF)	58
4.4 Haptic Assistance Functions	60
4.4.1 Haptic Virtual Walls	61
4.4.2 Haptic Grids	62
4.5 Conclusion	63
<b>5 Experimental Setup</b>	<b>65</b>
5.1 Introduction	65
5.2 System Architecture	66
5.2.1 Operator Side	67
5.2.2 Teleoperator Side	67
5.2.3 Central Controller	68
5.2.4 Hardware Components	68
5.2.4.1 Haptic Input Devices	68
5.2.4.2 Industrial Robot	70
5.2.4.3 Real-Time Platform (RT-Platform)	71
5.2.5 Communication Channels	72
5.2.5.1 Development-Time Communication Link	72
5.2.5.2 Run-Time Communication Links	73
5.3 Conclusion	74
<b>6 Experimental Evaluation</b>	<b>77</b>
6.1 Introduction	77
6.2 User Studies	77
6.2.1 Participants	78
6.2.2 Experiment A: Trajectory Tracking with Different Control Methods	78
6.2.2.1 Task Definition and Requirements	78

---

6.2.2.2	Experimental Design . . . . .	78
6.2.2.3	Hypothesis . . . . .	79
6.2.2.4	Procedure . . . . .	80
6.2.2.5	Data Analysis and Results . . . . .	80
6.2.2.6	Summary of Experiment A . . . . .	92
6.2.3	Experiment B: Surface Finishing Task with Model-based Force Feedback . . . . .	93
6.2.3.1	Task Definition and Requirements . . . . .	93
6.2.3.2	Industrial Relevance . . . . .	94
6.2.3.3	Experimental Design . . . . .	95
6.2.3.4	Hypothesis . . . . .	96
6.2.3.5	Procedure . . . . .	96
6.2.3.6	Data Analysis and Results . . . . .	97
6.2.3.7	Summary of Experiment B . . . . .	101
6.3	Conclusion . . . . .	101
<b>7</b>	<b>Operational and Economic Feasibility</b>	<b>103</b>
7.1	Operational Feasibility . . . . .	103
7.2	Economic Feasibility . . . . .	106
7.2.1	Cost-Benefit Analysis . . . . .	106
7.3	Conclusion . . . . .	108
<b>8</b>	<b>General Conclusion and Future Work</b>	<b>109</b>
	<b>Bibliography</b>	<b>113</b>



## List of Abbreviations

2D	2-dimensional
3D	3-dimensional
A/D	Analog-to-digital
ANOVA	Analyses of variance
AR	Augmented reality
CAD	Computer aided design
COTS	Commercial off-the-shelf
CS	Command station
DOF	Degree(s) of freedom
e.g.	For example
etc.	And so forth (Latin: et cetera)
FRB	forbidden region borders
FTS	Force-torque sensor(s)
HibC	Human intention-based control
HMI	Human machine interface
HRI	Human-Robot Interaction
HSI	Human-System interface(s)
HVW	Haptic virtual wall(s)
HPF	Haptic path follower
I/O	Input/Output
IbFF	Impedance-based force feedback
ISO	International Organization for Standardization
i.e.	That is (Latin: id est)
K	Interest
L	Lifetime
M	Maintenance
PC	Personal computer
PCI	Position control with indexing
PK	Payback period
RC	Rate control
ROV	Remotely operated vehicle
RT	Real-time
RTOS	Real-time operating system
SME	Small and medium enterprise(s)
T	Training
TCP	Tool center point

## Contents

---

TCP/IP	Transmission control protocol
TCT	Task completion time
TN	Target node
TPTA	Telepresence and teleaction
U	Annual usage
UDP/IP	User datagram protocol
VbFF	Vibration-based force feedback

## List of Symbols

$T$	Transformation matrix ( $4 \times 4$ )
$R$	Rotation matrix ( $3 \times 3$ )
$\mathbf{p}, \mathbf{q}$	Position vector
$\mathbf{p}_r$	Position vector of the teleoperator end-effector
$\mathbf{v}_r$	Velocity vector of the teleoperator end-effector
$\mathbf{p}_h$	Position vector of the haptic device handle
$\alpha$	Position scaling factors
$\beta$	Force reflection scaling factor
$\gamma$	Velocity scaling factors
$v_{th}$	Threshold value
$W_h$	Workspace of the haptic device
$W_r$	Workspace of the teleoperator
$x_m$	Master (haptic device) position
$x_s$	Slave (teleoperator) position
$f_m$	Reflection force at the master side
$f_e$	Measured environmental force at the teleoperator side
$\hat{f}_e$	Calculated environmental force (model-based)
$m_m$	Effective inertia of the haptic device
$m_s$	Effective inertia of the teleoperator
$b_m$	Damping of the haptic device
$b_s$	Damping of the teleoperator
$k_m$	Stiffness of the haptic device
$k_s$	Stiffness of the teleoperator
$k_e$	Stiffness of the environment
$k_f$	Stiffness of virtual spring
$b_e$	Damping of the environment
$f$	Frequency
$t$	Time
$\delta v_m$	Change in velocity of haptic device
$\delta v_s$	Change in velocity of teleoperator
$Num$	Numerator
$Den$	Denominator
$F_{vib}$	Vibrational force
$N$	Sample size
$p$	Significance of a test
$M$	Mean value

## Contents

---

<i>SD</i>	Standard deviation
<i>F</i>	F-ratio (test statistic used in ANOVA)
<i>t(.)</i>	t-test
<i>r</i>	Effect size
$\Delta I$	Investment costs
<i>L</i>	System lifetime
<i>R</i>	Interest rate
<i>SV</i>	Average time saved (%)
<i>LC</i>	Labor cost
<i>T</i>	Training costs
<i>M</i>	Maintenance costs
<i>K</i>	Interest
<i>D</i>	Depreciation
<i>U</i>	Annual usage
<i>TS</i>	Time saved
$\Delta B$	Total annual benefits
<i>PK</i>	Payback period

## List of Figures

1.1	Operational number of total-world industrial robots at the year-end of 2007 and 2008 sorted by applications (IFR 2009)	2
1.2	Spatial Classification of Human-Robot Interaction (HRI)	4
1.3	Artist’s Concept of Mars Rover [Source: NASA/JPL]	5
1.4	HRI classification based on task and temporal division	6
1.5	Cobot scooter (left) and assembly of car doors using cobots (right) (PESHKIN & COLGATE 1999)	7
1.6	Robotic assist system (ROB@WORK 2010)	8
1.7	PowerMate assembly work-cell (SCHRAFT ET AL. 2005)	8
1.8	Intelligent Power Assist Device (IPAD) (KRÜGER ET AL. 2006)	9
1.9	Human-robot interaction in SME manufacturing facilities (SMEROBOT 2010)	10
1.10	Interactive user interface for programming of industrial robots (VOGL 2008)	11
1.11	Universal workpiece based approach for programming of cooperating industrial robots (REINHART & ZAIDAN 2009)	12
1.12	Diagram of thesis structure	13
2.1	General TPTA-system structure	16
2.2	The first teleoperation system for handling nuclear materials	19
2.3	da Vinci®: the telepresence system for performing minimally invasive surgery (INTUITIVE SURGICAL 2011)	20
2.4	Telepresence system for applications in space: Operator side (left) and SpaceJustin as a teleoperator (right) (DLR 2011)	21
2.5	ROVs: Remote operated vehicles (left) (photo: Schilling Robotics) and the operator control room (right) (photo: BP p.l.c.)	22
2.6	Examples of haptic devices available in market: PHANTOM Desktop from Sensable (left), Impulse Engine 2000 from Immersion Corp. (middle) and Falcon from Novint Technologies Inc.(right)	25
2.7	Scaling Issue	27

## List of Figures

---

3.1	Projecting the two degrees of freedom of the haptic device onto the motion plane within the teleoperator workspace	36
3.2	Motion command vector $\mathbf{q}$ lying on a motion plane parallel to $xy$ -plane of $\mathbf{C}_w$ frame	37
3.3	Motion command vector $\mathbf{q}$ lying on a motion plane parallel to $yz$ -plane of $\mathbf{C}_w$ frame	37
3.4	State-transition diagram of the PCI	40
3.5	Discontinuity of robot trajectory because of switching between two scaling factors (left) and continuous robot trajectory in the case of LSF (right)	40
3.6	State-transition diagram of the position control with LSF	41
3.7	State-transition diagram of the RC with elastic force feedback	42
3.8	Block diagram of the single zone intention-based control	43
3.9	Illustration of the mode selection based on velocity values	44
3.10	Double zones with intention-based scaling factor: $R$ is the radius of the inner zone, $D$ is the distance between haptic device handle and the center, and $\vec{r}$ is the unit vector pointing outside the inner zone	45
3.11	State-transition diagram of the double zones control method	46
4.1	Abstracted model of TPTA-system	50
4.2	Direct force feedback	51
4.3	Mass-damper-spring model of the TPTA-system: $m_m$ , $b_m$ and $k_m$ are the lumped mass, damping and stiffness of the haptic device and the human hand, respectively, $m_s$ , $b_s$ and $k_s$ are the mass, damping and stiffness of the teleoperator, respectively, and $k_e$ is the environment stiffness.	52
4.4	Root Locus of the TPTA-system with different scaling factors	53
4.5	Unstable teleoperator motion with product of scaling factors $\alpha\beta = 0.04$	54
4.6	Relation between environmental stiffness $k_e$ and scaling factors $\alpha\beta$	55
4.7	Model-based force feedback	57
4.8	Vibration-based force feedback	58
4.9	Impedance-based force feedback	59
4.10	Schematic representation of a viscoelastic environment (left) and a pure elastic environment (right)	60
4.11	Haptic virtual walls: the haptic path follower (left) and forbidden region borders (right)	61
4.12	Haptic grid	62

5.1	The developed TPTA-system architecture . . . . .	67
5.2	Haptic input devices utilized in this work . . . . .	69
5.3	The industrial robot KR100-HA is used as a teleoperator in our TPTA-system . . . . .	70
5.4	The hardware and software configuration of the RT-platform . . . . .	72
5.5	Communication channels . . . . .	73
5.6	Overall TPTA-system with its hardware components and communication links . . . . .	75
6.1	Schmidt trajectory used in the first experiment . . . . .	79
6.2	The system configuration for experiment A . . . . .	80
6.3	Mean values of TCT, overall and maximum deviations for the curve . . . . .	82
6.4	Mean values of TCT, overall and maximum position deviations for the circle . . . . .	83
6.5	TCT mean values of different control strategies for tracking the line segment . . . . .	84
6.6	Mean values of the overall and maximum position deviations of the line segment . . . . .	85
6.7	Mean values of TCT for the slope segment . . . . .	86
6.8	Mean values of overall and maximum position deviations of the slope segment . . . . .	87
6.9	Mean values of TCT and overall deviation of the large corner . . . . .	88
6.10	Mean values of TCT and overall position deviation of the small corners . . . . .	89
6.11	Mean values of the TCT and position deviation of the entire trajectory . . . . .	90
6.12	Means of usability ratings for each control method by joystick experience . . . . .	91
6.13	The teleoperator configuration for experiment B . . . . .	93
6.14	The four phases of the surface finishing task (experiment B)	94
6.15	Forces acting on the tool during grinding process . . . . .	95
6.16	Mean task completion time for each trial irrespective of force feedback type . . . . .	98
6.17	Mean task completion time for each trial by force feedback type . . . . .	98
6.18	Mean values of the average forces applied onto the object's surface for each trial by feedback type . . . . .	99
6.19	Mean values of the maximum forces applied onto the object's surface for each trial by force feedback type . . . . .	100

## List of Figures

---

7.1	Qualitative comparison between the developed TPTA-system and a conventional teleoperation system . . . . .	105
-----	--	-----

## List of Tables

2.1	Overview of mapping techniques . . . . .	26
2.2	Overview of scaling techniques . . . . .	28
2.3	Stability problems and solutions in the case of haptic feedback	33
3.1	Advantages and disadvantages of the implemented workspace scaling techniques . . . . .	48
4.1	TPTA-system parameters . . . . .	53
4.2	Experimentally determined stability of our TPTA-system . . .	54
5.1	Technical specifications of the deployed haptic input devices .	70
6.1	Pairwise comparisons of TCT for the curve segment . . . . .	81
6.2	Pairwise comparisons of overall position deviations for the curve . . . . .	82
6.3	Pairwise comparisons of maximum position deviations ( <i>mm</i> ) for the curve . . . . .	83
6.4	Pairwise comparisons of TCT for the circle segment . . . . .	84
6.5	T-statistics pairwise comparisons of TCT for the line segment	84
6.6	Pairwise comparisons of overall position deviations for the line segment . . . . .	85
6.7	Pairwise comparisons of maximum deviations for the line segment . . . . .	86
6.8	Pairwise comparisons of TCT for the slope segment . . . . .	86
6.9	Pairwise comparisons of overall position deviations for the slope segment . . . . .	87
6.10	Pairwise comparisons of maximum deviations for the slope segment . . . . .	87
6.11	Pairwise comparisons of TCT for the large corner . . . . .	88
6.12	Pairwise comparisons of TCT for the small corners segment .	89
6.13	Pairwise comparisons of overall deviations for the small corners segment . . . . .	89
6.14	T-statistics pairwise comparisons of overall TCT for the entire trajectory . . . . .	90
6.15	Pairwise comparisons of mean usability scores . . . . .	91

**List of Tables**

---

7.1 Cost-Benefit Analysis . . . . . 107

# 1 Introduction

*“For, usually and fitly, the presence of an introduction is held to imply that there is something of consequence and importance to be introduced.”*

---

*Arthur Machen*

## 1.1 Industrial Robots as Handling Machines

Robotics is regarded as one of the most important technologies in industrial societies. This is attributed to the precision, speed, endurance and reliability of industrial robots. Nevertheless, the world robot market has already been affected by the economical downturn of 2008, which led to stagnated worldwide sales of industrial robots at about 113,300 units. Regardless of this fact, the non-automotive sectors in Germany<sup>1</sup>, especially the metal and food industry, substantially increased their robot purchases (IFR 2009). In Germany alone, about 15,200 industrial robots were sold in 2008 (4% more than in 2007). In addition, the growth rate of industrial robot investments in the European Union is nowadays higher than in Japan<sup>2</sup>, which meanwhile sees a continuing decline in industrial robots purchase. It is also estimated that the worldwide number of operational industrial robots will increase from about 1,036,000 units at the end of 2008 to 1,057,000 at the end of 2011, corresponding to an average annual growth rate of about 2% (IFR 2009).

Material handling and machine tending had the highest share of operational number of industrial robots in the world at the end of 2008. This accounted for about 38%, while welding tasks account for 30% (see Figure 1.1). Reasons for utilization of robots in material handling processes are that they beat humans especially in the areas of precision, speed of execution and their capacity for huge achievable load-bearing. Industrial robots carry out their tasks by always repeating the same program sequence which is written by a programming specialist. Programming of industrial robots takes usually a long time because

---

<sup>1</sup>Germany is considered the largest market for industrial robots in Europe

<sup>2</sup>Japan is traditionally the largest market for industrial robots worldwide

# 1 Introduction

---

many iterations are needed. Thus, the reconfiguration of these machines is usually time-consuming and expensive. In addition, the initial costs are very high. Consequently, the use of industrial robots is economically efficient only for mass production or for processes requiring precision not attainable by humans.

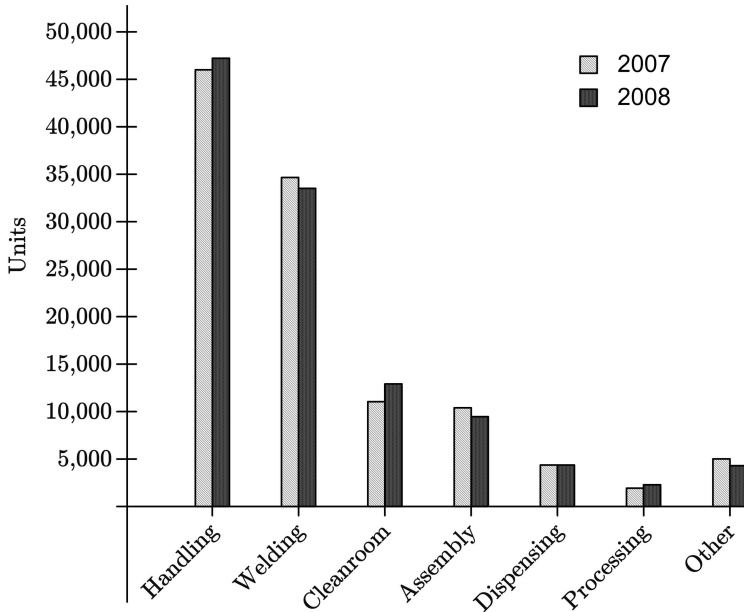


Figure 1.1: Operational number of total-world industrial robots at the year-end of 2007 and 2008 sorted by applications (IFR 2009)

In spite of significant advances in the field of industrial automation using robots, human intelligence is far superior in terms of reasoning, decision making and creative thinking, among others. Several tasks require both the acute reasoning and perceptive abilities of humans. In addition, the production trend of recent years is to produce individualized and short life-time products in small and/or medium batches. This calls for new production technologies that can cope with these challenges.

In manual assembly, human workers use their superior sensory capability and intelligence to accomplish complex tasks. This makes the manual workstation more suitable for production with the aforementioned challenges, because in this case the production work-cell is more flexible and changeable than the automated one. Therefore, manual assembly continues to be an important feature

of many industrial processes. However, the production rate of manual workstations is very slow and the running costs including labor costs are high. In addition, for specific tasks, such as the assembly of heavy parts, some pieces of raw materials or equipments are too heavy to be safely handled by workers. Therefore, assistant devices such as industrial robots is mandatory as human ability is hindered by physical limitations. Furthermore, the aging and demographic change in European societies projects a decline of the population at working age. Forecasts show that until 2050 the median age in European Union member states will rise to 48 years (MÜNZ 2007). This calls for systems where the worker could easily and ergonomically manipulate parts to be assembled without exerting huge physical efforts. This in turn can reduce or eliminate the risk of manual handling injuries and give older workers the chance to actively perform and stay on their jobs for a longer time. The main reasons for using robot assistance in such cases are (a) to increase productivity and efficiency by dividing the tasks into human-oriented and robot-oriented sub-tasks, and (b) to comply with ergonomic guidelines. One commonly used guideline to determine safe lifting limits is the standard ISO 11228 part 1 (2003), part 2 (2007a) and part 3 (2007b). In this standard a reference mass for two handed lifting under ideal conditions has been set to 25 kg for 95% of males and 15 kg for 99% of females.

Combining skills of humans such as adaptability and decision making ability with industrial robot manipulation capability enables new concepts for flexible systems and opens up new application scopes. In this manner, robots will assist humans in manufacturing through close interaction with them, instead of replacing them. The robot and the human worker are, therefore, partners in joint manufacturing tasks. One way to realize such a combination is Human-Robot Interaction (HRI).

## 1.2 Human-Robot Interaction

HRI is a research field aiming at understanding, designing and evaluating robots interacting with humans (GOODRICH & SCHULTZ 2007). In order to get the interaction in HRI systems the human operator should interact with the robot. Several classifications of HRI based on temporal and spatial division of humans and robots can be found in the literature. Based on the spatial region of human and robot, HRI can be classified (as shown in Fig. 1.2) into two main categories (GOODRICH & SCHULTZ 2007) (YANCO & DRURY 2004) (HELMS 2006):

1. Proximate interaction (common workspace), where humans and robots are co-located; either they have a common workspace or overlapping workspaces.
2. Remote interaction (discrete workspaces), where humans and robots are not co-located and are separated in two discrete workspaces.

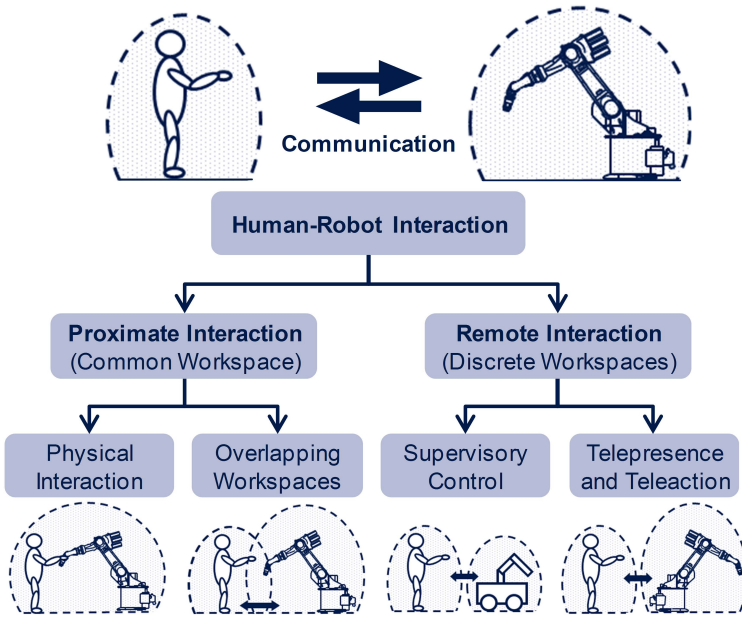


Figure 1.2: Spatial Classification of Human-Robot Interaction (HRI)

Within these general categories, there are several subcategories based on system configurations and applications. Under proximate interaction there would be an HRI system with direct physical contact. Here the human operator and the robot have a common or shared workspace and they physically contact each other. Human safety is a fundamental requirement for such systems, since the direct contact can lead to accidents or even human injuries. An example of this configuration is the direct guidance of a robot, provided that the robot has an input device mounted directly on it. The input device can be a joystick, a 3D space mouse or a force-torque sensor (FTS). The latter measures the forces that the human operator applies for moving the robot. These forces are then translated to motion commands sent to the robot controller through a force control strategy, e.g. zero gravity or compliance control. Providing this setup, the human and the robot are able to jointly perform a handling or assembly task at the same time, i.e. time-sharing. It is here to mention that the coexistence of human and robot is in the meantime allowed by the current standard ISO 10218, which specifies the safety requirements (ISO 10218-1 2006) and system integration (ISO 10218-2 2011) of such a configuration.

The second subcategory within the proximate interaction is characterized by overlapping workspaces, in which the human and the robot have their own

workspaces and these workspaces overlap to provide a common/shared region. This allows both to work together within this region to accomplish a common task, and at the same time they can separately perform other sub-tasks within the unshared spaces. The human and robot do not necessarily make physical contacts in this case, but human safety is still crucial to allow collision-free interaction.

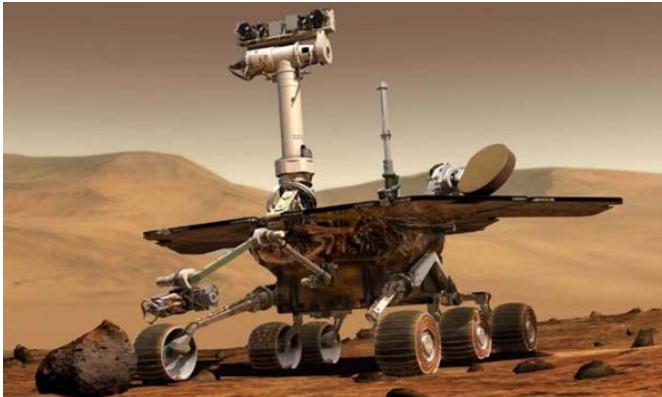


Figure 1.3: Artist's Concept of Mars Rover [Source: NASA/JPL]

Remote interaction with a mobile robot, e.g. the Mars rover (Figure 1.3), is often referred to as supervisory control. With this control strategy, the human operator sends high level programs to an autonomous system and supervises task execution. For this purpose, the operator divides a problem into a sequence of tasks and the robot performs them on its own. Once the full control is given to the robot, the operator typically assumes a monitoring role and will not be part of the control loop. However, the operator may also occasionally interfere and control the robot by closing a command loop or he/she may change some control variables manually while leaving the others to the robot. When the human operator remotely interacts with a mobile robot or a robotic arm to perform physical manipulation tasks, it is usually referred to as physical telemanipulation or *telepresence and teleaction (TPTA)*. In this case, the human operator is part of a bilateral control loop. The motion commands are sent from the operator side to the robot side, and several sensory information, such as haptic, vision and auditory, are sent from the robot side back to the operator side. This multimodal interaction leads to a more immersive experience of the operator.

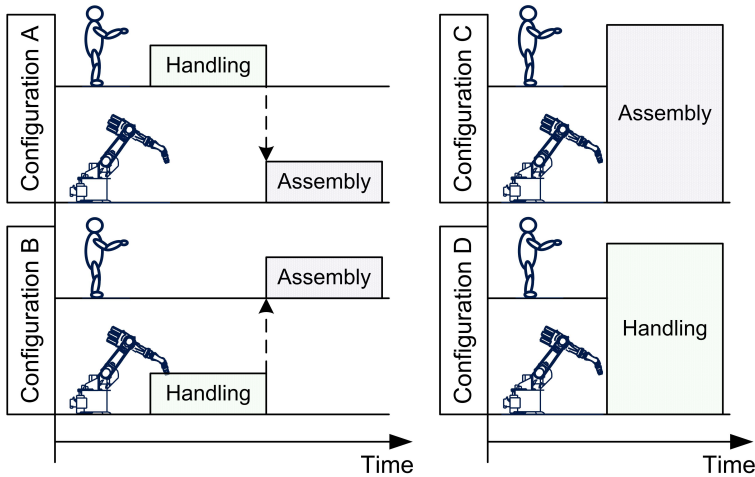


Figure 1.4: HRI classification based on task and temporal division

Another classification of HRI is based on task and temporal division (KRÜGER ET AL. 2009), i.e. whether the human and the robot perform a common task or different tasks at the same time or sequentially (see Figure 1.4). Here four configurations can be distinguished. In the first configuration (A) the robot performs the assembly task and the human operator performs the handling one. In the second configuration (B) the robot performs the handling task and the operator performs the assembly task. These two configurations belong to the overlapping workspaces category (cf. Figure 1.2). In the third configuration (C) the operator and the robot perform a common assembly task at the same time. An example is the assembly of heavy parts. Here the robot assists the human operator by carrying the heavy part while the operator tries to assemble them. In the fourth configuration (D) the human operator and the robot perform a handling task at the same time, e.g. transporting heavy loads. The last two configurations belong to either proximate interaction with physical contact or remote interaction with TPTA (cf. Figure 1.2).

## 1.3 Recent Research in Human-Robot Interaction

In this section, some advances in HRI research which have a focus on industrial applications are briefly reviewed. In production engineering, HRI can be considered as assistant robotic systems, which are industrial robots that assist people in value-added process chains (REINHART & SPILLNER 2010). An exam-

### 1.3 Recent Research in Human-Robot Interaction

---

ple of the field-tested assistant robots is Cobot (Collaborative Robot) invented by COLGATE ET AL. (1996). It is a mechanical device guided directly by a human operator, who is responsible only for motion commands, and the motion power is provided by the use of servomotors. Cobot also offers assistance functions such as virtual surfaces, virtual stops or preprogrammed trajectory in order to simplify handling operations. An important feature of Cobot compared with a simple balancer is the ability to provide power support to the worker in a way that the apparent inertia of heavy workpieces can be reduced by a factor of ten or more. This leads to a significant reduction of the physical efforts that the worker must apply during handling tasks. An alternative approach to provide power support to the human worker during handling of heavy parts is the use of robotic exoskeletons (SNYDER & KAZEROONI 1996) (KAZEROONI & GUO 1993). Compared with Cobots the exoskeleton systems provide a higher degree of mobility but on the other hand the adaptation to workers is time-consuming.

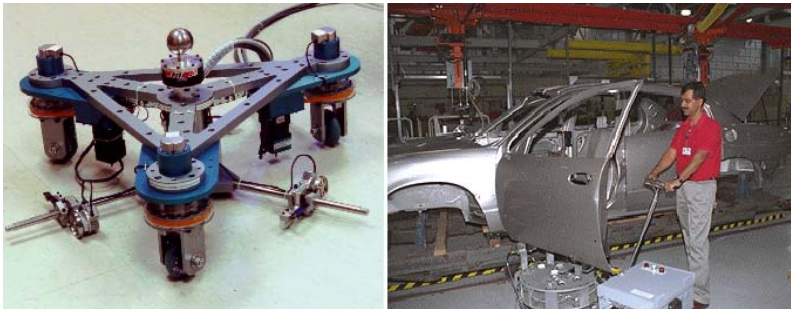


Figure 1.5: Cobot scooter (left) and assembly of car doors using cobots (right) (PESHKIN & COLGATE 1999)

Several robotic assistance systems developed for research purposes provide a multimodal sensor-based interaction with workers. For example, the assist robot *rob@work* developed by HELMS ET AL. (2002) consists of a mobile platform with differential gear drives, seven degrees-of-freedom (DOF) robot, control unit and power supply with nine-hour capacity (Figure 1.6). In this system, the worker is responsible for giving commands and supervising the execution of tasks, while the robot carries out repetitive and fatiguing operations such as lifting and carrying loads as well as tool handling. Intended applications of this system are the manufacturing of small lot sizes as well as in maintenance tasks. One should mention here that the mobility of this system makes it more flexible

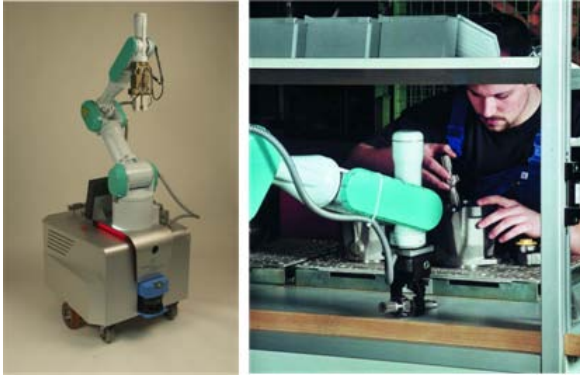


Figure 1.6: Robotic assist system (ROB@WORK 2010)

not only to perform logistic activities, but also to be moved to a location where assistance is needed.

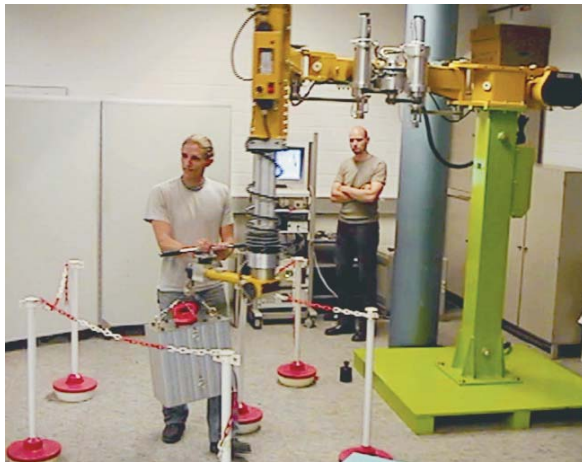
Another example is the system *team@work* (THIEMERMANN 2003), by which the robot and the human operator share the same workspace. For safe cooperation between the robot and the human, an image processing system is installed as monitoring sensor to observe the scene from above. The velocity of the robot is controlled upon the shortest distance between the human and the robot.



Figure 1.7: PowerMate assembly work-cell (SCHRAFT ET AL. 2005)

SCHRAFT ET AL. (2005) introduced the PowerMate as a robot assistant, which

works together with humans<sup>3</sup>. The interaction between robot and human is realized by a FTS which allows the direct manipulation of the robot by the worker. An example of the applications of PowerMate is the assembly of heavy parts of an automotive rear axle (see Figure 1.7). The main drawbacks of PowerMate are the need for a large floor space and the limited velocity in the area that the human operator has access to. KRÜGER ET AL. (2006) introduced an intelligent power assist device (IPAD) which also allows direct cooperation between robot and human worker (cf. Figure 1.8) and integrates force-feedback and programming functions, as well as compliant motion guidance and semi-autonomous functions. However, the IPAD system is restricted to only two geometrical DOF.



*Figure 1.8: Intelligent Power Assist Device (IPAD) (KRÜGER ET AL. 2006)*

Interactive robotic assistant systems are also investigated and developed within the research project MORPHA (LAY ET AL. 2001). One of these systems, among others, is developed at DaimlerChrysler Research and Technology's Cognition and Robotics Group. It provides an interactive robot programming by workers through pointing to objects with a laser pointer (STOPP ET AL. 2003). Another example within this project is CoRA (Cooperative Robot Assistant) introduced by IOSSIFIDIS ET AL. (2002). It has been designed to be anthropomorphic and it interacts with the human worker through several modalities, e.g. by visual/gesture recognition, speech recognition and haptic through the so called artificial skin.

---

<sup>3</sup>PowerMate conforms to safety category 3 according to DIN ISO 954

## 1 Introduction

---

Within the SMEROBOT<sup>4</sup> initiative (2010), several examples for using robots to assist workers in small and medium enterprises (SME) were developed (see Figure 1.9). The focus of this project was on the needs and culture of such manufacturing facilities with regards to planning, operation and maintenance. For safety assessment of human-robot-cooperation systems, OBERER-TREITZ ET AL. (2011) introduced a new methodology based on an injury model. This model is a numerical simulation of human-robot-collision which is integrated into the system controller to analyze injury criteria. This allows the system to dynamically respond to danger potentials.



*Figure 1.9: Human-robot interaction in SME manufacturing facilities (SMEROBOT 2010)*

Another assistant robot has been developed within the research project LiSA (**L**ife **S**cience **A**ssistant) to assist humans in biological and pharmaceutical laboratories by conducting repetitive tasks such as filling and transporting micro-plates (SCHULENBURG ET AL. 2007). The interaction between lab technicians and LiSA is multimodal through speech and touchscreen inputs.

The interaction between human and robot is not only necessary during the execution of tasks, but also during the programming phase. In this area, several works have been conducted to facilitate the programming of industrial robots. For example, gestures (OSAKI ET AL. 2008) and facial expressions (HEINZMANN & ZELINSKY 1999) can be used as interaction means for generating robot programs. BRECHER ET AL. (2010) introduced a hybrid programming technique which combines the advantages of online and offline robot programming methods.

---

<sup>4</sup>An integrated project funded under the European Union's Sixth Framework Programme (FP6)

The human operator can intuitively teach a task either in the real robot cell or in a synchronized simulation model. At the Institute for Machine Tools and



*Figure 1.10: Interactive user interface for programming of industrial robots (VOGL 2008)*

Industrial Management (*iwb*) several research setups have been built up for HRI during programming of industrial robots. An interactive spatial user interface based on Augmented-Reality technology (AR) was developed by VOGL (2008). This system included projection-based visualization, automatic capturing of geometrical information and an interactive 3D input device (Figure 1.10). Another example is the use of FTS and input devices, e.g. Wii-Remote and Novint Falcon, for programming of cooperating industrial robots (see Figure 1.11) based on a universal workpiece-based method (REINHART ET AL. 2010b).

### 1.4 Thesis Structure

Figure 1.12 shows the chapter structure of this thesis, which is organized into eight chapters. **Chapter 1** gives a short overview of the recent research in Human-Robot Interaction (HRI). Afterwards, **chapter 2** introduces the Telepresence and Teleaction Technology (TPTA) and its potentials for industrial applications. This chapter focuses also on the challenges and problems that exist when deploying TPTA-technology in industrial environments and provides a review of previous work in similar and related fields. A section is also dedicated to the research objectives of this work.

**Chapter 3** explains in detail the scaling and mapping techniques, which are developed and implemented in this work. Several techniques are described and



*Figure 1.11: Universal workpiece based approach for programming of cooperating industrial robots (REINHART & ZAIDAN 2009)*

discussed, and motivation for considering scaling and mapping in such cases is given. **Chapter 4** concentrates on the problem of force feedback provision and the effects of teleoperator's inertia on the stability of the TPTA-system. The problem is manifested using stability analysis and experiments, and a solution using a model-based force feedback is introduced. Assistance haptic functions which are implemented within this work are also described in this chapter.

**Chapter 5** introduces the general concept of the developed TPTA-system and its hard- and software components, while **chapter 6** is dedicated to the evaluation experiments. The designs of the two main experiments are presented, followed by the results and a conclusion of the findings. The first experiment aims at the evaluation of three different scaling techniques, namely position control with indexing, rate control and human intention-based control, with regard to speed, position accuracy and usability in a standardized tracking task. The second experiment studies the effect of model-based force feedback on task performance. Specifically, it was ascertained whether model-based force feedback would provide additional assistance over that offered by the visualization of applied forces during task execution.

In **chapter 7**, an operational and economic assessment of the developed industrial TPTA-system is given. For the operational feasibility, the system has been compared with conventional teleoperation systems that do not have all the features such as force feedback and different scaling techniques. For the economic feasibility, the model-based force feedback has been representatively used to quantitatively assess the performance and economic benefits of the developed system. Finally, **chapter 8** concludes the findings of the entire thesis, and presents avenues for future work.

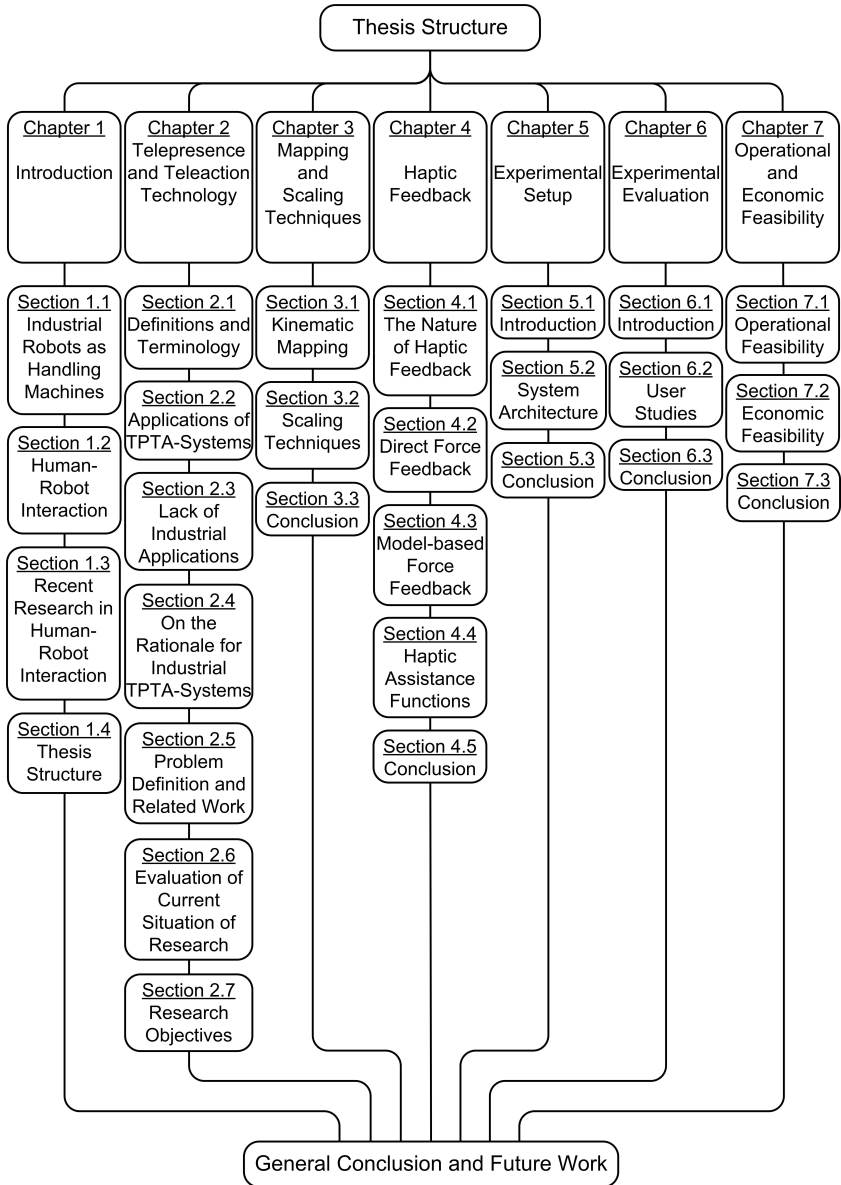


Figure 1.12: Diagram of thesis structure



## 2 Telepresence and Teleaction Technology

*“Presence refers to the natural perception of an environment, and telepresence refers to the mediated perception of an environment”*

---

STEUER (1992)

This chapter introduces the telepresence and teleaction technology (TPTA) as a way to realize HRI. As shown in Figure 1.12, this chapter is divided into seven sections. The first section provides definitions of the important terms associated with the TPTA-technology. The second section shows the general applications of this technology. Despite the apparent potentials of industrial TPTA-systems (section 2.4) there is a visible deficient for large-scale deployment of this technology in the industrial field. The reasons of this lacking are highlighted in section 2.3. Section 2.5 concentrates on the challenges and problems that exist by deploying TPTA-technology in industrial applications and previous work conducted to cope with these challenges. Afterwards, a brief evaluation of current research is given in section 2.6, while section 2.7 clarifies the research goals of this work.

### 2.1 Definitions and Terminology

Before starting the discussions about the aspects considered in this thesis, the important terms associated with the TPTA-technology are defined in this section. Figure 2.1 shows a general structure of a TPTA-system with human operator.

**Presence** is defined as the sense of being in an environment (STEUER 1992) and **Telepresence** is realized when technical means enable humans to feel present in other, remote, or not accessible environments. This can be achieved when a sufficient amount of sensor information (vision, sound, haptic information) is sensed at the remote side, transmitted to the local side, and displayed in a natural way to the human operator. When humans are no longer able to differentiate easily between whether their sensory impressions result from direct interaction with the environment or result from technical means, the telepresence system is considered as a highly transparent system. Simple examples of telepresence systems are the television and telephone, by which the human visual and/or auditory senses are used to perceive a remote environment.

## 2 Telepresence and Teleaction Technology

---

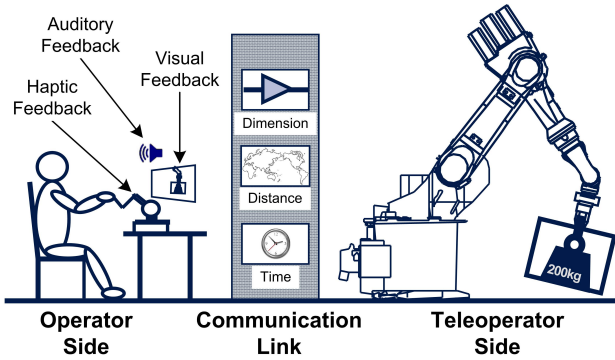


Figure 2.1: General TPTA-system structure

**Teleaction:** It means that the human operator is not only passively present at the remote place, but he/she can also actively change and interact with the remote environment. This is achievable when some tools and end-effectors are installed at the remote side and the human operator is given full control over these tools.

**Telepresence and Teleaction** is usually performed when the human operator remotely interacts with a mobile robot or a robotic arm to perform physical manipulation tasks. The overall system is called TPTA-system and it covers the entire structure including hardware as well as software that is needed to perform telepresent tasks. According to ROSENBERG (1993), the fundamental purpose of a telepresence system is to extend the human operator's sensory-motor facilities and problem solving abilities to a remote environment.

**Haptics:** Haptics refers to all that the human sense of touch concerns, i.e. sensing and manipulating through touch. It entails both *tactility* and *kinesthesia*. Tactility is the sensory perception of the mechanical interaction with the skin (KERN 2009), and it is responsible for sensing surface characteristics such as roughness, and detecting contact of the human body with its environment. Kinesthesia covers the internal sensing of forces and movements inside muscles, tendons and joints (HANNAFORD & OKAMURA 2008), and it is responsible of detecting the position and the motion of the human body.

**Haptic Input Device:** They are robotic manipulators that enable manual interactions with virtual environments or telerobotic systems. They are employed for tasks that are usually performed manually in the real world, such as manual exploration and manipulation of objects. In general, they receive action commands from humans and display appropriate haptic images to them.

**Human Operator:** The operator is a human who uses a TPTA-system to perform a task in a remote environment. The human operator is considered part of the closed control loop of a TPTA-system, which makes the design of this control loop more difficult because of the unknown and variable human dynamics.

**Human-Machine Interfaces (HMI):** Using a TPTA-system, the human operator interacts with the remote environment by means of technical devices. Hereby, the human operator uses Human-Machine Interfaces (HMI), which are also referred to in the literature as Human-System Interfaces (HSI), to input his/her commands. These commands are then transmitted from the operator side (local side) to the teleoperator side (remote side) over an appropriate communication link. HMI are designed to receive and display multimodal feedback in form of visual, auditory, and haptic information. They can, therefore, render a realistic feeling of contact and dynamic interaction with the remote environment.

**Teleoperator/Telerobot:** Teleoperators or telerobots (also referred to as slaves in the literature) are real or virtual handling equipments, for example industrial robots, that interact with nearby, remote or virtual environments. They perform handling tasks on an inaccessible remote/virtual site. These tasks are initiated by the human operator through the HMI and the teleoperators perform them either (semi-) automatically (intelligent teleoperation), or by simple teleoperation.

**Local Side:** On the local side, the operator is located with a human-machine interface (HMI) needed to couple the human operator with the TPTA-system. The local side is often referred to in the literature as operator side or master side.

**Remote Side:** This is the place where the teleoperator and handling tasks to be performed are found. It is also called slave side in the literature. This term is now applied indiscriminately for distant, miniaturized and virtual environments - in any case usually inaccessible for the human operator. This inaccessibility is either because of the danger, such as the handling of radioactive materials, or because of the physical size, such as microassembly. In comparison to the local side, the remote side consists of all devices and equipments such as grippers, fixtures and sensors, which are needed by the teleoperator to perform handling tasks and also to send sensory information from this side to the local side.

**Modalities:** They are human senses - vision, hearing, touch (or haptic), smell and taste. From these classical sense modalities, the first three are relevant for TPTA-systems.

**Multimodality:** It refers to inputs from more than one sense modality at a time (EPSTEIN 1985). In telepresence context this means that the human operator is provided with all telepresence-relevant modalities (visual, auditory, and haptic) at the same time. This gives far greater information about the handling task than one sense alone.

**Crossmodality:** It refers to the use of one modality to convey information that originally entered in another modality (EPSTEIN 1985). Reading is one example for crossmodality, by which the visual input is transformed into auditory information. Another example is the car parking assistance by which the auditory information is used to inform the driver about the distance to obstacles.

**Vision System:** This is the system used to provide the human operator with the visual feedback from the remote side. It usually consists of a camera system (including 2D camera, stereo-camera or 3D camera), which is located on the remote side, and a visual display (monitor, head mounted display or 3D visual workstation), which is located on the local side.

**Audio System:** To provide the human operator with the auditory information, microphones should be installed on the remote side to capture audio data, which is sent back to the local side and displayed by loudspeakers. To increase the degree of immersion, real time 3D sound synthesis algorithms can be used for spatial audio reproduction (KEYROUZ & DIEPOLD 2007).

**Transparency:** After stability, transparency is a major goal when designing TPTA-systems. In this context, ideal transparency means that the TPTA-system gives the human operator the feeling as if he/she is manipulating the remote environment directly (RAJU ET AL. 1989)(LAWRENCE 1993), i.e. the user is not able to distinguish between remote presence and local presence. This is achieved when all barriers between the human operator and the remote environment are overcome.

**Degrees of Freedom:** In a mechanics context, degrees of freedom (DOF) of a rigid body are the total number of coordinates or independent displacements and/or rotations required to completely describe the configuration of that body in space (HARTENBERG & DENAVIT 1964, p.133)(PENNESTRI ET AL. 2005). Thus a rigid body in  $d$ -dimensions has  $d(d + 1)/2$  DOF ( $d$  translational and  $d(d - 1)/2$  rotational DOF). Translational DOF is the ability to move the body without rotating, while the rotational DOF indicates the angular motion of a body about an axis. For example, a free rigid body has six DOF in 3D space (three translational and three rotational DOF) and 3 DOF in 2D space (two translational DOF and one rotational DOF).

**Workspace:** It is the reachable area (in 2D space) or volume (in 3D space) of a device's or manipulator's end-effector.

**Communication Link:** The communication link usually consists of a computer network (e.g. Internet) or sometimes a dedicated communication medium such as a direct cable connection or a broad bandwidth radio link. Through this link the human commands are sent from the local side to the remote side, and sensory information is also sent back from the remote side to the local side.

### 2.2 Applications of TPTA-Systems

Venues for several practical applications of TPTA-technology are found in areas as diverse as handling of hazardous materials, minimally invasive surgery, space and deep sea exploration, training and education, and the entertainment industry. The following are some of these applications.

#### 2.2.1 Handling of Materials in Hazardous Environments

According to SHERIDAN (1989), the first idea to manipulate hazardous objects from a safe distance dates back to the mid 1940s, when handling of nuclear materials was performed using the first teleoperation system (Figure 2.2). The connection between the operator and teleoperator was at that time purely mechanical, i.e. no time delay present between the two sides. However, due to this mechanical coupling a reduction of the apparent inertia of the teleoperator was not possible and wide separation was also difficult to realize. For these reasons, the first electronic remotely operated manipulators were implemented in 1954 (HOKAYEM & SPONG 2006). The mechanical coupling between the operator and robot sides was replaced by a data transmitting connection. This system is considered a basic model of all modern TPTA-systems.



*Figure 2.2: The first teleoperation system for handling nuclear materials*

### 2.2.2 Medicine

In addition to the application of TPTA-technology for handling nuclear materials, there are several research works for implementing this technology in medicine (e.g. TENDICK & CAVUSOGLU (1997), ORTMAIER (2003) and MAYER ET AL. (2007), among others). This has several reasons, one of them being that TPTA-technology allows expert surgeons to perform advanced surgeries at distance where they can not be present, e.g. in natural disaster areas or in battlefields (SATAVA 1995). Another reason is that it offers the possibility for minimally invasive surgeries to be conducted. In this case, the incisions are very small in comparison to open surgery and pain and trauma will be reduced, leading to shorter rehabilitation time (MACK 2001), (ORTMAIER 2003). In order to facilitate the operation and improve the performance of the task, there are various special surgical devices developed for teleoperated minimally invasive surgery. These are usually equipped with specially designed sensors (KÜBLER ET AL. 2005) to enable the surgeon feeling the interaction forces occurring at the tool during surgery (OTTENSMEYER ET AL. 2000) (MAYER ET AL. 2007). In addition, assistance functions were investigated by semi-autonomous tasks (e.g. by guiding the surgeon or moving the camera along the changing focus of surgery) (GROEGER ET AL. 2008). To sum up, TPTA-systems used in medicine (Figure 2.3) overcome the barriers of distance, inaccessibility and also facilitate minimally invasive surgeries.



*Figure 2.3: da Vinci<sup>®</sup>: the telepresence system for performing minimally invasive surgery (INTUITIVE SURGICAL 2011)*

### 2.2.3 Space Explorations and Maintenance

Automating tasks to be carried out in space, such as maintenance of space stations, is inconceivable since the tasks in this environment are changeable and unpredictable. Therefore, these tasks are usually conducted by astronauts. However, sending astronauts to space is very expensive and risky in such missions. Here, using TPTA-technology is considered reasonable, where a robot can be sent to space instead of an astronaut and this robot will be controlled by a human operator from the earth (Figure 2.4). To achieve this, several experiments on space telerobotics have been proposed in the literature (HIRZINGER 1994) (LANDZETTEL ET AL. 1999) (REINTSEMA ET AL. 2007). In addition, several research studies have been conducted to overcome the communication problems in this case, such as time delay in the communication channel (SHERIDAN 1993) (ARTIGAS ET AL. 2006) (RYU ET AL. 2010), which can be up to several seconds and leads to instability in the system. Furthermore, research works are conducted on the reliability of the communication channel in space TPTA-systems (STOLL 2009).

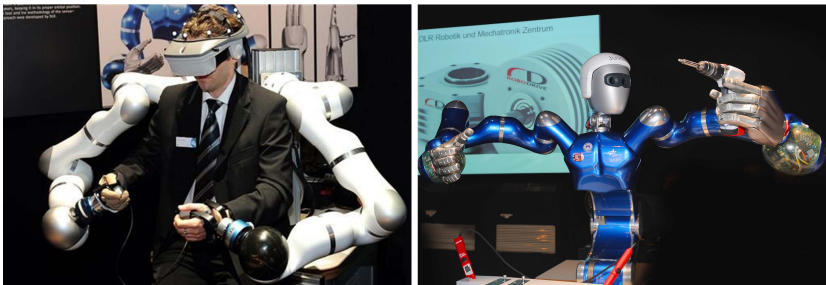


Figure 2.4: Telepresence system for applications in space: Operator side (left) and Space-Justin as a teleoperator (right) (DLR 2011)

### 2.2.4 Underwater Explorations and Maintenance

What happened in the Gulf of Mexico on 20th April 2010, when the BP's Deepwater Horizon oil rig exploded, is considered a big challenge for TPTA-technology in this field. Sending human divers to conduct underwater tasks, such as maintenance, is risky and very expensive, especially when it comes to depths below 200 meters. The oil well in the Gulf of Mexico sits at about 1500 meters, which is only reachable by remotely operated vehicles (ROVs) (Figure 2.5). Several cooperating ROVs have carried out their tasks with impressive success and were

## 2 Telepresence and Teleaction Technology

---

able to stop the oil leak on 15th July 2010 by capping the running wellhead (BBC.NEWS 2010).

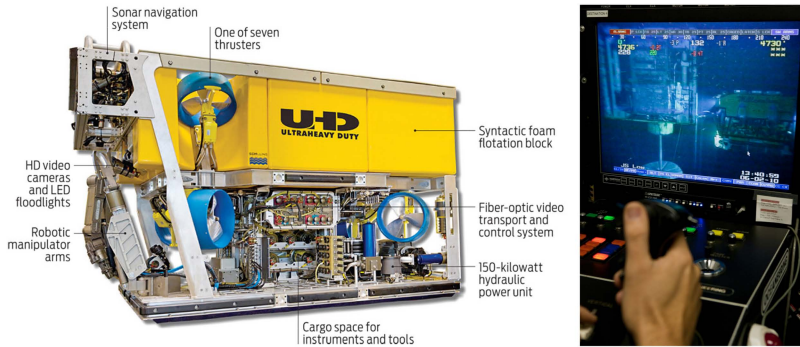


Figure 2.5: ROVs: Remote operated vehicles (left) (photo: Schilling Robotics) and the operator control room (right) (photo: BP p.l.c.)

### 2.2.5 Training, Education and Entertainment

TPTA-systems are used for training purposes in complex and/or crucial tasks, for which it is too difficult, dangerous or expensive to provide direct training in the real environment. For example, training new surgeons can be performed using TPTA-systems so that a doctor can practice in a simulation environment before the real operation (LIU ET AL. 2003) (SUZUKI ET AL. 2005). Besides training, TPTA-technology has applications in many educational and entertainment industries. For instance, the Insect Telepresence project (ALL & NOURBAKHSI 2001) allows students and museum visitors, through mediated telepresence, to enter the small-scale world of insects to learn more about them and their daily life. TOURBOT and WebFAIR projects (TRAHANIAS ET AL. 2005) provided techniques for using mobile robots as interactive agents in populated environments, such as museums or trade fairs.

### 2.3 Lack of Industrial Applications

In spite of numerous distinguished research undertakings in the field of telepresence and teleaction, wide scale deployment of this technology in the industrial and commercial realm has yet to materialize. This could be attributed to the

cost effectiveness and design guidelines of such novel types of systems. Most of the developed systems shown in the previous sections are designed for special applications, which makes them very expensive and suitable only for those intended applications. Therefore, several modifications and extensions have to be performed during designing and deploying TPTA-systems in order to enhance the usability of such systems and make them appropriate for industrial applications (see section 2.5).

### 2.4 On the Rationale for Industrial TPTA-Systems

There are several circumstances under which TPTA-technology may meet specific industrial needs. The following factors point out the fundamental reasons of deploying TPTA-systems in the industrial realm.

#### Scaling factor

TPTA-technology is economically reasonable when the ability of the human worker is hindered by physical limitations (RADI ET AL. 2010a). For example, the use of haptic devices as a human interface allows the perceived impedance by the operator to be adjustable depending on the task. This could be used to lessen the stress impact on an operator responsible for handling heavy loads, and therefore gives the operator the ability to strike a balance between realistic feeling and manageable amount of stress.

Another example is the handling of micro products. In this case the range of human motor skills and visual perception are rendered insufficient to perform precise movements and accurate placement adequately. Parts with dimensions smaller than 1 mm also require highly accurate assembly, where common tolerances of 0.1 mm are insufficient. Human workers need a lot of training to fulfill these requests (GROSS & DIRKS 2004). Therefore, the deployment of TPTA-systems solves this problem because human movements will be recorded by an input device and scaled down in a sufficient manner, so that they can be executed by a very precise and accurate teleoperator's kinematics. Furthermore, and especially for elders who have problems like tremor (vibrating movement), the high frequency tremor can be filtered out using adequate signal processing algorithms. Also, the visualization of the task can be scaled up by the use of image processing techniques, so it becomes more intuitive for humans.

#### Safety factor

The deployment of TPTA-systems to carry out tasks in dangerous and/or highly inaccessible areas is exclusively needed. For example, handling radioactive materials is required to be remotely maintainable to minimize exposure to human workers. All space applications and deep sea operations are also considered typical applications in this case.

### Flexibility factor

TPTA-systems are relatively flexible than automated robotic systems with regard to the environmental structure. As the structure of the environment decreases or when the environment is dynamic, the TPTA-systems become more suitable if the automated systems lack the ability to create environment models from real-time sensory data.

Although TPTA-technology is considered a promising solution for conducting manual tasks, it is not as profitable when switching from unique individual products to small batch sizes. Hereby, an approach combining the advantages of TPTA-technology and automation techniques forms an efficient solution (RADI ET AL. 2010b), by providing a high degree of flexibility for production.

### Economic factor

The TPTA-system is controlled by humans, i.e. expensive testing and monitoring equipments, such as optical sensors, which are needed for automated systems, can be avoided. This reduces the investment costs compared to automated systems. However, special devices are also needed for TPTA-systems such as haptic devices and force-torque sensors. Therefore, one should perform an economical study to find out whether TPTA-systems can be profitable for an intended application. Nevertheless, it should be here mentioned that there are several factors such as safety and ergonomics, which play a very important role and can not be disregarded. These factors may have a higher priority than others and they should not be underestimated. In some cases, TPTA-technology is considered a solution from these factors point of view.

## 2.5 Problem Definition and Related Work

For TPTA-technology to become a viable solution in an industrial context, its impact on the overall process performance needs to be addressed. Several modifications and/or extensions to TPTA-technology are needed to make it better suited for industrial deployment. In industry, the use of commercially purchased devices - **Commercial Off-The-Shelf (COTS)** components - for designing and constructing new systems is preferred to specially designed and fabricated devices because this:

1. reduces overall design and construction costs of a system,
2. reduces spare parts inventories,
3. minimizes operator-training time, and
4. decreases costly downtime.

However, the use of such devices poses several challenges and problems which should be solved during the design of new TPTA-systems in order to enhance the usability of TPTA-systems in industrial environments. These problems are highlighted in the following sections.

### 2.5.1 Kinematic Mapping and Workspace Scaling

Most of HMIs, especially standard haptic devices (cf. Figure 2.6), are limited in their degrees of freedom and have only small workspaces. Therefore, using these devices to maneuver heavy-duty teleoperators in TPTA-systems will pose a problem. This problem is twofold: the kinematic mapping and the workspace scaling. The former considers the mapping between DOF of the haptic device and the teleoperator, while the latter focuses on the issue of manipulating a huge teleoperator through its entire workspace by using a relatively small haptic device.



Figure 2.6: Examples of haptic devices available in market: PHANTOM Desktop from Sensable (left), Impulse Engine 2000 from Immersion Corp. (middle) and Falcon from Novint Technologies Inc.(right)

Regarding the first aspect, the kinematic mapping, if the haptic device and teleoperator are mechanically identical, then the teleoperator is always able to duplicate the motions of the haptic device (SAYERS 1999). However, controlling six DOF with one hand is very difficult (RICE ET AL. 1986), and maneuvering an input device with high number of DOF results in less coordinated motions (ZHAI & MILGRAM 1998)(DEML 2007). Moreover, designing a haptic input device which is kinematically similar to the teleoperator would have technical challenges and it in turn would make the device very expensive. Therefore, the haptic devices, which are used as input devices for human movements, should not be kinematically designed to be similar to the teleoperator structure. It has been shown that using a coordinate transformation allows for connecting two kinematically different master and slave devices (CORKER & BEJCZY 1985). Hence, the use of simple standard haptic devices is preferable in this case. But suppose that a haptic device with e.g. two DOF is selected to perform a task

## 2 Telepresence and Teleaction Technology

---

which requires controlling more than two DOF. Then adequate solutions for such situation should be sought.

Several methods have been developed in the past to solve this kinematic problem (see Table 2.1). Based on isometric projection, SATO ET AL. (1992) developed a method by which a two dimensional operating surface in the input device workspace was mapped to a curved working plane in the teleoperator workspace. Another way to cope with the DOF-deficiency is to enable only the required DOF or task-specific DOF. MANOCHA ET AL. (2001) used virtual linear fixtures and virtual planar fixtures to constrain the motion of a simulated teleoperator to coincide with a given line or plane, respectively. This allows having an input device with less number of DOF as the extra DOF of the teleoperator will be constrained by these fixtures during task execution. DUBEY ET AL. (2001) solved the problem by using an intermediate transformation to relate the two workspaces of the input device and teleoperator.

Method	Pros	Cons
Mechanically identical master and slave	-Easy to duplicate motions	-Difficult to control many DOF -Less coordinated motions -Very expensive haptic devices
Isometric projection	-Mapping a surface in the master workspace to a curved plane in the slave workspace	-Limited shapes
Virtual fixtures	-Master device with less number of DOF	-Only simulated teleoperator
Intermediate transformation	-Master devices with different DOF and shapes can be utilized	-Complex implementation -Time-consuming

Table 2.1: Overview of mapping techniques

The second aspect is the workspace scaling. Having different devices with different workspace sizes leads to scaling problems. As mentioned before, the human operator uses a haptic device to steer e.g. a huge robot during handling processes. These devices are usually designed to the convenience of the human operator, i.e. they should not be sized to the huge size of teleoperators, which are mainly used for handling heavy loads. Therefore, the physical workspace of a grounded haptic device is significantly smaller than the target workspace of the teleoperator (cf. Figure 2.7), and the human operator will not be able

to reach and interact with objects located outside this limited workspace. To overcome this problem, several scaling techniques have already been reported in the literature (see Table 2.2).

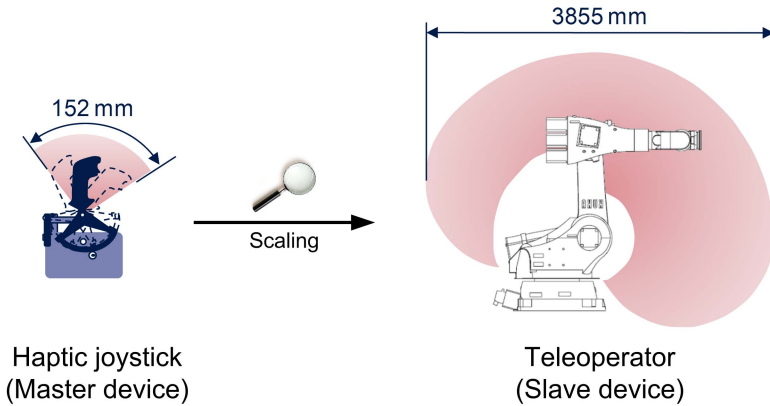


Figure 2.7: Scaling Issue

The first commonly used technique is position control, by which the displacements of the haptic device are scaled with an appropriate scaling factor and mapped to motions of the teleoperator. This means that the scaled displacements of the haptic device dictate displacements of the steered teleoperator. Depending on the application, the scaling factor can be smaller than or greater than one. For example, the scaling factor for moving a robot in micro scale workspaces is usually smaller than one (ZÄH ET AL. 2006), while for a robot in large-scale domain is greater than one. Position control with indexing is used to solve the problem when the operator reaches the workspace limits of the haptic device during position control. This is achieved by disconnecting the communication between the haptic device and the teleoperator and then moving the handle of the device back to the origin. Afterwards the communication is resumed.

Ballistic Control (MALLETT ET AL. 2004) is another way to solve the problem of reaching the workspace limits of the haptic device. It sets the scaling factor of the position control based on the velocity at which the device is traveling within its workspace. When the operator moves the haptic device slowly, the ballistic controller assumes that a fine motion is desired and therefore a small scaling factor is applied. When the operator moves the device very quickly, the controller assumes that a coarse motion is desired and a larger scaling factor is applied. Furthermore, the scaling factors can be either linear or nonlinear

## 2 Telepresence and Teleaction Technology

---

function of the velocity. For example, the scaling factor during fine motion of the robot can be adjusted based on a linear relationship with the device motion, while for coarse motion it is adjusted based on an exponential relationship with the device motion.

Rate control is another method used to solve the scaling problem. It refers to a class of mapping, in which the displacement of the haptic device is interpreted as a velocity command for the teleoperator, i.e. the haptic device can be held at a fixed position but the teleoperator keeps moving according to a related commanded velocity. This is principally similar to the gas pedal in vehicles; the further the haptic device is moved from the initial position, the greater the velocity of the steered robot. It has been found that applying an elastic force (spring force) improves the rate control (ZHAI 1995), i.e. the operator can feel the effect of his/her control actions very well by the attracting spring force toward the initial position (zero velocity).

Method	Pros	Cons
Position control	<ul style="list-style-type: none"> <li>-Simple</li> <li>-Understandable</li> <li>-Direct kinematic correspondence</li> </ul>	<ul style="list-style-type: none"> <li>-Poor spatial resolution in case of large scaling</li> </ul>
Ballistic control	<ul style="list-style-type: none"> <li>-Adaptive scaling factor</li> <li>-Linear and non-linear scaling factors</li> </ul>	<ul style="list-style-type: none"> <li>-Complex implementation</li> </ul>
Rate control	<ul style="list-style-type: none"> <li>-Simple</li> <li>-Understandable</li> <li>-Infinite workspace</li> </ul>	<ul style="list-style-type: none"> <li>-No direct kinematic correspondence</li> </ul>
Workspace drift control	<ul style="list-style-type: none"> <li>-Manipulating large objects</li> <li>-Using small haptic device</li> </ul>	<ul style="list-style-type: none"> <li>-Only virtual environments</li> <li>-Conservative method</li> </ul>
Hybrid position/rate control	<ul style="list-style-type: none"> <li>-Position and rate control at once</li> <li>-No manual switching</li> </ul>	<ul style="list-style-type: none"> <li>-Complex implementation</li> </ul>

*Table 2.2: Overview of scaling techniques*

Another scaling technique called workspace drift control was introduced by CONTI & KHATIB (2005) and was used to manipulate large objects inside a 3D virtual environment. Based on the observation that people do not notice small deviations of their hands unless that small deviation has a corresponding

visual component, the physical workspace of the haptic device is shifted towards an unreachable area within the robot workspace without affecting the human perception. As indicated by CONTI & KHATIB (2005), there are some conditions required to ensure that the drift of the workspace remains imperceptible to the operator. First, the shifting should occur only when the user hand is in motion, otherwise the operator will recognize this drift as an action which is unrelated to his/her hand motion. Second, the velocity of the shifting should be proportional to the velocity of the operator hand. The third condition is that the object to be manipulated should be at least partially within the haptic device workspace.

As the position control can solve the kinematic correspondence and contact force feedback problems encountered with rate control and rate control can solve the spatial resolution problem encountered with position control, the hybrid position/rate control allows the operator to have both techniques available at once (HOLLIS & SALCUDEAN 1993). This is realized by dividing the haptic device workspace into an inner zone designated for position control and an outer zone designated for rate control. As the operator keeps the device within the inner zone, the robot is guided under position control. When the operator moves the device into the outer zone, the rate control is activated. Therefore, the effort incurred in manual switching between the two different modes is reduced.

### 2.5.2 Haptic Feedback and System Instability

Apart from visual feedback, haptic feedback is in several cases mandatory and the lack of it will lead to longer task completion times or even to unfeasible tasks. Examples of situations where the use of haptic feedback is necessary are:

1. Poor or inadequate visual feedback from the slave side.
2. Accurate and fine positioning tasks by assembly in complex environments.
3. Handling of delicate materials.
4. Providing physical information about the material characteristics such as material stiffness, weight of objects, surface roughness, etc.

Numerous studies have been conducted to evaluate the effects of haptic feedback on human task performance with TPTA-systems, with most being performed on peg-in-hole tasks. It has already been shown that incorporating haptic feedback into TPTA-systems reduces the maximum contact forces, the variance in applied forces and the task completion times. For instance, DRAPER ET AL. (1987) stated that the provision of haptic feedback allowed the human operators to reduce the maximum peak forces applied to the task objects, but no noticeable effect on the task completion time has been found. They showed also that task

## 2 Telepresence and Teleaction Technology

---

error rates are lowered with force feedback. Later on, HANNAFORD & WOODS (1989) reported reductions of the sum of squared applied forces by a factor of 7 with haptic feedback. They found that haptic feedback reduces also the task completion time by approximately 30% for peg-in-hole tasks. MASSIMINO & SHERIDAN (1989) showed significant reductions of the mean task completion time when operators received haptic feedback in a peg-in-hole scenario. In another study, KIM (1992) showed that reductions of cumulative contact forces are achieved by haptic feedback in such tasks, but almost no effects on the task completion time is reported. In contrast, KONTARINIS & HOWE (1996) and DENNERLEIN ET AL. (2000) showed that force feedback significantly decreases the task completion times. In another task, SALLNÄS (2001) showed that the time needed for constructing a tower of virtual objects such as cubes is significantly reduced when the operators receive haptic feedback. JACOBS ET AL. (2007) found that the time needed to cut out round figures and to perform double dot suture lines is decreased with haptic feedback. FARKHATDINOV & RYU (2008) showed that the sway of the load in an industrial overhead crane is reduced using the haptic feedback. RADI ET AL. (2010a) investigated the effect of force and vibration feedback on the performance of pick-and-place tasks. They determined that force feedback reduced the pressure forces applied on the surface when placing a cube on it, but not when vibration is used.

However, not all studies showed that force feedback increases the task performance. Other studies mentioned that haptic feedback showed small or even non-significant improvements in task completion time, while improving the accuracy and reducing the number of errors (e.g. WALL ET AL. (2002) and OAKLEY ET AL. (2000), among others).

The haptic feedback in force-reflecting TPTA-system is measured at the teleoperator side either by FTS, by position sensors in both haptic device and teleoperator, or by motor current of the teleoperator. However, closing the control loop by having this haptic feedback could cause system instability. Sources of this instability in TPTA-systems can be either the time delay in communication channels or the dynamic masking.

### 2.5.2.1 Time Delay

TPTA-systems have often been associated with the time delay problem since the introduction of electrical servo-control instead of the direct mechanical connections between the haptic devices and the teleoperators. This imposed the use of bilateral closed-loop<sup>1</sup> control between the local side and the remote

---

<sup>1</sup>The loop from the haptic device to the teleoperator and back

side. FERRELL (1964) showed that the existence of time delay in the control loop of force-reflecting teleoperation systems causes instability. This is because the delayed force feedback introduces unexpected disturbances to the system which, in turn, confuses the human operator. To avoid this instability at that time, Ferrell used either a move-and-wait strategy or supervisory control (FERRELL & SHERIDAN 1967).

Many control strategies have been proposed in the literature to overcome the instability in bilateral TPTA-systems due to communication time delays. The passivity-based approaches, e.g. time-domain passivity (HANNAFORD & RYU 2001) (ARTIGAS ET AL. 2006) or wave variables (NIEMEYER & SLOTINE 1997), have opened the way for stable teleoperation with constant time delays in communication links. After the Internet began to be used as a communication medium in the mid 1990s, teleoperation through the Internet imposed other problems such as randomly varying time delays, discrete-time data exchange and data loss. It has been shown that teleoperation systems may experience instability when the time delay varies (CHOPRA ET AL. 2003). Various research works have consequently been carried out to adapt the used control methods to varying time delays (YOKOKOHI ET AL. (1999), CHOPRA ET AL. (2003) and RYU & PREUSCHE (2007), among others) and discrete-time communication (SECCHI ET AL. (2003) and BERESTESKY ET AL. (2004), among others). Prediction has been also investigated to solve the problem of varying time delays and data loss (MUNIR & BOOK (2002) and CLARKE (2006), among others). Another source of time delay - beside this transmission delay - is the local position control loop at the robot side. This control loop ensures the high position accuracy of industrial robots, but it includes both control delay and actuators delay (mechanical time constants) in the overall bilateral closed control loop of TPTA-systems.

Usually teleoperators in TPTA-systems are developed for teleoperation purposes, i.e. the communication links are implemented and specially adapted to be used between haptic devices and teleoperators. Standard industrial robots are, however, designed for automation processes and not to be connected to haptic input devices in a TPTA-system. But there are some industrial robots that have interfaces to be connected to external devices. These usually have special industrial communication protocols and, in turn, extra inherent time delays. Yet there are several efforts by industrial robot manufacturers to develop new robot interfaces which allow users to connect their robots with external devices and sensors.

The time delay issue is out of the scope of this thesis because:

- in this work the utilized communication link between the haptic device and teleoperator is one of the state-of-the-art industrial robot interfaces. This communication link has real-time characteristics with 4 msec sampling rate and has no time delay.

- the work here focuses on haptic feedback in TPTA-systems with heavy-duty teleoperators. This imposes other problems, e.g. the dynamic masking which is explained in the following section.

### 2.5.2.2 Dynamic Masking

Several mechanical characteristics of haptic devices, such as stiffness, friction and inertia, and/or the intrinsic dynamics of the teleoperator can mask the reflected forces from the teleoperator side and may cancel them (SHERIDAN 1992, pp. 174:175) or even force an instability in the system. This dynamic masking effect is perceptible when the force feedback is either scaled-up, such as in the case of micro-manipulation (CHIN ET AL. 1993), or directly fed back in the case of heavy-duty teleoperators. In the case of scaling up the force feedback, this is very critical for some tasks such as telesurgery and manipulation of delicate materials (e.g. microassembly), because the human operator may not feel the real interaction forces between the teleoperator and the environment and he/she will keep moving the input device, which, in turn, could cause serious damages. COLGATE (1993) introduced the *impedance shaping bilateral control* to solve this problem in micro-manipulation tasks. The idea of impedance shaping was to augment the sensor-based force feedback by a model based on priori information of the environment. PETZOLD (2007) has also used a model-based force feedback at the operator side in a micro-telemanipulation system.

In the case of heavy-duty teleoperators - normally used for handling heavy loads - the forces at the teleoperator side, which are directly fed back to the human operator through haptic interfaces, must be scaled down in order to have a stable haptic feedback. KIM (1992) has found that the forces should be scaled down by a factor of 10% to maintain system stability. However, scaling down the forces will distort the real feeling of the interaction forces at the teleoperator side and consequently will decrease the transparency of the TPTA-system. It has been also shown that the scaling factors are limited by the ratio of haptic device's mass and teleoperator's mass (DANIEL & MCAREE 1998) (SHULL & NIEMEYER 2008). Therefore, various methods have been suggested to stabilize and increase transparency of teleoperation systems with heavy-duty teleoperators. For example, MCAREE & DANIEL (2000) used estimates of the distance between the teleoperator and objects in its workspace to limit the momentum of the teleoperator at impact. The use of local force feedback at the robot side is proposed by HASHTRUDI-ZAAD & SALCUDEAN (2002) and SHULL & NIEMEYER (2007) to convert the robot into an impedance device in order to hide the large inertial and frictional properties of it and to maintain system stability. However, SHULL & NIEMEYER admitted that the telerobotic system they used is limited by the internal time delay of the industrial robot, which makes it difficult to maintain stability.

## 2.6 Evaluation of Current Situation of Research

As this issue is one of the main aspects addressed in this work, it is explained in detail in chapter 4 and also a proposed solution is introduced and discussed.

Problem	Consequences	Solutions
Time delay in communication channels	<ul style="list-style-type: none"><li>-Unexpected disturbances</li><li>-Human operator confusion</li><li>-System instability</li></ul>	<ul style="list-style-type: none"><li>-Move-and-wait strategy</li><li>-Time-domain passivity</li><li>-Wave variables</li><li>-Prediction</li></ul>
Dynamic masking	<ul style="list-style-type: none"><li>-Masking the reflected forces</li><li>-Distortion of the real feeling <math>\Rightarrow</math> less transparency</li><li>-System instability</li></ul>	<ul style="list-style-type: none"><li>-Impedance shaping bilateral control</li><li>-Model-based force feedback for micro-manipulation tasks</li><li>-Downscaling in the case of heavy-duty teleoperators</li><li>-Distance-to-contact estimation</li><li>-Local force feedback at teleoperator side</li></ul>

*Table 2.3: Stability problems and solutions in the case of haptic feedback*

## 2.6 Evaluation of Current Situation of Research

Several methods, e.g. position control with indexing and rate control, are used for tracking tasks in TPTA-systems to solve the problem of workspace limitation of haptic input devices. Most of the conducted research has focused on the implementation issues and few of them have evaluated these methods. In this work, three methods have been implemented and comprehensive evaluation experiments have been conducted to show in detail the performance of these methods during tracking a standardized trajectory with different shapes.

Furthermore, numerous research undertakings have confirmed the improvement of task performance by directly feeding back the interaction forces to the human operator in TPTA-systems and virtual reality. However, having heavy-duty teleoperator showed difficulties in maintaining the stability of TPTA-systems and, therefore, the direct force feedback cannot be used without scaling down the forces to certain values that allows stable haptic feedback. This scaling affects the

transparency of the TPTA-system. Therefore, the idea of implementing a model-based force feedback instead of directly feeding back the measured interaction forces have recently been suggested by several researchers to overcome this stability problem. However, several problems which are faced by researchers, such as the internal time delay of industrial robots, makes the stability issue harder and hinders the further evaluation of this method.

### 2.7 Research Objectives

Unlike existing research, this work focuses on enhancing the industrial usability of TPTA-systems. One way to achieve this objective is by utilizing COTS components. This can reduce the overall design and construction costs of TPTA-systems and therefore makes them more suitable for industrial applications. However, the utilization of COTS components poses several challenges and problems especially when deploying industrial TPTA-systems with heavy-duty teleoperators. In this work, two challenges are addressed, namely the *kinematic mapping and workspace scaling* and the *provision of haptic feedback*. Hence the goal of this research is twofold:

- **With regard to kinematic mapping and workspace scaling**  
Several techniques, as described in chapter 3, have been developed in this work. Furthermore, a human subject experiment has been conducted (see Section 6.2.2) to evaluate the implemented techniques in a standardized tracking task with regard to usability and various measures of task performance, e.g. speed and position accuracy.
- **With regard to haptic feedback**  
To solve the problem of having force feedback in the case of heavy-duty teleoperator and small haptic device, a model-based force feedback is used rather than scaling down the measured forces to ensure stability of the TPTA-system (see chapter 4). In order to assess this solution, another human subject experiment has been conducted (see Section 6.2.3) to investigate whether this model-based force feedback would improve task performance as the direct force feedback does.

## 3 Mapping and Scaling Techniques

*“To solve any problem, here are three questions to ask yourself: First, what could I do? Second, what could I read? And third, who could I ask?”*

---

*Jim Rohn*

This chapter serves as an overview of the methods developed in this work to overcome the kinematic mapping and workspace limitation of haptic devices. In Section 3.1, the mechanisms used in this work for transforming the motion commands of the haptic device held by the human operator into motions of the teleoperator are described. This includes the kinematic mapping strategy that solves the DOF-deficiency of the haptic device. Scaling techniques, namely position scaling with indexing, rate control and human intention-based control, are described in Section 3.2. Finally, Section 3.3 concludes the chapter with a brief discussion of the advantages and disadvantages of these techniques.

### 3.1 Kinematic Mapping

When the haptic device has insufficient DOF, the simultaneous control of all translational and rotational DOF of the teleoperator is impossible. Therefore, a mapping strategy is needed to cope with this challenge. Suppose  $N_{op}$  is the number of the DOF at the operator side (DOF of the haptic device), and  $N_{to}$  is the number of degrees of freedom at the teleoperator side (DOF of the robot). One solution is to map the available DOF  $N_{op}$  onto selected DOF of the teleoperator, defined as controllable teleoperator DOF and termed  $N_{to_{ctrl}} \subseteq N_{to}$ . For example, if  $N_{op} = 2$ , the mapping in this case can be done by projecting these DOF onto a plane within the workspace of the teleoperator. This plane is called the *motion plane* (cf. Figure 3.1).

It should be mentioned here that motions need simultaneous control of more than  $N_{op}$  are impossible using this technique (REINHART & RADİ 2009). However, by switching between several motion planes within the workspace of the teleoperator, it is possible to successively control all DOF of the teleoperator (see Figure 3.2 and Figure 3.3). This is similar to the case of interacting with 3D graphics (e.g. CAD models) using only a two DOF computer mouse. The

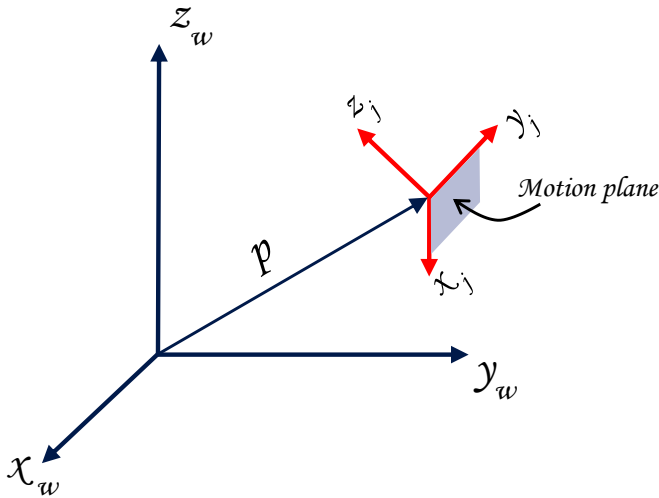


Figure 3.1: Projecting the two degrees of freedom of the haptic device onto the motion plane within the teleoperator workspace

operator must change the plane-of-view consecutively to manipulate graphs lying on other planes. In this work, the uncontrollable DOF are kept constant in order to help the operator concentrate on the controllable ones. For example, if the operator performs only translational motions, the rotational DOF will not be changed.

#### 3.1.1 Transformation

The homogeneous transformations are applied in this work to convert the motion commands from the joystick coordinate frame ( $C_j$ ) to the robot world coordinate frame ( $C_w$ ) and it is mathematically<sup>1</sup> defined as (PAUL 1981, Page 13)

$$T = \begin{bmatrix} R & \mathbf{P} \\ \mathbf{0}^T & 1 \end{bmatrix} \in \mathcal{R}^{4 \times 4} \quad (3.1)$$

---

<sup>1</sup>Throughout this thesis, the *italicized small* letters are used to represent scalars, the *ITALICIZED CAPITAL* letters to represent matrices, **bold small** letters to represent vectors, and **BOLD CAPITAL** letters to represent coordinate frames

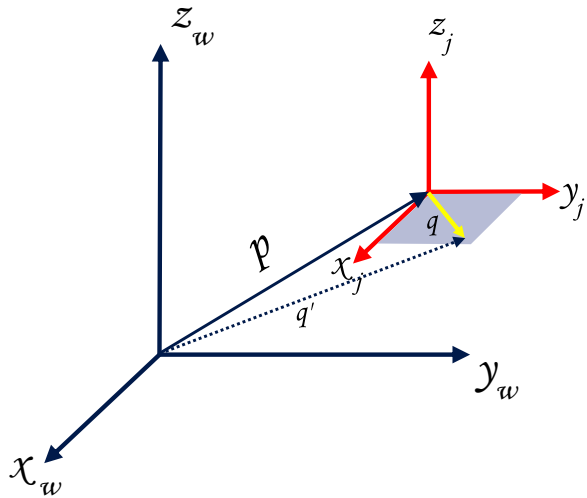


Figure 3.2: Motion command vector  $\mathbf{q}$  lying on a motion plane parallel to  $xy$ -plane of  $\mathbf{C}_w$  frame

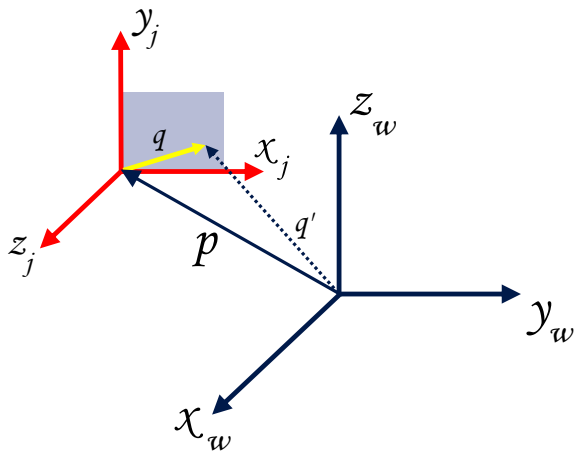


Figure 3.3: Motion command vector  $\mathbf{q}$  lying on a motion plane parallel to  $yz$ -plane of  $\mathbf{C}_w$  frame

### 3 Mapping and Scaling Techniques

---

where  $\mathbf{p} = [ p_x \quad p_y \quad p_z ]^T$  is a displacement vector representing the position of the new coordinates relative to the old one, and  $R \in \mathcal{R}^{3 \times 3}$  is a rotation matrix representing the orientation of the new coordinates relative to the old one.

Let  $\mathbf{q} = [ q_x \quad q_y \quad q_z ]^T$  be a point in the  $\mathbf{C}_j$  frame and these motion commands should be sent to the robot controller (Figure 3.1). This requires calculating the coordinates of the point  $\mathbf{q}$  in terms of the  $\mathbf{C}_w$  frame. First, the position and orientation of  $\mathbf{C}_j$  frame relative to  $\mathbf{C}_w$  frame should be mapped using a transformation matrix  $T$ . This is done by multiplying several transforms one by another. In general, the coordinates of a motion command  $\mathbf{q}$  in the robot coordinate frame are given by  $\mathbf{q}'$  (see Figure 3.2):

$$\mathbf{q}' = T \begin{bmatrix} \mathbf{q} \\ 1 \end{bmatrix} \quad (3.2)$$

where  $T$  is the total transform matrix produced by multiplying all needed intermediate transforms to get the motion commands in the  $\mathbf{C}_w$  frame.

## 3.2 Scaling Techniques

As mentioned before, the human operator uses haptic devices to steer the telerobot during handling processes and the physical workspace of such devices ( $W_h$ ) is significantly smaller than the target workspace ( $W_r$ ) of teleoperators used for heavy duty tasks. Hence the operator will not be able to reach and interact with objects located outside this limited workspace. In this section, the scaling techniques developed in this work are explained in detail and advantages and disadvantages of each are also mentioned (REINHART ET AL. 2010a). In general, workspaces of haptic devices and robots may have up to  $N$  dimensions ( $\mathcal{R}^N, N_{max} = 6$ ) with multiple translational and rotational degrees-of-freedom. However, for illustration purposes two dimensional workspaces ( $\mathcal{R}^2$ ) are used throughout this section.

### 3.2.1 Position Control

Position control is the most commonly used technique and is obtained by scaling the displacements of the haptic device with an appropriate scaling factor and mapping these to teleoperator motions, i.e. the scaled displacements of the haptic device dictate displacements of the telerobot. Equation 3.3 describes the

relationship between the position of the haptic device handle ( $\mathbf{p}_h \in \mathcal{R}^2$ ) and the position of the robot end-effector ( $\mathbf{p}_r \in \mathcal{R}^2$ ) in the target workspace.

$$\mathbf{p}_r = \alpha \times \mathbf{p}_h \quad (3.3)$$

where  $\alpha \in \mathfrak{R}$  is a constant scaling factor.

The value of the scaling factor depends solely on the application. In the case of microassembly, the scaling factor is usually smaller than one. In this work, however, teleoperators with large workspace are considered, i.e.  $\alpha \geq 1$ .

Although this technique allows the operator to navigate through a larger portion of the robot workspace with a small workspace haptic device, using a large scaling factor leads to poor spatial resolution and, therefore, the operator will not be able to perform precision manipulation tasks. For accurate positioning, a small scaling factor should be selected and, consequently, only a small part of the teleoperator workspace can be traversed. This problem can be solved either by indexing (JOHNSEN & CORLISS 1971) or ballistic control (MALLET ET AL. 2004).

### Position Control with Indexing

Position control with indexing (PCI) is performed by stopping the communication between the haptic device and the telerobot when the operator reaches the workspace limits of the haptic device and then moving the handle of the device back to the origin. Afterwards, the communication is resumed. This procedure is performed either by using buttons located on the haptic device or even by software switches within the operator interface. Figure 3.4 describes this technique.

Unfortunately, PCI becomes cumbersome since the operator needs to perform this action frequently to reach new regions of the teleoperator workspace. Besides, the disconnection of the communication between the haptic device and the telerobot causes a discontinuity of the robot motion. Furthermore, changing the scaling factor during motion introduces discontinuities in the command signals sent to the robot (see Figure 3.5-left). Thus, one concludes that PCI is more natural and easier to learn, but it is more fatiguing in case of indexing and generates discontinuous robot trajectories.

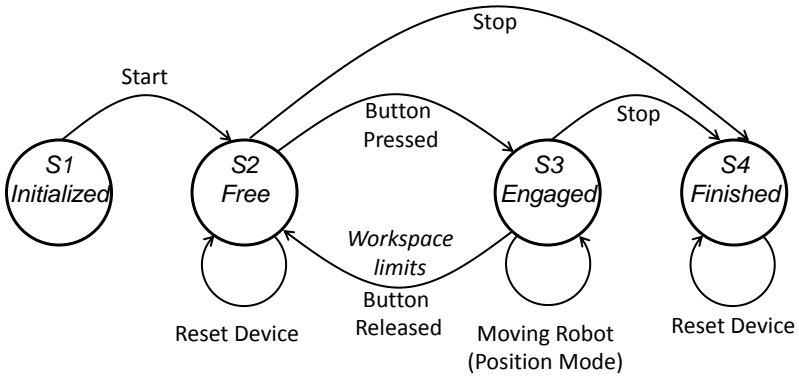


Figure 3.4: State-transition diagram of the PCI

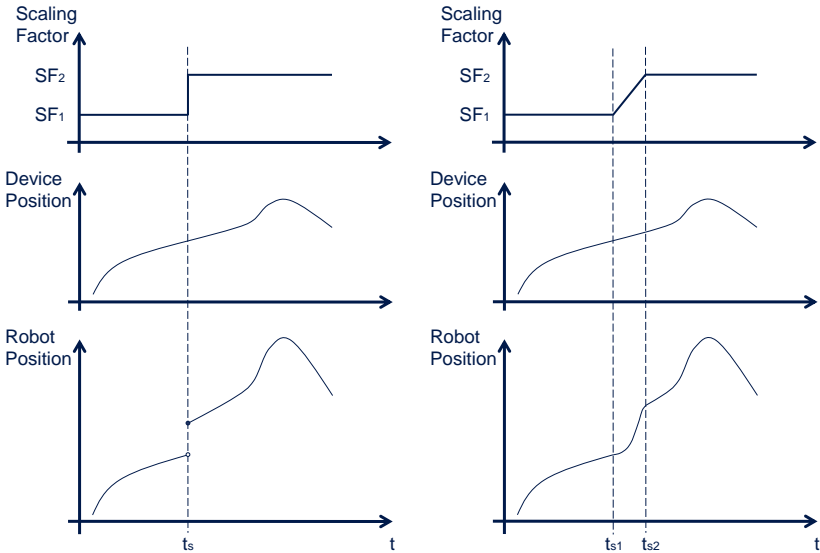


Figure 3.5: Discontinuity of robot trajectory because of switching between two scaling factors (left) and continuous robot trajectory in the case of LSF (right)

### Position Control with Linear Scaling Factor

Since the PCI is cumbersome and generates discontinuous robot trajectories, a position control with linear scaling factor (LSF) that allows the user to smoothly change the scaling factor (SF) during motion is here proposed. Hence, the discontinuity and inconsistency brought by PCI are avoided (see Figure 3.5). In addition, the loss of resolution problem, which the position control with large scaling factors suffers from, is solved by allowing the user to adapt the SF to the intended motion, i.e. for fine positioning the user reduces the SF and for gross motions he/she increases it.

Figure 3.6 describes the state transition diagram of this technique. After initializing the haptic device (S1) the robot and the haptic device are engaged and the position mode takes place (S2). When the user finds that the SF is not adequate for the intended motion, he/she linearly increases (S3) or decreases (S4) this SF by pressing dedicated buttons of the haptic device, respectively. Note that the SF in the state S2 is variable.

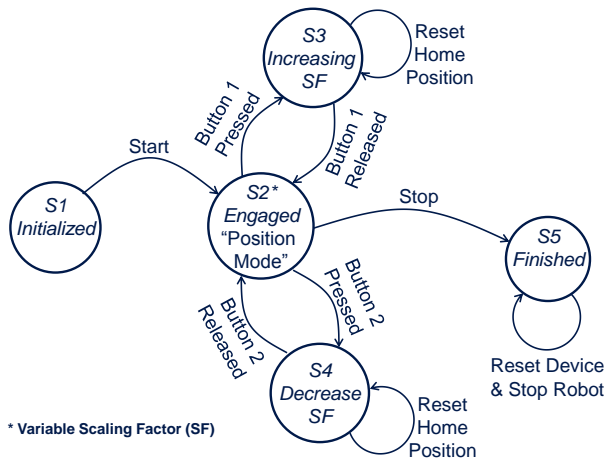


Figure 3.6: State-transition diagram of the position control with LSF

### 3.2.2 Rate Control

Using rate control (RC) the displacements of the haptic device are translated to velocity commands for the teleoperator. This means that the human operator can hold the handle at a specific position and the telerobot will keep moving

### 3 Mapping and Scaling Techniques

---

at constant speed based on the deflection of the haptic device. Both Figure 3.7 and Equation 3.4 describe this technique. Here,  $\mathbf{v}_r$  is the velocity of the telerobot within the target workspace ( $W_r$ ),  $\mathbf{p}_h$  is the position of the haptic device handle and  $\gamma$  is a velocity scaling factor.

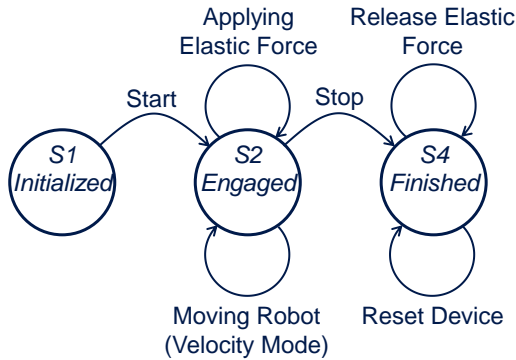


Figure 3.7: State-transition diagram of the RC with elastic force feedback

$$\mathbf{v}_r = \gamma \times \mathbf{p}_h \quad (3.4)$$

As mentioned in the previous chapter, the addition of an elastic force (spring force) will improve the RC (ZHAI 1995). Equation 3.5 shows the relationship between the elastic force  $\mathbf{f}_h$  and the position of the device  $\mathbf{p}_h$ . The constant  $k_f$  is the stiffness of the virtual spring.

$$\mathbf{f}_h = k_f \times \mathbf{p}_h \quad (3.5)$$

In comparison to the position control, rate control has both advantages and disadvantages. On the one hand, it compensates for the physical limitations of the haptic device by enabling an essentially infinite workspace. On the other hand, there is no direct kinematic correspondence between the haptic device and the robot, imposing a possibly higher cognitive load on the operator. Furthermore, this loss of kinematic correspondence produces an unnatural perception of the environment, unless the force derivative is fed back to the haptic device (PARKER ET AL. 1993).

### 3.2.3 Human Intention-based Control (HIBC)

Combining position and rate control modes is advantageous in cases when each of them separately does not guarantee successful execution of teleoperated tasks. A typical task of TPTA-systems might be to have the teleoperator grip an object, move it to a target position which is at distance from the initial position, and then position this object with high accuracy. Gripping and positioning the object requires precise manipulation with high resolution and, therefore, the position control is here pertinent. On the other hand, this high accuracy is not required in the case of transporting the object for a long distance. In this case, RC is more suitable to reduce the time needed to accomplish the task. However, changing alternately between the two modes entails a switching mechanism, which leads to a highly complicated control system. In order to decrease this complexity, human intention is used in this work to perform the switching from one mode to another automatically. There are two variants of this method: the **Single Zone with Intention-based Mode Selection** and the **Double Zones with Intention-based Scaling Factor**. The following sections describe these variants in detail.

#### 3.2.3.1 Single Zone

The idea behind this method is to estimate human intentions by observing the velocity with which he/she moves the haptic device in order to comfortably switch between two modes: the position control mode and the rate control mode. Figure 3.8 shows the block diagram of the proposed approach.

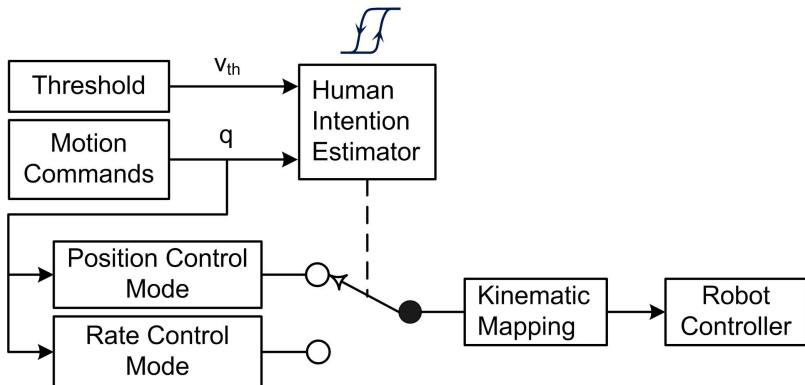


Figure 3.8: Block diagram of the single zone intention-based control

#### Intention Estimator

Several methods on the estimation of human intention are reported in the literature. For example, the floor reaction forces are used for estimating the walking intention by extracting the position of the center of gravity, which is shifted by humans to the side of the supporting leg before he/she starts swinging the other leg (SUZUKI ET AL. 2005). Another example of human intention estimation is proposed by DUCHAINE & GOSSELIN (2007), by which the measured velocity and force derivative are used to obtain whether the human operator wants to accelerate or decelerate. In this work, the velocity with which the human operator moves the haptic device is used to predict the human intention.

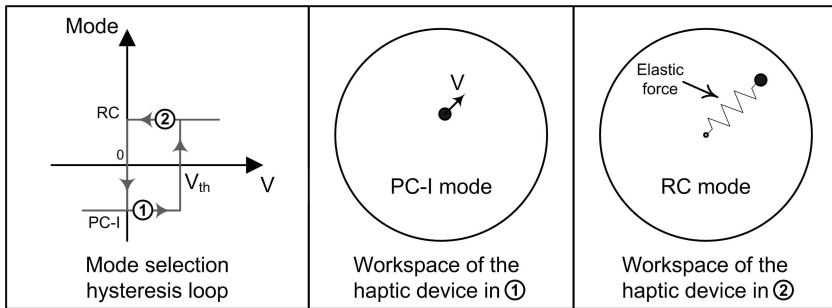


Figure 3.9: Illustration of the mode selection based on velocity values

As shown in Figure 3.9, when the velocity of the haptic device exceeds a certain threshold value ( $v_{th}$ ), this implies that the human operator intends to move faster to reach a target at a long distance and, therefore, the control mode will be changed from PCI to RC. This control mode incorporates an elastic force that assists the human operator to know the direction that he/she should move the haptic device to reduce the velocity. When the user comes closer to the target position, he/she will reduce his velocity toward zero, which implies that the operator wants to precisely position the teleoperator. At this moment, the control method will be changed from velocity mode back to position mode again. The following describes the logic of this control method

**if**  $Mode = PCI$  **and**  $V_{human} \geq V_{th}$  **then**  $Mode = RC$ ,  
**if**  $Mode = RC$  **and**  $V_{robot} \approx 0$  **then**  $Mode = PCI$ .

3.2.3.2 Double Zones

The control method described herein is closely related to the approach used in by HOLLIS & SALCUDEAN (1993). This is made up by dividing the haptic device workspace into an inner zone ( $W_{h1}$ ) designated for position control and an outer zone ( $W_{h2}$ ) designated for rate control as shown in Figure 3.10. As long as the operator keeps the device within  $W_{h1}$ , the robot is guided under position control and when the operator decides to apply rate control he moves the device into  $W_{h2}$ . Equation 3.6 and Figure 3.11 describe this technique.

$$\mathbf{p}_r = \alpha \times \mathbf{p}_h + \mathbf{p} \tag{3.6}$$

where

$$\dot{\mathbf{p}} = \begin{cases} \gamma \times \mathbf{p}_h & \text{if } \mathbf{p}_h \in W_{h2} \\ 0 & \text{if } \mathbf{p}_h \in W_{h1} \end{cases}$$

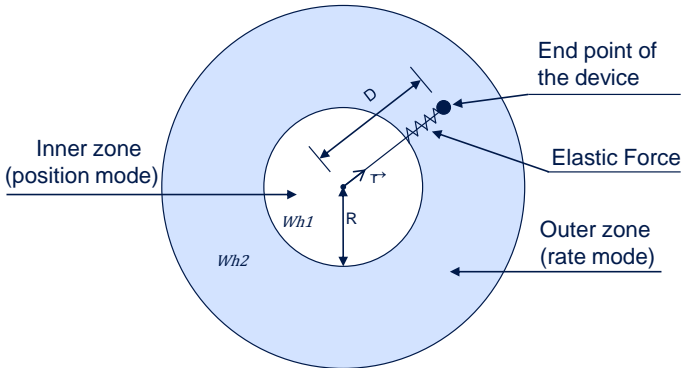


Figure 3.10: Double zones with intention-based scaling factor:  $R$  is the radius of the inner zone,  $D$  is the distance between haptic device handle and the center, and  $\vec{r}$  is the unit vector pointing outside the inner zone

In addition, the following assistance features are proposed and implemented to improve the intuitiveness of this method:

1. **Variable radius of the inner zone:** The user can change the radius of the inner zone using the dedicated switches available on the haptic device.

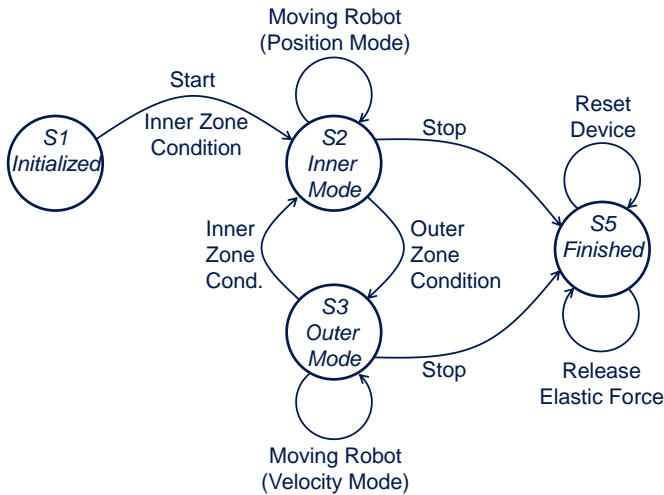


Figure 3.11: State-transition diagram of the double zones control method

One switch is used to increase the radius and the other is to reduce it. This is similar to the zoom in and out function in computer graphics software.

2. **Damping force and haptic grids in the inner zone:** The damping force is proportional to the measured velocity of the handle (velocity of the operator hand) and is used to limit the acceleration and, therefore, smoothen the motion commands sent to the teleoperator. Haptic grids (cf. Section 4.4.2) are also included as an option within this zone. This assists the human operator by snapping his/her hand to a predefined points on the grids.
3. **Adaptive Scaling based on user intention:** When the haptic device is moved within the inner zone, the controller examines whether it has been moved completely within a predefined small region for longer than a predetermined period of time. This implies that the operator is attempting to perform fine motions. The scaling factor is automatically adapted to allow the operator to perform the fine movements he/she intends to. The predetermined period of time can be manually configured and it should be long enough to identify the user's intention. This means that the scaling factor is a function of time, human velocity and the size of the manipulation region. The automatic adaption of the scaling factor reduces the mental effort of the operator and lets him/her concentrate only on the task.
4. **Elastic force in the outer zone:** This elastic force is proportional to the distance between the zones-boundary and the handle position and it is

used to inform the user about the entrance into the outer zone and to assist him/her bringing back the handle to the inner zone.

5. **Zones visualization:** This is done by visualizing the zones within the workspace of the haptic device and can provide a useful method to aid the user in mode selection. This makes the method more perceptible and increases the intuitiveness.

### 3.3 Conclusion

As discussed in chapter 2, the utilization of COTS components incorporates several challenges. In this chapter, the mapping technique used in the case of insufficient degrees of freedom of haptic devices is introduced. This can be performed by projecting the available degrees of freedom of the utilized haptic device onto a motion plane within the workspace of the teleoperator. Using the homogeneous transformation the motion commands on the motion plane can be transformed into motion commands in a stationary coordinate frame of the teleoperator. Nevertheless, the simultaneous control of all degrees of freedom of the telerobot is difficult in this case. It is, however, possible to successively control these degrees of freedom by moving the motion plane to different locations within the workspace of the teleoperator. Thus the motion plane is movable and the human operator can easily and comfortably decide the position and orientation of this plane.

The second aspect addressed in this chapter is the workspace scaling. Three workspace scaling techniques, namely position control, rate control and human intention-based control, are described in detail in this chapter. It is also noted that each method incorporates advantages and disadvantages, which are here summarized in Table 3.1.

After the theoretical and technical description of the mapping and scaling techniques introduced in this chapter, a comprehensive psychophysical experiment has been conducted to extensively evaluate these methods with regard to usability and various measures of task performance in a standardized robotics tracking task. This experiment and its results are introduced and discussed in chapter 6.

### 3 Mapping and Scaling Techniques

Method	Pros	Cons
Position control	<ul style="list-style-type: none"> <li>-Simple implementation</li> <li>-Understandable</li> <li>-Direct kinematic correspondence</li> </ul>	<ul style="list-style-type: none"> <li>-Poor spatial resolution in case of large scaling</li> <li>-PCI is cumbersome</li> <li>-PCI produces discontinues robot trajectory</li> <li>-With PC-LSF: high mental efforts of the operator</li> </ul>
Rate control	<ul style="list-style-type: none"> <li>-Simple implementation</li> <li>-Understandable</li> <li>-Theoretically infinite workspace</li> </ul>	<ul style="list-style-type: none"> <li>-No direct kinematic correspondence</li> <li>-High cognitive load on the operator</li> <li>-Unnatural feel of environment in case of force feedback</li> </ul>
Human intention-based control	<ul style="list-style-type: none"> <li>-No manual switching between modes</li> <li>-Lessen the cognitive load on the operator</li> <li>-Combine advantages of both position and rate control</li> </ul>	<ul style="list-style-type: none"> <li>-Complex implementation</li> <li>-Need for automatic switching mechanisms</li> </ul>

Table 3.1: Advantages and disadvantages of the implemented workspace scaling techniques

## 4 Haptic Feedback

*“Some classes of animals have all the senses, some only certain of them, others only one, the most indispensable, touch.”*

---

*Aristotle 350 B.C.*

Several studies suggested that haptic feedback enhances the immersive user experience, leading to improved task performance. This chapter deals with the provision of haptic feedback in a TPTA-system with heavy-duty teleoperator. Closing the control loop of the system by feeding back the interaction forces at the remote environment to the human operator would lead to stability problems, especially when a heavy-duty teleoperator is deployed. This challenge and several solutions are presented in this chapter.

### 4.1 The Nature of Haptic Feedback

Haptics refers to everything that concerns the human sense of touch, i.e. sensing and manipulating through touch. It entails both *tactility* and *kinesthesia*. Tactility means the tactile sensory perception via mechanical, thermal and pain-sensitive receptors in the different dermal layers of the skin (KERN 2009). It is responsible for sensing surface characteristics such as temperature and smoothness as well as detecting contact of the human body with its environment. Kinesthesia covers the proprioceptive sensory perception of the position and movements of the body and the forces acting on it (HANNAFORD & OKAMURA 2008). This perception is provided via different receptors located in the muscles, tendons and joints.

In terms of devices, haptic interfaces are manipulators that enable manual interactions with virtual environments or telerobotic systems, producing haptic impressions ranging from kinesthetic feeling (movements and forces) to tactile feeling (roughness, vibration and temperature). They are employed for tasks that are usually performed manually in the real world, such as manual exploration and manipulation of objects. In general, they receive action commands from humans and display appropriate haptic signals. To increase the degree of immersion, haptic interactions are usually accompanied by other modalities, namely visual and auditory feedback.

## 4 Haptic Feedback

In this work, the term haptics is limited to kinesthetic sensing, and therefore the utilized haptic devices are those which interact with the muscles and tendons to give humans a sensation of forces being applied on their hands. These forces can be either measured forces that arise between manipulated objects or a rendered virtual signals to facilitate a specific task.

An abstracted model of a TPTA-system is shown in Figure 4.1. In this model, the human operator and the haptic device are lumped into one block on one side, and the teleoperator and environment into another group on the other side. A communication link connects both groups and consists of two scaling factors: the position forward scaling factor<sup>1</sup> ( $\alpha$ ) and the force reflection scaling factor<sup>2</sup> ( $\beta$ ). Accordingly, the following equations govern the relationship between the master and slave sides:

$$x_s = \alpha x_m \quad (4.1)$$

$$f_m = \beta f_e \quad (4.2)$$

where  $x_m$  and  $x_s$  are positions of the haptic device (master) and the teleoperator (slave) respectively,  $f_m$  is the reflected force at the master side and  $f_e$  is the measured environmental force at the teleoperator side.

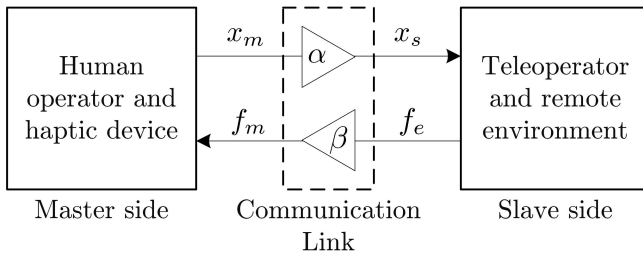


Figure 4.1: Abstracted model of TPTA-system

### 4.2 Direct Force Feedback

As mentioned in chapter 2, it has been found that feeding back the interaction forces that arise between a heavy-duty teleoperator and manipulated objects

<sup>1</sup>The scaling factor of the position commands from the haptic device to teleoperator

<sup>2</sup>The scaling factor of the forces fed back from the teleoperator to haptic device

directly to a small haptic device induces instability problems in TPTA-systems. In general, the contact process can be divided into two phases: *Impact* phase and *In-Contact* phase (DANIEL & MCAREE 1998) (SHULL & NIEMEYER 2008). During the impact phase, DANIEL & MCAREE (1998) stated that with perfect force feedback the impulse generated by the contact will be perfectly transmitted from the teleoperator to the haptic device, and the following equation is applied:

$$m_m \delta v_m = m_s \delta v_s \Rightarrow \delta v_m = \frac{m_s}{m_m} \delta v_s \quad (4.3)$$

where  $m_m$  and  $m_s$  are the effective inertia of the haptic device and the teleoperator, respectively, and  $\delta v_m$  and  $\delta v_s$  are the changes in velocities of haptic device and teleoperator, respectively, after impact.

This implies that for the case of heavy-duty teleoperators ( $m_s \gg m_m$ ), the resultant change in velocity of the small haptic device is very large, i.e. right after the moment of collision the haptic device will recoil violently and the human operator will not be able to bring the teleoperator in contact with the environment. This is determined by the mass ratio of the teleoperator and the haptic device  $\frac{m_m}{m_s}$  (DANIEL & MCAREE (1998), SHULL & NIEMEYER (2008)). Thus, the forces fed back to the haptic device should be attenuated by a factor equal to  $\frac{m_m}{m_s}$  in order to stabilize the system and allow bringing the teleoperator in contact with the environment (see Figure 4.2).

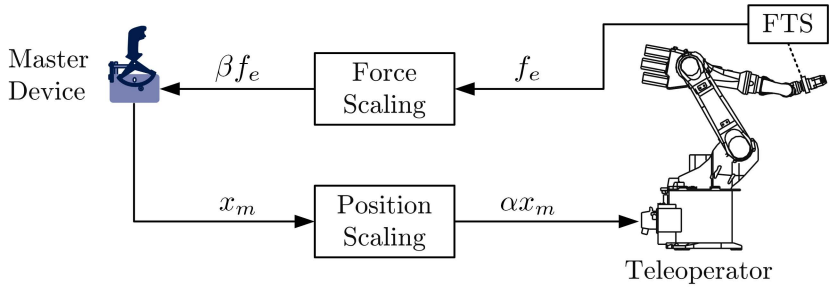


Figure 4.2: Direct force feedback

The second phase is the in-contact one, which starts after the teleoperator gets in contact with the environment and continues to be in contact with it. To study the effect of the scaling factors on system stability during this phase, the two blocks of the system shown in Figure 4.1 can be modeled as mass-damper-spring system with lumped parameter equivalents (cf. Figure 4.3). Following the analysis procedure detailed by DANIEL & MCAREE (1998), the critical value of

## 4 Haptic Feedback

the product of scaling factors that maintains the system stability is given by the following equation<sup>3</sup>

$$(\alpha\beta)_c = \frac{Num_1}{Den_1} + \frac{Num_2}{Den_2} \quad (4.4)$$

with

$$\begin{aligned} Num_1 &= m_s(b_s b_m^3 - 2k_m b_s b_m m_m) + 2k_s b_s b_m m_m^2 + b_m^2 b_s^2 m_m \\ Num_2 &= m_m m_s (2b_m^3 k_s b_s + 2b_m^2 k_m b_s^2 - 4k_m b_s b_m m_m k_s) + \\ & 2k_m^2 b_s b_m m_s^2 m_m + 2k_s^2 b_s b_m m_m^3 + \\ & m_m^2 (2k_s b_s^2 b_m^2 + 2k_m b_s^3 b_m) \\ Den_1 &= k_s (b_m^2 m_s^2 + 2b_s b_m m_m m_s + b_s^2 m_m^2) \\ Den_2 &= k_s (b_m^2 m_s^2 + 2b_s b_m m_m m_s + b_s^2 m_m^2) \times \\ & [k_m (m_m b_s^2 + m_s (m_s k_m - 2m_m k_s + b_m b_s)) + \\ & k_s (m_s b_m^2 + m_m (m_m k_s + b_m b_s))]^{0.5} \end{aligned}$$

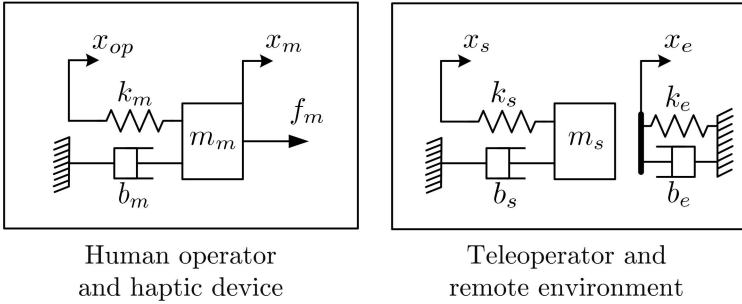


Figure 4.3: Mass-damper-spring model of the TPTA-system:  $m_m$ ,  $b_m$  and  $k_m$  are the lumped mass, damping and stiffness of the haptic device and the human hand, respectively,  $m_s$ ,  $b_s$  and  $k_s$  are the mass, damping and stiffness of the teleoperator, respectively, and  $k_e$  is the environment stiffness.

To find this critical value for the developed TPTA-system<sup>4</sup>, the parameters listed in Table 4.1 were experimentally identified. Substituting these parameters to Equations 4.4 gives the critical value  $(\alpha\beta)_c = 3.8\%$ . That is, the developed TPTA-

<sup>3</sup>As the equation is very long, it is divided into two fractions to make it readable. *Num* stands for numerator and *Den* stands for denominator

<sup>4</sup>The system structure is described in detail in Chapter 5

system is marginally stable if the product of scaling factors is equal to 0.038. This implies that an intensive downscaling is needed to guarantee the system stability, e.g. for a unity position forward scaling factor the forces should be scaled down by a factor less than 0.038.

	Parameter	Value	Unit
Haptic device	$m_m$	0.034287	kg
	$b_m$	22.778	Ns/m
	$k_m$	39.57	N/m
Teleoperator	$m_s$	0.71	kg
	$b_s$	16,094	Ns/m
	$k_s$	624,750	N/m

Table 4.1: TPTA-system parameters

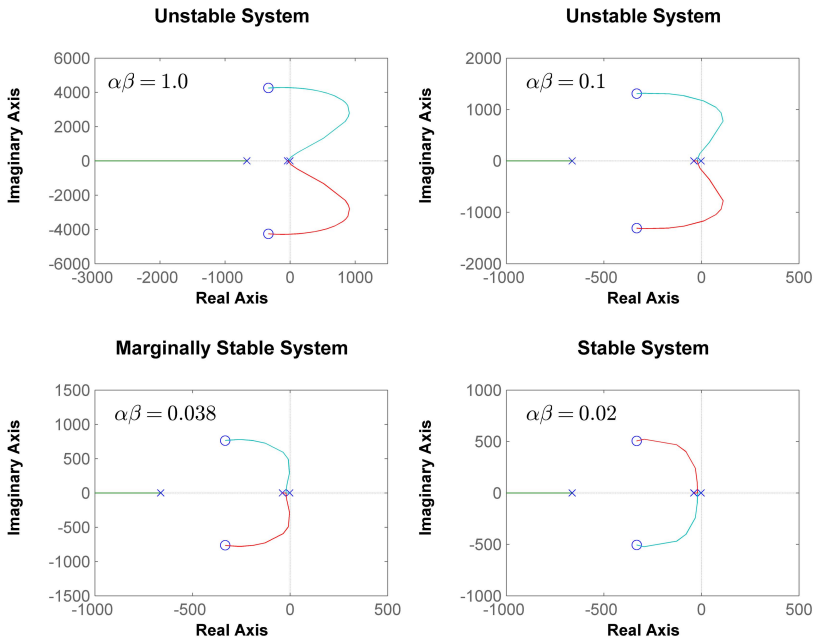


Figure 4.4: Root Locus of the TPTA-system with different scaling factors

The root locus of the developed TPTA-system with different scaling factors

## 4 Haptic Feedback

is shown in Figure 4.4. Obviously, the system is conditionally stable, i.e. the system can be stable for a range of environmental stiffness. For instance, a unity product of scaling factors (see Figure 4.4:Top-left) makes the system theoretically unstable if the stiffness of the environment lies within the range  $1.35 \times 10^4$  to  $4.5 \times 10^8$  N/m. These stability conditions have been empirically proven. Table 4.2 shows the experimentally determined stability of the developed TPTA-system. Furthermore, Figure 4.5 shows an unstable motion of the teleoperator with  $\alpha = 4$  and  $\beta = 0.01$ .

Scaling factors	Stable (imperceptible FF)	Marginally stable	Unstable			
$\alpha$	0.5	1.5	2.0	2.5	3.0	4.0
$\beta$	0.01	0.01	0.01	0.01	0.01	0.01
$\alpha\beta$	0.005	0.015	0.02	0.025	0.03	0.04

Table 4.2: Experimentally determined stability of our TPTA-system

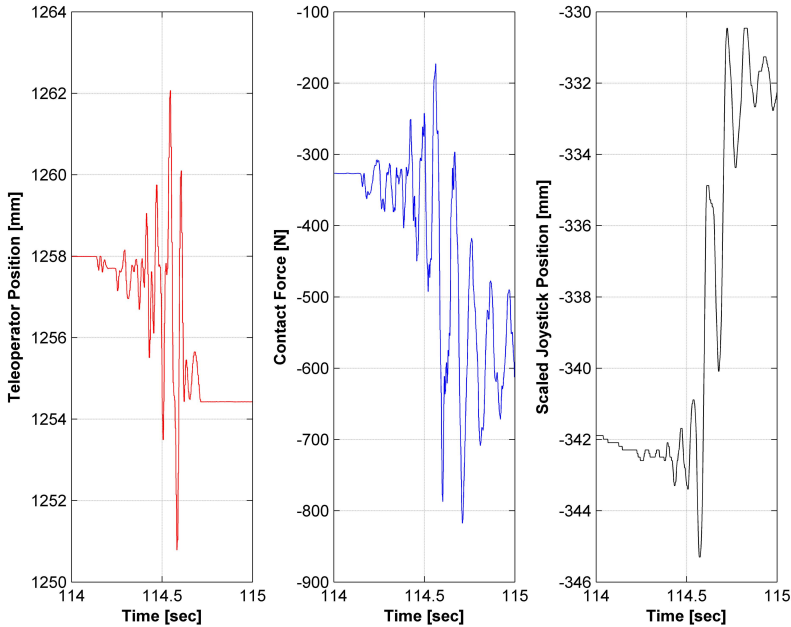


Figure 4.5: Unstable teleoperator motion with product of scaling factors  $\alpha\beta = 0.04$

Nevertheless, the maximum scaling factors that can be applied depend essentially on the stiffness of the environment, i.e. the softer the material of the manipulated objects, the higher the scaling factor that can be applied. Figure 4.6 shows theoretically the relation between the maximum scaling factors and the environmental stiffness.

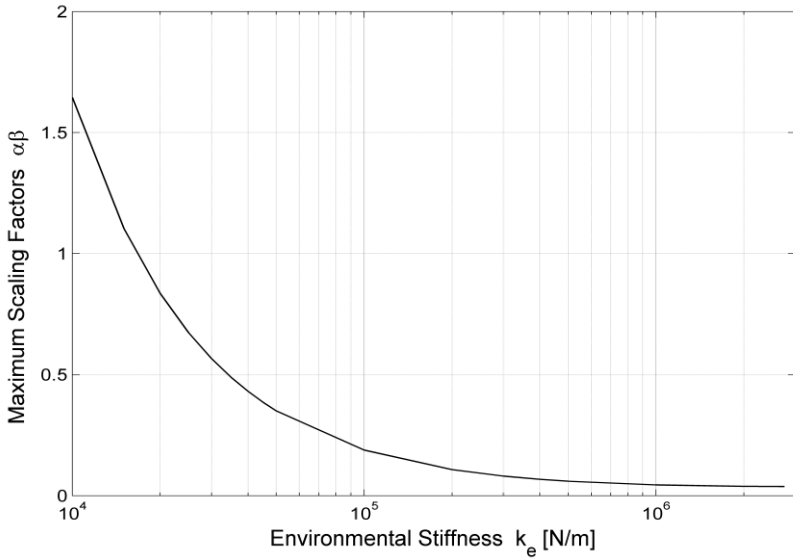


Figure 4.6: Relation between environmental stiffness  $k_e$  and scaling factors  $\alpha\beta$

### Stability/Transparency Dilemma

The most critical issue in TPTA-systems is to ensure stable and safe HRI with a high rendering performance. This is a challenge when taking into account serious issues, such as unknown and variable human dynamics, nonlinear characteristics of common environments (VUKOBRATOVIC ET AL. 2009), as well as many disturbances in the communication link such as time delay and packet-loss (CLARKE 2006). Previous works exhaustively explained why the pursuit of stability compromises transparency once the teleoperator comes in contact with the environment (LAWRENCE 1993)(YOKOKOHI & YOSHIKAWA 1994)(DANIEL & MCAREE 1998). As mentioned before, the excessive downscaling of the feedback forces will maintain the stability of the TPTA-systems with heavy-duty teleoperators. However, the human operator will consequently perceive a distorted feeling of the environment, e.g. if the teleoperator is in contact with a very

stiff environment the human operator will perceive a *sponge-like* contact. This might negatively affect the performance of the system and result in increasing the time needed to accomplish the given tasks. Moreover, as the human operator thinks that he/she brings the teleoperator in contact with a soft material, he/she would ignore the weak force feedback and try to move the robot further. This may damage the material and/or the teleoperator, resulting in degrading the quality of products. This is the opposite of what is actually intended by having haptic feedback in TPTA-systems, as several studies have suggested that force feedback can have the effect of enhancing task performance and reducing the pressure forces applied on objects by teleoperators (WAGNER ET AL. (2007) and RADI ET AL. (2010a), among others). To cope with this challenge an approach advocating utilization of model-based force feedback is proposed in the following section.

### 4.3 Model-based Force Feedback

As the force feedback is used in TPTA-systems to increase the immersion of the human operator into the remote environment and also to convey information about the interaction between the teleoperator and its environment, the model-based force feedback (MbFF) can be classified according to the information that should be delivered to the human operator:

1. **Vibration-based force feedback:** is used to inform the human operator about the contact state (*contact* and *no-contact*) without information about the material which the teleoperator is in contact with. This is suitable for some tasks such as pick-and-place tasks or for virtual walls.
2. **Impedance-based force feedback:** is used to give the human operator not only the state of the contact, but also information about it (e.g. the stiffness of the material which the teleoperator in contact with). This is suitable for tasks in which the characteristics of the material plays a role in quality of the task performance. Typical tasks include assembly tasks and surface operation tasks such as deburring and polishing.

To realize the MbFF approach, the following components are required. Their interaction together is depicted in Figure 4.7.

#### Event Extractor

The event extractor is responsible for extracting the contact events that occur at the moment when the teleoperator touches parts in its environment. The output of the event extractor is a trigger signal that is mainly used to enable the model-based force feedback. FTS or proximity sensors can be utilized to detect contact events. In some environments, such as radioactive environments, it is not

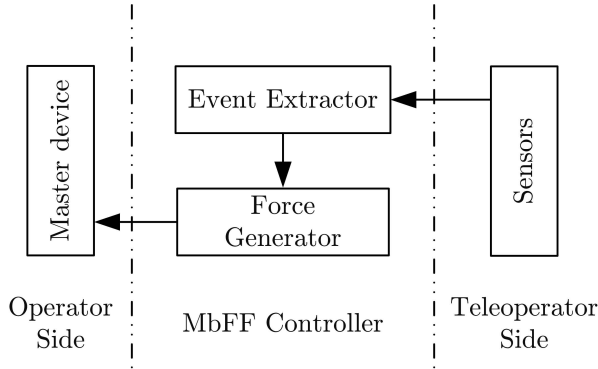


Figure 4.7: Model-based force feedback

feasible to have sensors on the teleoperator sides. Detecting the contact events in this case can be either indirect, such as measuring the motor currents of the teleoperator, or estimated using prior knowledge about the remote environment. The second case is also suitable for industrial environments where the positions of manipulated objects and teleoperator are mostly known in advance.

### Force Generator

This is a generic block which denotes the source of the model-based force signals. It is responsible for producing a force signal based on the type of the force feedback. For example, the generated force feedback could be a vibration signal (vibration-based force feedback) or a continuous signal (impedance-based force feedback). The type is defined before the operation starts, but it could also be varied during run-time.

#### 4.3.1 Vibration-based Force Feedback (VbFF)

Using this type of force feedback, the human operator is provided with vibration signal instead of a continuous one. This signal is generated and applied to the joystick at the moment of contact. Thus the real contact forces between the teleoperator and the manipulated objects do not show up directly as a force, but in a modified form which nevertheless provides information about the contact events on the teleoperator side. Equation 4.5 shows the signal produced using this type of haptic feedback. The amplitude value  $A$  and the frequency  $f$  can be changed according to the task and user preference. Figure 4.8 shows the system configuration in this case.

$$F_{vib} = A \cdot \sin(2\pi ft) \quad (4.5)$$

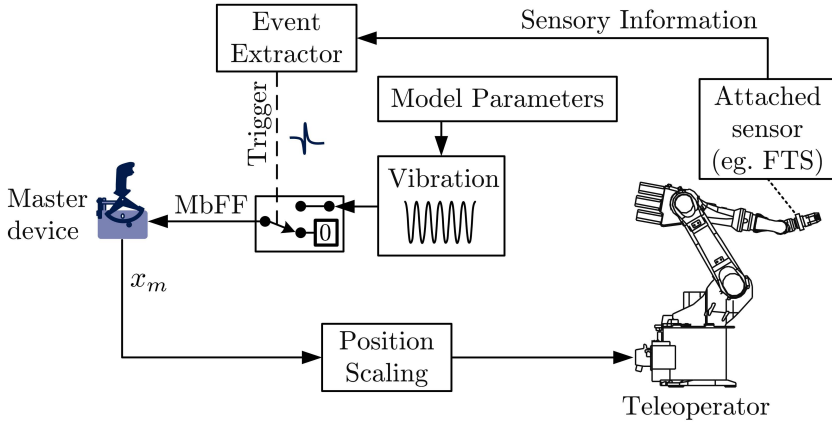


Figure 4.8: Vibration-based force feedback

### 4.3.2 Impedance-based Force Feedback (IbFF)

Instead of feeding back the measured forces from the remote teleoperator to the haptic input device, the forces will be computed in this approach by using a simple virtual environment model located at the operator side. When a contact event arises, the model is triggered by discrete event triggers. The following is a description of the components that comprise the IbFF system (cf. Figure 4.9).

#### Environment Model

Several environment models representing stiff and soft environments can be found in the literature. Apart from a few objects, most of the parts to be manipulated in industrial environments are mechanically very stiff. Therefore, a simple model<sup>5</sup> is used to represent viscoelastic environments in this work (see Figure 4.10). This model is only valid if the following general assumptions are fulfilled:

1. The robot is stiff enough and encounters no compliance.

<sup>5</sup>a mechanical equivalent of *Kelvin-Voigt* model

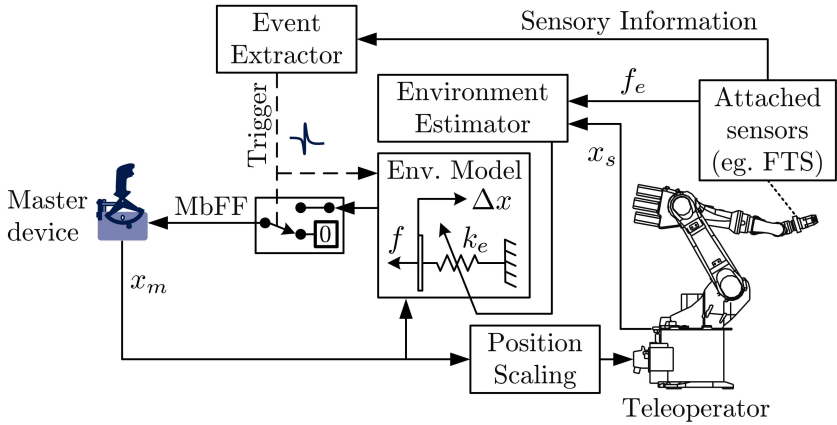


Figure 4.9: Impedance-based force feedback

2. The environment is passive.
3. The contact surface is smooth<sup>6</sup>.

The equation that governs the relationship between the contact force and the teleoperator motion is given by:

$$\hat{f}_e = \begin{cases} \hat{k}_e \Delta x + \hat{b}_e v & \text{if } \Delta x \geq 0 \\ 0 & \text{if } \Delta x < 0 \end{cases} \quad (4.6)$$

where

$\hat{f}_e$  is the calculated contact force,  $\Delta x$  is the distance or the penetration of the robot's tool in the environment material,  $v$  is the velocity that the teleoperator moves with in the environment material after contact, and  $\hat{k}_e$  and  $\hat{b}_e$  are the stiffness and damping of the virtual environment, respectively.

If the robot's tool does not move in or penetrate into the stiff environment, the viscous damper can be set to zero in this model, and thus the resultant model will consist of a pure virtual spring<sup>7</sup> as shown in Figure 4.10-right. Because the teleoperator/environment stiffnesses are usually much higher than that of the human/haptic device (KIM 1992), the value of the virtual spring is set at the

<sup>6</sup>The friction effect can be also included in the model.

<sup>7</sup>first-order stiffness control law



Figure 4.10: Schematic representation of a viscoelastic environment (left) and a pure elastic environment (right)

beginning to a very high value in order to not underestimate the environment stiffness.

### Event Extractor

Impedance-based force feedback is an event-triggered model, i.e. the output calculated force will be displayed to the haptic device only if a trigger signal is generated by the event extractor component, otherwise zero force is displayed on the haptic device.

### Environment Estimator

As mentioned before, the stiffness of the virtual spring is set at the beginning of the task to a very high value. This value can be adapted after bringing the teleoperator in contact with the environment. The environment estimator component receives the position and force signals directly after the contact event and identifies the stiffness of the environment. The stiffness of the virtual spring is then changed gradually to match the identified value. However, if the identified value is close to the previous applied value, then no changes will be made.

## 4.4 Haptic Assistance Functions

Haptic feedback in TPTA-systems is not only used to convey information about the interaction between the teleoperator and the manipulated objects, but also to provide assistance to the human operator during task execution. Several assistance functions can be found in the literature. In this work, two kinds of assistance function are developed, namely the haptic virtual walls and haptic grids.

#### 4.4.1 Haptic Virtual Walls

Virtual walls are usually used by robot manufacturers as virtual fences for safety reasons to prevent the robots entering particular regions. However, these virtual walls are usually position-based and in the case of guiding a robot by a control panel they can be only perceived visually by the operator. The haptic virtual walls (HVW) are used in this context to haptically convey information to human operators about the teleoperator surrounding environment. They can be either implemented as haptic path follower (HPF) or as forbidden region borders (FRB) (cf. Figure 4.11). The HPF is used as a guiding tool when the target position and the path to be followed by the operator are previously known. This forces the operator to follow a specific path while guiding the robot to the target position, and therefore reduces the risk of collision with other parts in the environment. Using the second type, the FRB, a particular region within the teleoperator environment can be surrounded and will haptically prevent the operator entering this region. Therefore, unintended collisions with other devices or machines can be avoided.

The HVW tool is not to be confused with the local model-based haptic feedback which is mentioned in the previous section. In the case of HVW there is no physical contact between the manipulated objects and the environment. To assure that this HVW function will be accepted by the human operator and will not disturb him, abrupt force cues should be avoided. This means that the forces generated by the HVW model should be gradually and gently displayed to the human operator.

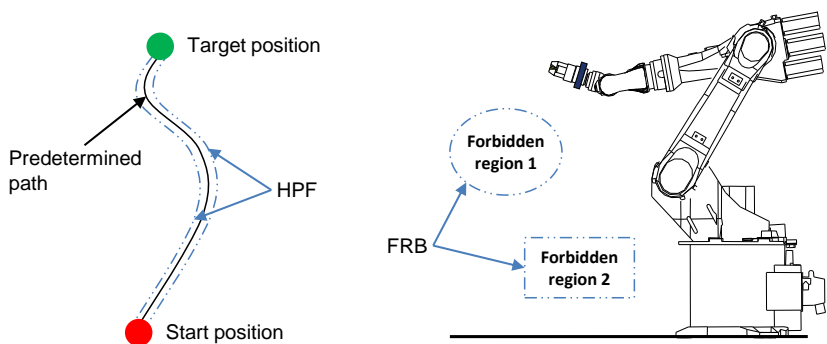


Figure 4.11: Haptic virtual walls: the haptic path follower (left) and forbidden region borders (right)

### 4.4.2 Haptic Grids

Geometric grids are a widely used tool in drawing software such as CAD-systems, by which the mouse pointer is restricted to equally spaced points. This feature can be considered as a visual clue which aids the user in placing a selected object in a specific location. A haptic grid utilizes the same concept as the visual grid, but the haptic device in this case snaps to predefined grid points by means of force feedback. Grid points in this respect behave as a magnetic field pulling the haptic device to them and away from the other points in their immediate neighborhood (see Figure 4.12). This is similar to an array of gravity wells located uniformly in space. The parameters affecting the grid are (REINHART ET AL. 2008):

1. **Grid Spacing:** the distance between two consecutive grid points,
2. **Gravity Well Radius:** how far away from a grid center the pulling force begins to appear on the device, and
3. **Pulling Force:** how the strength of the force on the haptic device is directly determined by the stiffness and damping properties of the well.

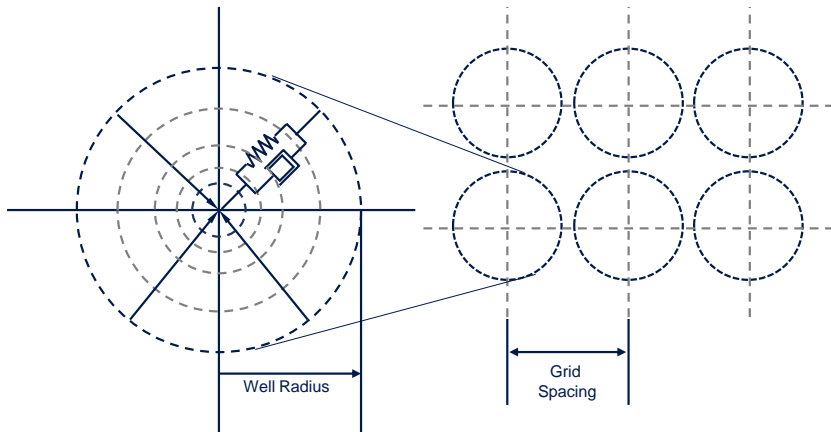


Figure 4.12: Haptic grid

Using this feature allows the human operator to accurately move the robot across predefined equally spaced points. The spacing between two points can be changed either manually or automatically based on the adaptive scaling factor (cf. section 3.2.3.2), i.e. the longer the operator tries to position the robot, the smaller the grid spacing. Although the haptic grid assists the user to move the

robot precisely within a discrete workspace, the user can disable this feature when a smooth motion is desired. The decision of using haptic grids depends entirely on the task to be performed.

### 4.5 Conclusion

The provision of haptic feedback in TPTA-system enhances the immersive user experience, leading to improved task performance. However, closing the control loop of the system by feeding back the interaction forces between the teleoperator and manipulated objects to the human operator leads to stability problems, especially when a heavy-duty teleoperator is deployed. Scaling down the interaction forces before displaying them to the human operator can solve the stability problem. This, nevertheless, reduces the transparency of the system.

In this chapter, different methods and approaches to utilize haptic feedback in an industrial robotic system have been presented. Instead of downscaling and feeding back the measured interaction forces to the operator side, model-based haptic feedback is used to overcome the stability problem. Two kinds of this model are introduced in this chapter. The first one is the vibration-based force feedback, by which a vibration signal is applied to the human operator to inform him about the contact state of the teleoperator. The second type is the impedance-based force feedback, by which a continuous force signal is generated based on the mechanical impedance of the interaction between the teleoperator and the environment. Features and advantages of the developed impedance-based force feedback are:

1. Simple environment model (e.g. spring model)
2. Online adjustment of stiffness value of the environment model
3. Measured force as event trigger (event extraction)
4. No force scaling needed
5. Better stability and performance

Not only are the interaction forces between the teleoperator and the manipulated objects used for haptic feedback, but also haptic assistance functions such as virtual walls and haptic grid are deployed to increase the intuitiveness and the performance of the task.



## 5 Experimental Setup

*“All our dreams can come true, if we have the courage to pursue them.”*

---

*Walt Disney*

### 5.1 Introduction

After describing the methods to overcome the two challenges faced during the deployment of TPTA-technology in an industrial setup, namely the **workspace scaling** and the **haptic feedback**, this Chapter introduces the developed system which will be used to validate and evaluate the developed techniques. Before starting with the technical details, it is imperative to highlight the design requirements of such system. These requirements can be divided into three categories as follows:

#### General requirements:

1. **Simplicity and ergonomics** - the design of the TPTA-system should be simple and cost effective while maintaining the quality at high level. In addition, the human ergonomic factors should be considered in order to avoid fatiguing during task execution.
2. **Compliance with safety** - as humans will be involved in TPTA-systems, several technical standards, that are explicitly and implicitly for the purpose of ensuring safety of humans during implementation and task execution, should be maintained (RADI & REINHART 2009). For this purpose, the generated force feedback is limited by a software limiter, ensuring that the maximum force applied on the human hand by the haptic device is inadequate to injure the human operator. Furthermore, strategies to guarantee the safety of the robot and objects within the robot’s environment should be addressed.
3. **Utilization of standard COTS components** - in general, this increases the flexibility and reliability of the designed system according to the advantages mentioned in section 2.5.

4. **Flexibility and extensibility** - the system architecture should be independent of any restrictions dictated by components manufacturers in order to allow the integration of the designed techniques into any robotics system which has the minimum technical requirements and settings.

### Requirements with regard to mapping and scaling:

1. **Haptic device with small workspace** - This is crucial to test and evaluate the developed techniques aimed at solving the problem of traversing a large robot's workspace with a small haptic device.
2. **Deficiency in the number of degrees of freedom** - the haptic input device should not have the same number of DOF of the robot in order to validate the kinematic mapping strategy described in section 3.1.
3. **Industrial robot with large workspace** - the teleoperator should be an industrial robot with a relatively large workspace. In addition, robot with high accuracy is of advantage to enable comparing different control strategies (e.g. position and rate control) in the trajectory tracking experiments.

### Requirements with regard to haptic feedback:

1. **Display of high stiffness** - the haptic device should be able to display high stiffnesses as the objects and environments to be manipulated are usually stiff.
2. **High bandwidth communication channel** - this is mandatory to allow a stable direct haptic feedback. In the context of the model-based force feedback, this allows faster environment identification as the position signals from the robot will be available at high frequency.
3. **High stiffness industrial robot** - a compliance in the industrial robot structure can be thought by the model-based force feedback as a compliance of the environment. Therefore, a high stiff industrial robot is to be utilized.

## 5.2 System Architecture

To meet the requirements identified in the previous section a TPTA-system consisting of the elements shown in Figure 5.1 has been developed. The system is divided into three parts: operator side, teleoperator side and central controller.

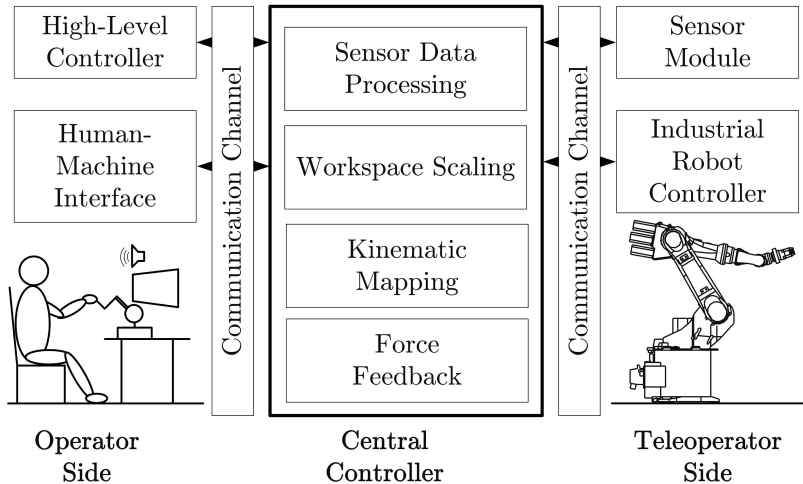


Figure 5.1: The developed TPTA-system architecture

### 5.2.1 Operator Side

Two modules constitute the operator side: the **human-machine interface** and the **high-level controller**. HMI is responsible for receiving the human motion commands and displaying the multimodal feedback information, i.e. visual, auditory, and haptic information. This includes the haptic device, the visual feedback display and audio speakers or headphones.

The **high-level controller** allows the human operator to enter and adjust the parameters of the control methods. For instance, the velocity threshold value used in the human intention-based control can be adapted through this module.

### 5.2.2 Teleoperator Side

At the teleoperator side a **sensor module** has been developed for acquiring information about the remote environment at run-time. This includes a camera system and a FTS. The camera system consists of two cameras that give a complete view of the teleoperator and its environment via a live video stream. A pan-tilt camera presents an overview of the whole remote scene, while another camera mounted at the robot with the optical axis parallel to the z-axis of the flange coordinate gives a close-up image of the objects to be manipulated. The FTS is mounted directly at the robot's flange and in a way that the coordinates of the last robot's axis are congruent to the coordinates of the sensor.

## 5 Experimental Setup

---

The second module at this side is the **industrial robot controller** which is responsible for executing the motion commands. In this system, a KRC2 controller from KUKA Roboter GmbH<sup>1</sup> is deployed and it has a vendor-specific real-time interface (cf. section 5.2.5.2) to connect it to any external computer-based system.

### 5.2.3 Central Controller

This is the core of the developed TPTA-system and it consists of several modules as seen in Figure 5.1. These modules are implemented on a real-time platform (see section 5.2.4.3). The **sensor data processing** module is responsible for dealing with direct sensor data and features derived from those sensors, e.g. filtering the force signals and magnifying, focusing and filtering the camera signals.

Techniques for the DOF mapping and workspace scaling are implemented within two modules, the **kinematic mapping** and **workspace scaling**. The last module of the central controller is the **force feedback** which generates the force feedback signals according to the selected mode (direct or model-based force feedback).

### 5.2.4 Hardware Components

In the following we give an overview about the hardware components utilized in this work. This consists of haptic devices, the teleoperator and the real-time platform.

#### 5.2.4.1 Haptic Input Devices

The haptic interface integrated into the system is the Impulse Engine (IE2000) from Immersion Corp.<sup>2</sup> (see Figure 5.2). This has been selected because it is a two DOF joystick, which is easier for the human operator to control and produce coordinated motions (as mentioned in section 2.5.1). The original interface card of the IE2000 provided by the manufacturer has a driver for Microsoft-Windows platforms. As the developed TPTA-system is designed on a real-time platform (cf. section 5.2.4.3), there are two possibilities to integrate this joystick into the system. The first one is to stick to the manufacturer specific interface card and connect the MS-Windows computer to the real-time platform through a server/client Ethernet communication link. This, however, has a drawback as

---

<sup>1</sup><http://www.kuka-robotics.com>

<sup>2</sup><http://www.immersion.com>

the purpose for which MS-Windows was developed does not guarantee the time restrictions needed for real-time computation, though the computer running it might be a state-of-the-art. Hence using MS-Windows to process input signals and calculate respective output signals would introduce a huge time delay into the system. Moreover, the Ethernet link itself poses additional communication time delay in the system.

As the developed system is a time-critical one, especially in the case of haptic feedback, and the focus of this work is not on the time delay problem, it was decided to go for the second option by replacing the interface card with another input-output (I/O) card which is compatible with the real-time platform. The card Sensoray Model 626 from Sensoray<sup>3</sup> is selected to connect the joystick directly to the real-time platform. The interface between the joystick and this card is described in section 5.2.5.2.

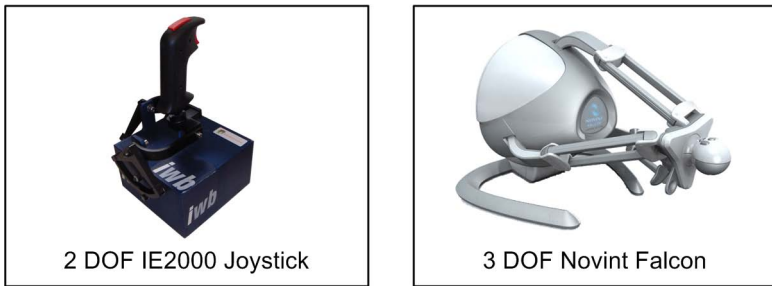


*Figure 5.2: Haptic input devices utilized in this work*

Another haptic input device incorporated into the developed system is the three DOF **Novint Falcon**<sup>4</sup> force feedback controller (see Figure 5.2). This device is, however, used for transportation tasks and not for tasks with haptic feedback, even though it has this feature. This is because a driver of the device has not been developed for the real-time platform yet. Hence a server/client Ethernet communication link (cf. section 5.2.5.2) is established between the real-time platform and the computer to which the Falcon is connected.

The specifications of the two utilized haptic devices are listed in Table 5.1.

<sup>3</sup><http://www.sensoray.com>

<sup>4</sup><http://www.novint.com>

## 5 Experimental Setup

---

	IE2000	Novint Falcon
DOF no.	2	3
Workspace [mm]	152.4 x 152.4	102 x 102 x 102
Position resolution [mm]	0.02	0.064
Maximum force [N]	8.9	9.0

Table 5.1: Technical specifications of the deployed haptic input devices

### 5.2.4.2 Industrial Robot

Since the company KUKA Roboter GmbH has developed a novel (for the time being) real-time robot interface to external systems, the robot KR 100 HA (High Accuracy) has been selected as a teleoperator in this work (see Figure 5.3). It is a six DOF articulated industrial robot with a nominal payload of 100 Kg at maximum TCP (Tool-Center-Point) velocity. With its special gear units and high mechanical stiffness, this robot provides a high positioning accuracy. It has a point repeatability of  $\pm 0.05$  mm and a linear path repeatability of  $\pm 0.2$  mm. It is provided with an optional arm extension of 400 mm which allows the robot to reach positions of up to 3000 mm.

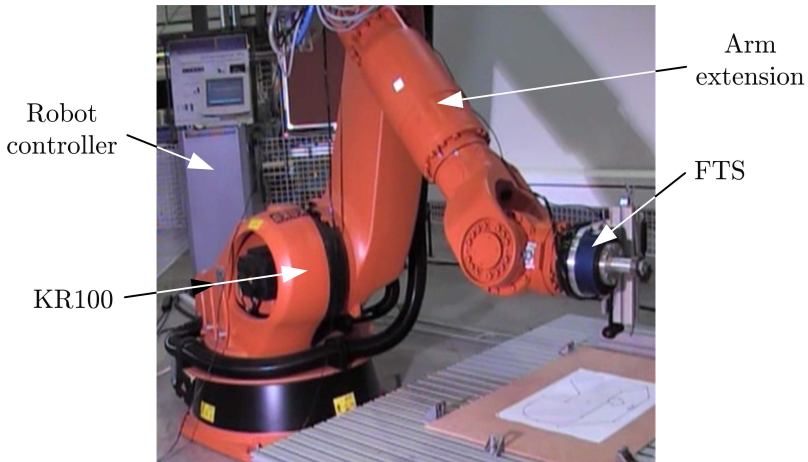


Figure 5.3: The industrial robot KR100-HA is used as a teleoperator in our TPTA-system

The JR3<sup>5</sup> 160M50A3 is a six DOF force-torque sensor which is used in our setup because it is a very stiff sensor, allowing it to be incorporated into the system with minimal degradation of positioning accuracy. The high stiffness also results in a high resonant frequency, providing fast response to rapid force changes. The sensor is 160 mm in diameter and 50 mm in thickness. Due to the bolt pattern (L60s) on top and bottom of the sensor there is no need for an additional mechanical adapter. Hence the FTS can simply be mounted between the robot's flange and the tool. The sensor has a built-in EEPROM which includes calibration data and RS485 serial driver. The sensor includes also a 16-bit analog-to-digital (A/D) converter.

### 5.2.4.3 Real-Time Platform (RT-Platform)

In this work, the developed TPTA-system is built using the concept of Hardware-in-the-Loop simulation (HIL), which allows for rapid prototyping and testing of control systems, while minimizing initial investment costs. For the real-time HIL solution in this work, RT-LAB<sup>TM</sup> from Opal-RT<sup>6</sup> has been selected as it is designed upon state-of-the art commercial-off-the-shelf (COTS) components such as the popular simulation tool **MATLAB/Simulink**<sup>®</sup> and the real-time operating system (RTOS) **QNX**<sup>®</sup> **Neutrino**<sup>®</sup>.

Based on the RT-LAB<sup>TM</sup> solution, the hardware configuration of the RT-platform consists of **Command Station** (CS) communicating with the **Target Node** (TN) through Ethernet communication link, **I/O** boards interfaced to the haptic device and the FTS mounted on the robot, and an **Ethernet card** interfaced to the remote sensor interface (RSI) of the industrial robot controller (see Figure 5.4). The CS serves as a user interface to build, edit and modify **MATLAB/Simulink**<sup>®</sup> control models, to generate and compile C code corresponding to the developed models, to send and execute the model onto the TN running the RTOS, and to change and adapt the control parameters in run-time. The TN performs the real-time execution of the developed control algorithms and also real-time communication interfaces between the TN and other components in the system, e.g. the haptic device and the industrial robot. The models of all control algorithms are designed and implemented in **MATLAB/Simulink**<sup>®</sup> from Mathworks Inc.<sup>7</sup>.

---

<sup>5</sup><http://www.jr3.com>

<sup>6</sup><http://www.opal-rt.com/>

<sup>7</sup><http://www.mathworks.com/products/simulink/>

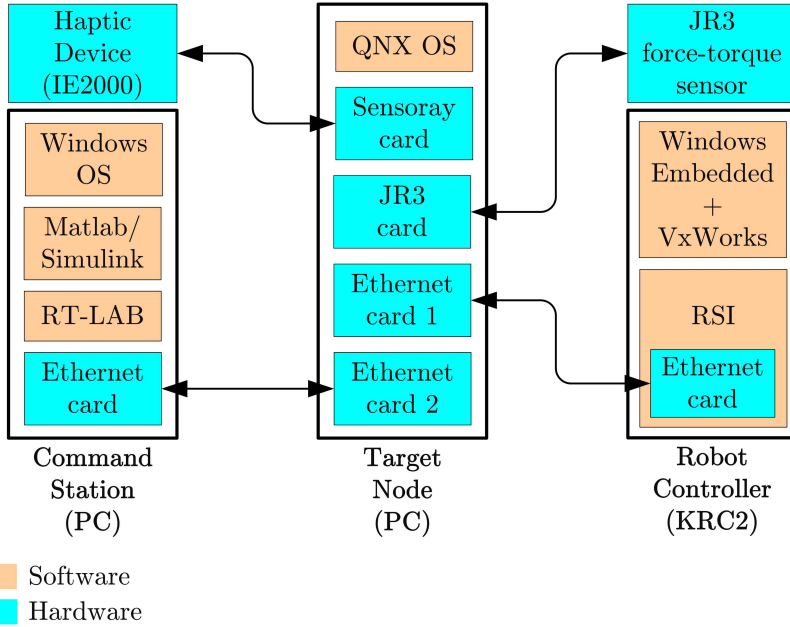


Figure 5.4: The hardware and software configuration of the RT-platform

### 5.2.5 Communication Channels

As shown in Figure 5.5, the communication links in our system can be divided into two categories, development-time communication link and run-time communication links.

#### 5.2.5.1 Development-Time Communication Link

The development-time communication link is responsible for transferring the compiled C code of the developed MATLAB/Simulink<sup>®</sup> models from the CS to the real-time TN. After getting the developed models compiled and transferred to the TN, this communication link becomes part of the run-time communication links, but it is used only for monitoring and run-time adapting of control parameters.

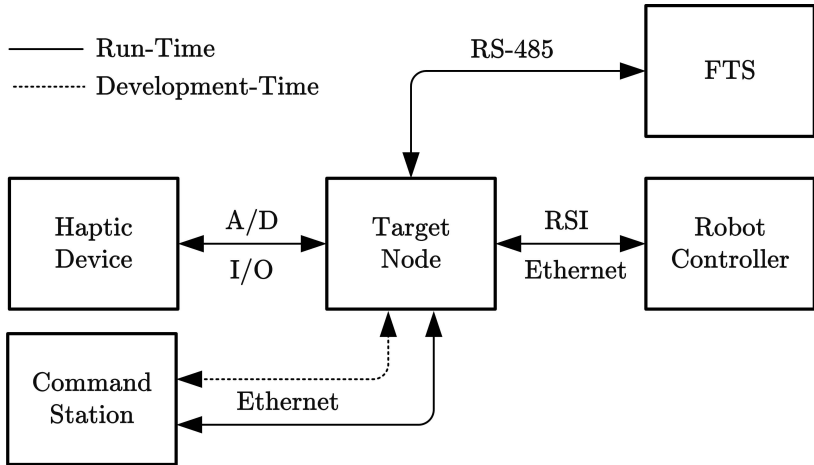


Figure 5.5: Communication channels

### 5.2.5.2 Run-Time Communication Links

The run-time communication links are used to send and receive signals between all system members during operation. A server/client architecture is used, so the RT-platform represents the server and all other components are clients. These links are presented in the following in more details.

#### Remote Sensor Interface

The Ethernet-based Remote Sensor Interface (RSI) is used to connect the industrial robot with the central controller running on the TN. The exchanged data is transmitted via the Ethernet TCP/IP (Transmission Control Protocol) as XML (Extensible Markup Language) strings. The cyclical data transmission rate is on the interpolation cycle of 4 milliseconds. This allows a direct intervention in the trajectory planning of the industrial robot during motion in real-time. Any delay during the transmission period terminates the connection between the robot and the TN.

#### Ethernet Link for the Falcon

This link is used only when the haptic device **Novint Falcon** is selected. Since the RT-platform is the server in this system, the computer to which the haptic device Falcon is connected acts as a client. By avoiding the overhead of checking whether every packet actually arrived makes UDP/IP (User Datagram Protocol) faster and more efficient than e.g. TCP/IP protocol. Therefore, it is decided upon a UDP/IP protocol to establish the connection between the Falcon and

RT-platform, because dropped packets are preferable to delayed packets which introduce a destabilizing effect in the control loop. Nevertheless, the communication link poses time delay to the system and thus it is decided to use the system with the Falcon only for transportation tasks (without haptic feedback). For tasks require haptic feedback the haptic joystick IE2000 from Immersion is selected.

### Data Acquisition and I/O Interfaces

A data acquisition interface (DAQ interface) is used for the connection between the FTS and the RT-platform. This is realized though a dedicated data acquisition card (DAQ card) from the same manufacturer of the FTS. A two Megabit per second serial data stream containing the complete six axis data (three forces and three torques) flows between the sensor and the card at a rate of 8kHz. The communication protocol for information exchange is EIA-485, also known as RS-485.

An analog-digital I/O interface is used to connect the haptic joystick **IE2000** to the RT-platform and it is realized using the I/O card from Sensoray (Model 626), as mentioned in section 5.2.4.1. This connection is established through three different connectors: encoder connector, D/A connector, digital I/O connector. The encoder connector is used for the two incremental encoders of the joystick (one encoder for each DOF of the joystick). The two DC motors used in the joystick to display the force feedback to the human operator are connected to the system through the D/A connector. The DC motors accept 0 to 5Volts, with 0V corresponding to  $-10\text{N}$  and 5V corresponding to  $+10\text{N}$  at the end point of the joystick's handle. The last connector, the digital I/O connector, is used to connect the two available buttons of the joystick.

### 5.3 Conclusion

In this chapter, it has been shown that COTS components can be principally used to build an industrial TPTA-system. Although the deployed devices have novel interfaces, considerable efforts have been spent in this work to connect all components together. This would be more efficient and easier if these interfaces were standardized. Therefore, we leave this as a recommendation for components manufacturers.

The overall developed TPTA-system with its hardware components and communication links is shown in Figure 5.6. Only one haptic device is engaged to the system at a time, with enabled force feedback feature only in the case of the joystick IE2000 from Immersion Corp.

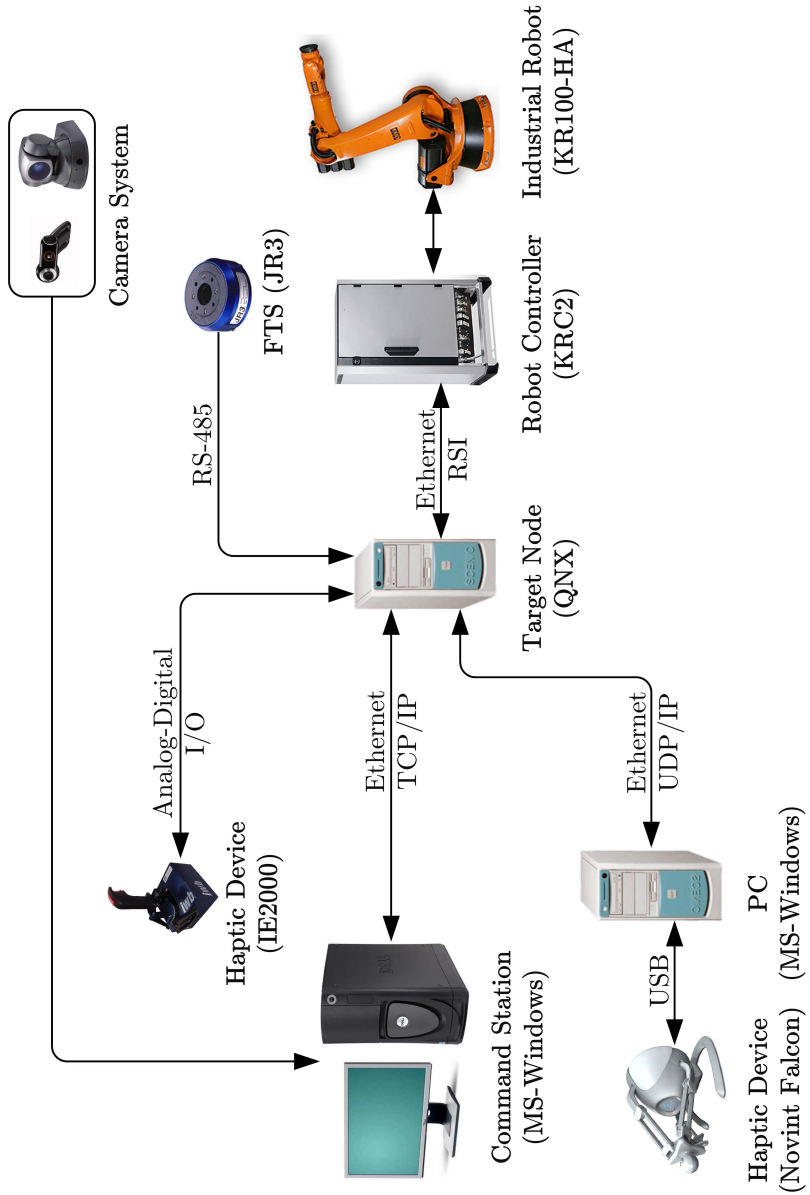


Figure 5.6: Overall TPTA-system with its hardware components and communication links



## 6 Experimental Evaluation

*“One of the great mistakes is to judge policies and programs by their intentions rather than their results.”*

---

*Milton Friedman*

### 6.1 Introduction

After describing the implementation of the control strategies used to cope with the two main challenges in the previous chapters, rigorous evaluation studies should be carried out to quantify the performance of each strategy against others during the execution of real tasks. In this chapter, two main psychophysical studies are introduced. These studies were conducted in the laboratory of the Institute for Machine Tools and Industrial Management (*iwb*) of Technische Universität München, jointly with the Human Factors Institute (IfA) of Universität der Bundeswehr München. The first study evaluates the scaling techniques described in chapter 3 while the second study investigated whether the model-based force feedback, which is described in chapter 4, can provide the benefits of having direct force feedback. For both studies, pilot experiments are conducted to test the control strategies and to determine the optimal parameters to be used during the user experiments. This is considered as the starting point for our evaluation studies.

### 6.2 User Studies

The tasks for the experiments were chosen based on real manufacturing processes, which users perform during handling and machining processes. The task of the first experiment was to precisely track a standardized trajectory. Hence the teleoperator motion is unconstrained, i.e. the robot is maneuvered in free space. This is relevant to the object’s transportation phase in assembly tasks.

A surface finishing task was chosen for the second experiment. This task involves teleoperator motion under geometrical constraints. Typically, such a task

requires the teleoperator to exert a certain amount of pressure onto an object during sliding across the surface of that object.

### 6.2.1 Participants

Thirty male and four female participants (mean age = 26.4 years, SD = 3.19 years) took part in both experiments. Although four participants stated that they are left-handed, all participants used their right hand to operate a computer mouse and intuitively grasped the joystick with their right hand. Seven participants stated to have no prior experience in the use of a joystick (novice), 16 further participants had experience of 1-70 hours over their lifetime (beginner), whereas 11 participants had experience of more than 70 hours of joystick operation (expert). Overall, participants had an average joystick experience of 154 hrs./lifetime.

### 6.2.2 Experiment A: Trajectory Tracking with Different Control Methods

#### 6.2.2.1 Task Definition and Requirements

The aim of this experiment is to evaluate three control methods, namely position control with indexing, rate control and human intention-based control, for a teleoperated system with regard to speed, position accuracy and usability. Furthermore, it is also of interest how the trajectory shape and size influence the performance of the control method used for trajectory tracking tasks. Thus, the experimental task was to track a standardized trajectory (EN ISO 9283:1998) as closely as possible from a predefined starting point to a particular end position. This trajectory is shown in Figure 6.1 and it consists of a two-dimensional route with segments that differ in shape and size. The  $400\text{mm} \times 400\text{mm}$  variant of this trajectory is selected.

#### 6.2.2.2 Experimental Design

A repeated measures within-subject design was used with control method as independent variable, which was manipulated on three levels (position control with indexing (PCI), rate control (RC), and human intention-based control (HIBC)). The order in which the three control types were tested was systematically varied for each participant, as well as the starting position (P10 or P35) (see Figure 6.1). Participants were seated in a sound attenuated room to shield them from disturbances.

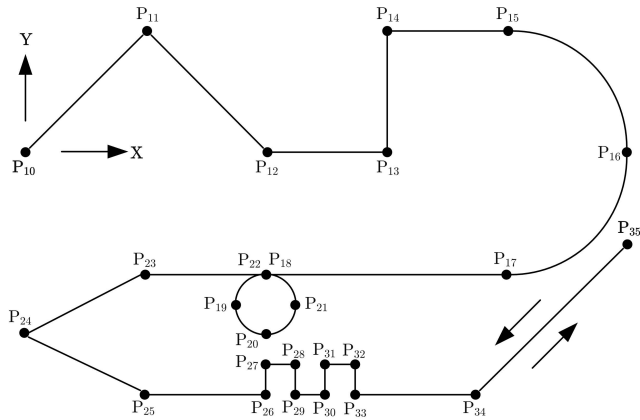


Figure 6.1: Schmidt trajectory used in the first experiment

The following performance measures were considered:

- **Task Completion Time (TCT):** the time the human operator takes to complete the entire trajectory, as well as pre-selected, individual trajectory segments.
- **Overall position deviation:** the area between the desired trajectory and the trajectory performed by users is used for accuracy comparisons.
- **Maximum position deviation:** The maximum position deviation from the desired trajectory is derived to compare the accuracy of the three control methods.
- **Usability:** based on a questionnaire, users rate the usability of the control method.

### 6.2.2.3 Hypothesis

The following null hypothesis is proposed for this experiment

- $H_0$ : There is no difference between the three control strategies during tracking trajectory segments, which differ in shapes and sizes.

## 6 Experimental Evaluation

---

### 6.2.2.4 Procedure

Using standardized instructions, participants were told to track the given trajectory as accurately and as quickly as possible (Figure 6.2). Before each trial, they were given the opportunity to familiarize themselves with the control, the task and the trajectory. After each trial, they were instructed to complete the usability questionnaire. Participants gave informed consent prior to the experiment and they were fully debriefed afterwards.

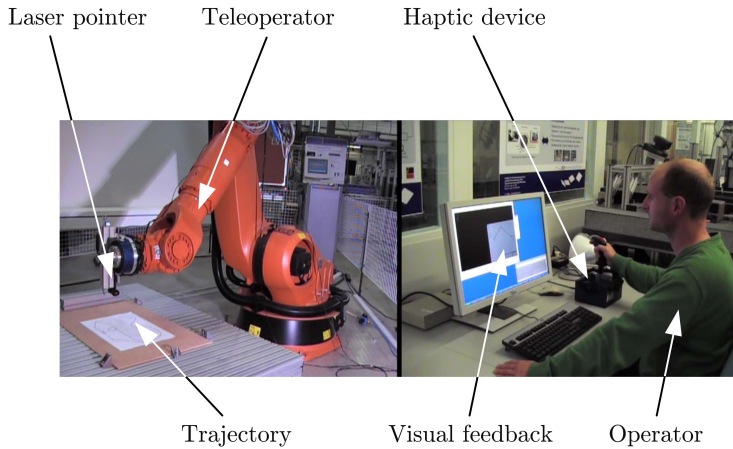


Figure 6.2: The system configuration for experiment A

### 6.2.2.5 Data Analysis and Results

The data were screened for outliers and data with  $z$ -scores of  $z > \pm 3.29$  ( $N = 17$ ) were removed from the data set and replaced with variable group means. Based on the central limit theorem, the data were assumed to be normally distributed. Assumptions of parametric data have been met. Therefore, parametric tests have been applied for further data analysis.

Different segments with different shapes and sizes have been extracted from the Schmidt trajectory and they were separately evaluated. Separate repeated-measures analyses of variance (ANOVA) have been applied with control method as independent variable and position deviation as well as task completion time for each tracking segment as dependent variables. For each of these analyses, it was investigated, whether the direction in which each segment was tracked had a significant influence on time or accuracy. Unless specifically stated, analyses

determined that the direction had no significant influence at the significance acceptance level  $p < .05$ . Furthermore, the influence of joystick experience on performance measures was examined. Unless specifically stated, analyses indicated that joystick experience did not change the effects of control method on the task performance measures for any of the investigated tracking segments. The following are the results obtained for different interesting segments as well as the overall trajectory as whole.

### Curve Segment

For the curve segment between P<sub>15</sub> and P<sub>17</sub> (cf. Figure 6.1), the assumption of sphericity<sup>1</sup> was violated. Therefore, the  $F$ -values were adjusted using the Greenhouse-Geisser correction,  $\epsilon = .74$ . After correction, there was a significant main effect of the method of control on TCT,  $F(1.48, 47.48) = 22.41, p < .001$ . T-test statistics for post-hoc pairwise comparisons were conducted<sup>2</sup>. As shown in Table 6.1, participants performed the task with HIbC ( $M = 15.42\text{sec.}, SD = 5.84\text{sec.}$ ) significantly faster than with PCI ( $M = 20.25\text{sec.}, SD = 7.76\text{sec.}$ ), which showed the slowest TCT. With RC, the task performance was the fastest ( $M = 14.27\text{sec.}, SD = 4.87\text{sec.}$ ), which was significantly faster than the performance with PCI, but not with HIbC. There was also a significant main effect of the

Pair	Dependent t-test <sup>a</sup>	Effect strength
PCI vs. RC	$t(33) = 5.24, p < .001$	$r = .67$
RC vs. HIbC	$t(33) = -1.79, p = .08$	-
PCI vs. HIbC	$t(33) = 4.89, p < .001$	$r = .65$

<sup>a</sup>accepted  $\alpha$ -level is  $< .017$

Table 6.1: Pairwise comparisons of TCT for the curve segment

control method on the overall position deviation (accuracy),  $F(2, 64) = 4.02, p < .05$ . As shown in Table 6.2 and Figure 6.3, t-statistics for pairwise comparisons showed that trials with PCI produced the smallest position deviations from the desired curve segment ( $M = 312.50\text{mm}^2, SD = 160.00\text{mm}^2$ ), which were significantly smaller than those performed with HIbC ( $M = 391.53\text{mm}^2, SD = 168.49\text{mm}^2$ ), but not to those with RC ( $M = 365.97\text{mm}^2, SD = 188.90\text{mm}^2$ ). Furthermore, the difference in mean position deviations between HIbC and RC was not significant.

<sup>1</sup>Homogeneity of variance

<sup>2</sup>As three T-test comparisons are conducted, the Bonferroni correction should be applied. Therefore, the Bonferroni-adjusted significance level for this multiple comparisons is  $p < .017$

## 6 Experimental Evaluation

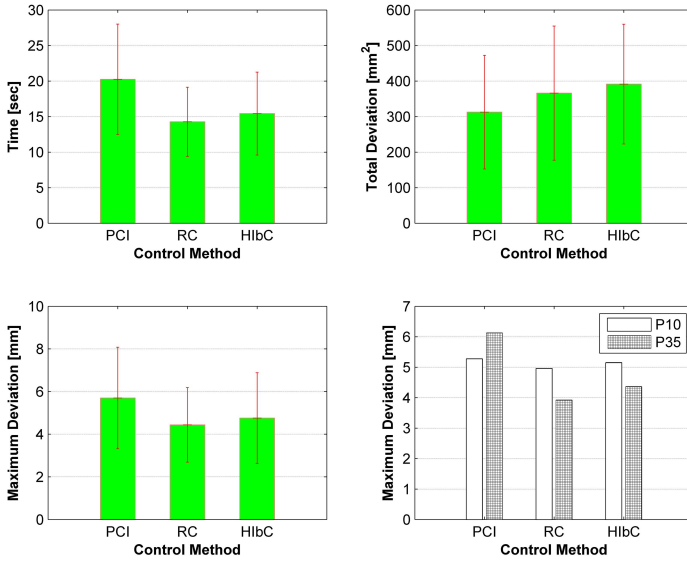


Figure 6.3: Mean values of TCT, overall and maximum deviations for the curve

Pair	Dependent t-test <sup>a</sup>	Effect strength
PCI vs. RC	$t(33) = -1.77, p = .09$	-
RC vs. Hlbc	$t(33) = -0.84, p = .41$	-
PCI vs. Hlbc	$t(33) = -3.28, p < .01$	$r = .50$

<sup>a</sup>accepted  $\alpha$ -level is  $<.017$

Table 6.2: Pairwise comparisons of overall position deviations for the curve

In addition, a significant main effect of control method on maximum deviation was also reported,  $F(2, 64) = 5.91, p < .01$ . Trials with PCI ( $M = 6.13mm, SD = 2.61mm$ ) showed the largest deviations, while using RC ( $M = 3.91mm, SD = 1.16mm$ ) led to the smallest maximum position deviations. Furthermore, there was a significant interaction effect between the control method and the tracking direction,  $F(2, 64) = 3.62, p < .05$ . This indicates that the differences in maximum position deviations were significant only for the group starting the task at P<sub>35</sub>. Further investigations showed that trials with PCI led to maximum deviation significantly larger than RC trials. The difference in maximum position deviations between Hlbc ( $M = 4.36mm, SD = 2.33mm$ ) and RC was not significant. Table 6.3 and Figure 6.3 summarize these results.

Direction	Pair	Dependent t-test <sup>a</sup>	Effect strength
P10-P35	PCI vs. RC	$t(16) = 0.76, p = .46$	-
	RC vs. HIbC	$t(16) = -0.49, p = .63$	-
	PCI vs. HIbC	$t(16) = 0.29, p = .78$	-
P35-P10	PCI vs. RC	$t(16) = 3.41, p < .01$	$r = .65$
	RC vs. HIbC	$t(16) = -0.86, p = .40$	-
	PCI vs. HIbC	$t(16) = 2.38, p = .03$	-

<sup>a</sup>accepted  $\alpha$ -level is  $<.017$

Table 6.3: Pairwise comparisons of maximum position deviations (mm) for the curve

### Circle Segment

The second segment was the circle found between P<sub>18</sub> and P<sub>22</sub>. There was a significant main effect of control method on task completion time,  $F(2, 64) = 20.16, p < .001$ . Pairwise t-statistics comparisons indicated that trials with HIbC were the slowest ( $M = 13.78\text{sec.}, SD = 5.18\text{sec.}$ ) (see Figure 6.4). Participants performed faster with PCI ( $M = 12.19\text{sec.}, SD = 4.25\text{sec.}$ ). However, the difference in TCT between trials with PCI and those with HIbC just scraped past the significance level of  $p < .017$ . Using the control method RC, the task performance was significantly faster ( $M = 10.06\text{sec.}, SD = 3.51\text{sec.}$ ) than those conducted with HIbC and PCI (see Table 6.4 and Figure 6.4).

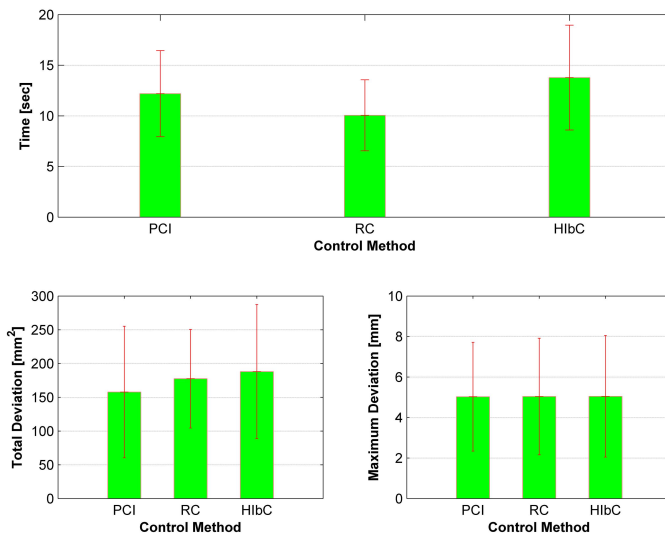


Figure 6.4: Mean values of TCT, overall and maximum position deviations for the circle

## 6 Experimental Evaluation

Pair	Dependent t-test <sup>a</sup>	Effect strength
PCI vs. RC	$t(33) = 4.60, p < .001$	$r = .63$
RC vs. HlbC	$t(33) = -5.91, p < .001$	$r = .72$
PCI vs. HlbC	$t(33) = -2.50, p = .018$	-

<sup>a</sup>accepted  $\alpha$ -level is  $< .017$

Table 6.4: Pairwise comparisons of TCT for the circle segment

Regarding tracking accuracy, there was neither a significant main effect of control method on overall deviation,  $F(2, 64) = 1.39, p = .27$ , nor on the maximum deviations,  $F(2, 64) = 0.00, p = 1.00$ . Nevertheless, trials with PCI produced less overall deviation than the other two control methods do (see Figure 6.4).

### Line Segment

There was a significant main effect of control method on TCT for tracking the straight line segment between P<sub>17</sub> and P<sub>18</sub>,  $F(2, 64) = 6.15, p < .01$ . As shown in Table 6.5, t-statistics indicated that trials with PCI ( $M = 6.92sec., SD = 2.64sec.$ ) were performed slower than those with HlbC ( $M = 5.95sec., SD = 1.36sec.$ ) (see Figure 6.5). However, the differences were insignificant. Furthermore, trials with RC ( $M = 5.62sec., SD = 1.27sec.$ ) were significantly faster than those conducted with PCI, but not significant to those with HlbC.

Pair	Dependent t-test <sup>a</sup>	Effect strength
PCI vs. RC	$t(33) = 3.03, p < .01$	$r = .47$
RC vs. HlbC	$t(33) = -1.21, p = .24$	-
HlbC vs. PCI	$t(33) = -2.50, p = .018$	-

<sup>a</sup>accepted  $\alpha$ -level is  $< .017$

Table 6.5: T-statistics pairwise comparisons of TCT for the line segment

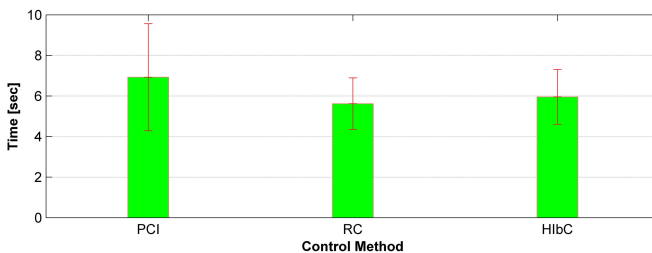


Figure 6.5: TCT mean values of different control strategies for tracking the line segment

There was also a significant main effect of the control method on the overall deviation,  $F(2, 64) = 5.26, p < .01$ . The differences in the mean overall position deviations between trials with PCI ( $M = 122.03\text{mm}^2, SD = 75.34\text{mm}^2$ ) and RC ( $M = 80.03\text{mm}^2, SD = 62.17\text{mm}^2$ ) were significant, while between PCI and HIbC ( $M = 83.97\text{mm}^2, SD = 61.77\text{mm}^2$ ) just failed to reach the significant level (see Table 6.6 and Figure 6.6-left). Furthermore, there was no significant difference in overall position deviations between RC and HIbC.

Pair	Dependent t-test <sup>a</sup>	Effect strength
PCI vs. RC	$t(33) = 3.33, p < .01$	$r = .50$
RC vs. HIbC	$t(33) = -0.28, p = .78$	-
PCI vs. HIbC	$t(33) = 2.47, p = .019$	-

<sup>a</sup>accepted  $\alpha$ -level is  $<.017$

Table 6.6: Pairwise comparisons of overall position deviations for the line segment

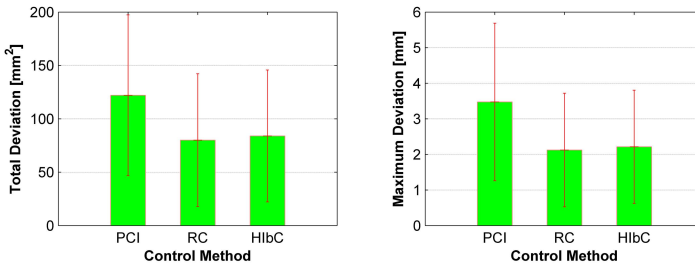


Figure 6.6: Mean values of the overall and maximum position deviations of the line segment

There was also a significant effect of the control method on the maximum position deviations during tracking the straight line segment,  $F(2, 64) = 7.46, p < .01$ . Post-hoc comparisons showed that trials with PCI produced the largest maximum deviations ( $M = 3.47\text{mm}, SD = 2.21\text{mm}$ ), which were significantly larger than those found with RC ( $M = 2.12\text{mm}, SD = 1.60\text{mm}$ ) and with HIbC ( $M = 2.21\text{mm}, SD = 1.59\text{mm}$ ). For this segment, there was no significant difference in maximum position deviations between trials with RC and those with HIbC (see Table 6.7 and Figure 6.6-right).

## 6 Experimental Evaluation

Pair	Dependent t-test <sup>a</sup>	Effect strength
PCI vs. RC	$t(33) = 3.57, p < .01$	$r = .53$
RC vs. HIbC	$t(33) = -0.26, p = .80$	-
PCI vs. HIbC	$t(33) = 2.82, p < .01$	$r = .44$

<sup>a</sup>accepted  $\alpha$ -level is  $<.017$

Table 6.7: Pairwise comparisons of maximum deviations for the line segment

### Slope Segment

There was a significant main effect of control method on TCT for the slope segment between  $P_{34}$  and  $P_{35}$ ,  $F(2, 64) = 4.39, p < .05$ . As shown in Table 6.8, t-statistics reported no significant differences between the control methods at  $p < .017$  when they were pairwise compared. However, trials with PCI ( $M = 8.24\text{sec.}, SD = 3.73\text{sec.}$ ) were on average slower than those with RC ( $M = 6.98\text{sec.}, SD = 1.89\text{sec.}$ ), while HIbC produced the shortest TCT ( $M = 6.96\text{sec.}, SD = 2.75\text{sec.}$ ) (see Figure 6.7).

Pair	Dependent t-test <sup>a</sup>	Effect strength
PCI vs. RC	$t(33) = 2.35, p = .03$	-
RC vs. HIbC	$t(33) = 0.07, p = .95$	-
PCI vs. HIbC	$t(33) = 2.41, p = .02$	-

<sup>a</sup>accepted  $\alpha$ -level is  $<.017$

Table 6.8: Pairwise comparisons of TCT for the slope segment

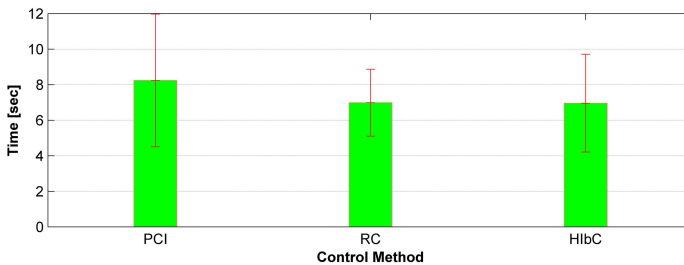


Figure 6.7: Mean values of TCT for the slope segment

There was also a significant main effect of the control method on the overall position deviation,  $F(2, 64) = 3.27, p < .05$ . T-statistics for pairwise comparisons

showed no significant differences at  $p < .017$  (see Table 6.9). Nevertheless, trials with PCI ( $M = 170.62\text{mm}^2, SD = 103.13\text{mm}^2$ ) were less accurate than those with HlbC ( $M = 133.58\text{mm}^2, SD = 75.43\text{mm}^2$ ) and RC ( $M = 124.82\text{mm}^2, SD = 79.71\text{mm}^2$ ) (see Figure 6.8-left). In addition, trials with RC were more accurate than those with HlbC.

Pair	Dependent t-test <sup>a</sup>	Effect strength
PCI vs. RC	$t(33) = 2.32, p = .03$	-
RC vs. HlbC	$t(33) = -0.56, p = .58$	-
PCI vs. HlbC	$t(33) = 1.81, p = .08$	-

<sup>a</sup>accepted  $\alpha$ -level is  $<.017$

Table 6.9: Pairwise comparisons of overall position deviations for the slope segment

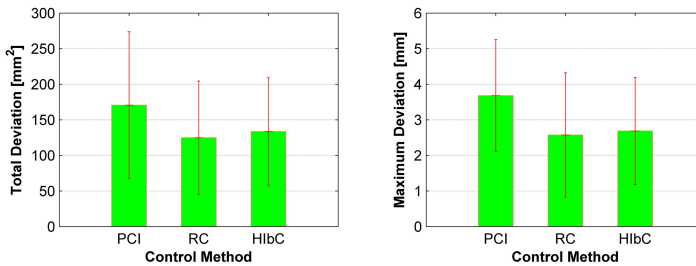


Figure 6.8: Mean values of overall and maximum position deviations of the slope segment

Regarding the maximum position deviations, there was a significant main effect of the control method,  $F(2, 64) = 5.76, p < .01$ . Pairwise comparisons showed that the maximum position deviations with PCI ( $M = 3.68\text{mm}, SD = 1.58\text{mm}$ ) were significantly larger than those produced with HlbC ( $M = 2.69\text{mm}, SD = 1.50\text{mm}$ ) and RC ( $M = 2.58\text{mm}, SD = 1.75\text{mm}$ ) (see Table 6.10 and Figure 6.8-right). The difference between RC and HlbC was insignificant.

Pair	Dependent t-test <sup>a</sup>	Effect strength
PCI vs. RC	$t(33) = 2.83, p < .01$	$r = .44$
RC vs. HlbC	$t(33) = -0.29, p = .77$	-
PCI vs. HlbC	$t(33) = 3.36, p < .01$	$r = .51$

<sup>a</sup>accepted  $\alpha$ -level is  $<.017$

Table 6.10: Pairwise comparisons of maximum deviations for the slope segment

## 6 Experimental Evaluation

### Large Corner Segment

For the large corner segment ( $P_{11}$ ) (cf. Figure 6.1), the assumption of sphericity was violated. Therefore, the Greenhouse-Geisser correction was applied,  $\epsilon = .76$ . After correction, there was found that a significant main effect of control method on the TCT exists,  $F(1.52, 48.64) = 8.85, p < .001$ . Further investigations by t-statistics indicated that trials conducted with RC ( $M = 2.99sec, SD = 1.50sec.$ ) were the fastest. As shown in Table 6.11, trials with RC were significantly faster than trials with HlbC ( $M = 4.46sec., SD = 2.60sec.$ ), but not than those with PCI ( $M = 3.54sec., SD = 2.60sec.$ ) (see Figure 6.9).

Pair	Dependent t-test <sup>a</sup>	Effect strength
PCI vs. RC	$t(33) = 2.39, p = .02$	
RC vs. HlbC	$t(33) = -3.76, p < .001$	$r = .55$
PCI vs. HlbC	$t(33) = -2.16, p = .038$	-

<sup>a</sup>accepted  $\alpha$ -level is  $< .017$

Table 6.11: Pairwise comparisons of TCT for the large corner

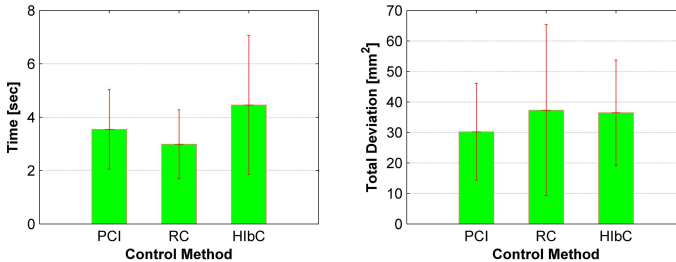


Figure 6.9: Mean values of TCT and overall deviation of the large corner

There was neither significant difference in TCT between trials with PCI and those with RC, nor between PCI and HlbC. Furthermore, there was no significant main effect of control method on the overall position deviation for this segment,  $F(2, 64) = 1.32, p = .28$ .

### Small Corners Segment

For the segment between  $P_{26}$  and  $P_{33}$ , there was a significant main effect of the control strategy on the TCT,  $F(2, 64) = 5.24, p < .001$ . As shown in Table 6.12, t-statistics indicated that trials with PCI ( $M = 12.85sec., SD = 4.19sec.$ ) were significantly faster than those conducted with HlbC ( $M = 18.77sec., SD =$

6.66sec.) and RC ( $M = 14,70\text{sec.}, SD = 6.56\text{sec.}$ ) (see Figure 6.10). Furthermore, trials with HibC were also significantly slower than those with RC.

Pair	Dependent t-test <sup>a</sup>	Effect strength
PCI vs. RC	$t(33) = -2.52, p < .017$	$r = .40$
RC vs. HibC	$t(33) = -4.80, p < .001$	$r = .64$
PCI vs. HibC	$t(33) = -8.48, p < .001$	$r = .83$

<sup>a</sup>accepted  $\alpha$ -level is  $< .017$

Table 6.12: Pairwise comparisons of TCT for the small corners segment

There was also a small significant main effect of control method on the overall deviations of the small corner segment,  $F(2, 64) = 5.24, p < .001$ . Table 6.13 shows the pairwise comparisons. It was found that trials with PCI ( $M = 72.98\text{mm}^2, SD = 29.67\text{mm}^2$ ) produced the smallest overall position deviations, which were significantly smaller than those conducted with RC ( $M = 96.37\text{mm}^2, SD = 45.46\text{mm}^2$ ) (see Figure 6.10). The difference in means of position deviations between trials with RC and HibC ( $M = 80.46\text{mm}^2, SD = 33.08\text{mm}^2$ ) was insignificant.

Pair	Dependent t-test <sup>a</sup>	Effect strength
PCI vs. RC	$t(33) = -3.07, p < .01$	$r = .58$
RC vs. HibC	$t(33) = 2.09, p = .05$	-
PCI vs. HibC	$t(33) = -1.15, p = .26$	-

<sup>a</sup>accepted  $\alpha$ -level is  $< .017$

Table 6.13: Pairwise comparisons of overall deviations for the small corners segment

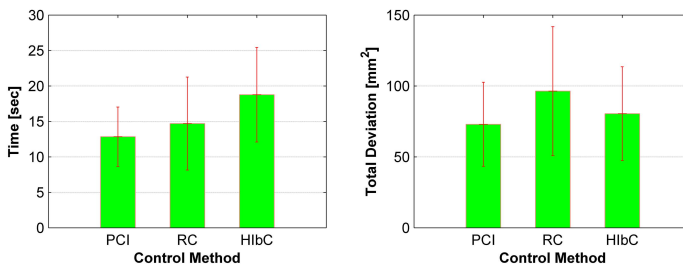


Figure 6.10: Mean values of TCT and overall position deviation of the small corners

**Overall Trajectory**

When the entire trajectory is considered, there was found a small significant main effect of the control strategy on the task completion time,  $F(1.55, 48.09) = 6.92, p < .01$ . As shown in Table 6.14, t-statistics pairwise comparisons indicated that trials conducted with RC led to the fastest TCT ( $M = 115.91sec., SD = 36.71sec.$ ), which were significantly faster than those conducted with HIbC ( $M = 135.23sec., SD = 50.14sec.$ ) and PCI ( $M = 139.71sec., SD = 69.56sec.$ ) (see Figure 6.11). The differences in TCT between trials conducted with PCI and HIbC were insignificant. There was no significant main effect of control strategy on the overall position deviations during tracking the complete trajectory,  $F(2, 62) = 1.63, p = .26$ . Therefore, these observed differences in the mean values of overall position deviations could be attributed to chance. Figure 6.11 shows these mean values.

Pair	Dependent t-test <sup>a</sup>	Effect strength
PCI vs. RC	$t(33) = 3.18, p < .01$	$r = .48$
RC vs. HIbC	$t(33) = -4.17, p < .001$	$r = .59$
PCI vs. HIbC	$t(33) = 2.85, p = .52$	-

<sup>a</sup>accepted  $\alpha$ -level is  $<.017$

Table 6.14: T-statistics pairwise comparisons of overall TCT for the entire trajectory

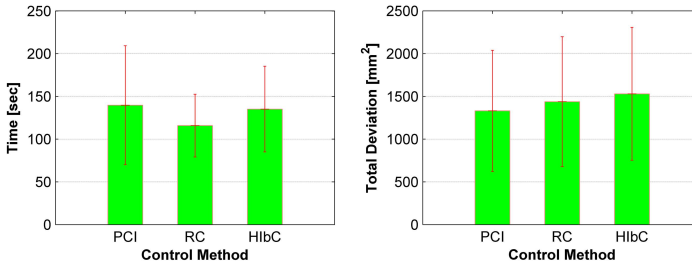


Figure 6.11: Mean values of the TCT and position deviation of the entire trajectory

**Usability**

Usability was assessed with the AttrakDiff2 (HASSENZAHL ET AL. 2003), a seven-point Likert-type questionnaire with the following items ranging from -3 to +3: technical/personal; complicated/simple; practical/impractical; cumbersome/manageable; unpredictable/predictable; confusing/clear. In general, this refers to the perceived ability of a product to accomplish a given task by offering usable functions. There was a significant main effect of the control

method on ratings of usability,  $F(2, 64) = 25.34, p < .001$ . As shown in Table 6.15, t-statistics revealed that usability scores of RC ( $M = 1.35, SD = 0.77$ ) were significantly higher than those of PCI ( $M = 0.19, SD = .76$ ) and HIBc ( $M = -0.41, SD = 1.02$ ). Furthermore, PCI was rated significantly more favourable than HIBc. There was no significant interaction effect between control method and joystick experience,  $F(4, 62) = 1.56, p = .20$ . However, an independent t-test comparing the HIBc usability ratings of novices ( $M = .22, SD = 1.10$ ) to experts ( $M = -1.03, SD = .78$ ) found a significant difference in ratings, with novices rating HIBc significantly more favourably than experts ( $t(16) = 2.83, p < .05, r = .58$ ). Figure 6.12 shows mean usability ratings for each control strategy by joystick experience group.

Pair	Dependent t-test <sup>a</sup>	Effect strength
PCI vs. RC	$t(33) = -5.06, p < .001$	$r = .66$
RC vs. HIBc	$t(33) = 6.67, p < .001$	$r = .76$
PCI vs. HIBc	$t(33) = 2.85, p < .01$	$r = .44$

<sup>a</sup>accepted  $\alpha$ -level is  $<.017$

Table 6.15: Pairwise comparisons of mean usability scores

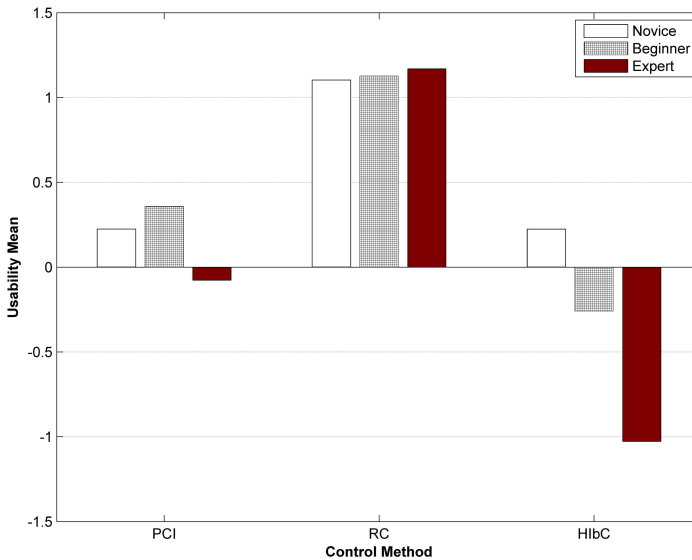


Figure 6.12: Means of usability ratings for each control method by joystick experience

### 6.2.2.6 Summary of Experiment A

The main goal of this experiment was to evaluate the performance of the implemented control methods, namely position control with indexing, rate control and human intention-based control, during tracking a standardized trajectory. The performance measures considered in this experiment were the task completion time, the maximum position deviation and overall deviation. Furthermore, the intuitiveness of the applied control methods was also investigated based on a usability questionnaire.

The results of the statistical analyses showed that rate control was not only faster than other methods, but also more accurate. The only exception here is the small corner segment, where the position control was significantly faster and more accurate. Regarding usability, rate control received the highest scores from users. However, if the user experience is taken into account, inexperienced users judged the usability of human intention-based control more favourable than rate control, whilst experienced participants judged it unfavourable.

The human intention-based control was found to significantly improve tracking accuracy compared to position control with indexing on straight segments, without slowing the task performance. It was also found that human intention-based control performed similarly to rate control on large segments, e.g. the curve segment. However, it was slower than rate control in small circle without significant improvement in accuracy. For corner segments, the human intention-based control was slower and inaccurate than position control (in the case of small corners) and rate control (in the case of large corners).

For the entire trajectory, the performance of control methods did not differ significantly with regard to accuracy. However, rate control was significantly faster than the other control methods.

In conclusion, it can be said that the developed human intention-based control seems to offer a valid compromise between position control and rate control, showing comparable performance to rate control on all accuracy measures and most speed measures apart from the tracking times of corners and circles, while showing significant improvement to position control in slope and line tracking accuracy as well as curve time. It seems that inexperienced users find it easier to handle the human intention-based control than experienced users, who are already trained in the use of other control strategies, mainly the rate control. Presumably, human intention-based control does not conform to expectations of experienced users, which is to be expected with new technologies. Future studies should be carried out to investigate the effects of prolonged training on performance and usability measures of the human intention-based control.

### 6.2.3 Experiment B: Surface Finishing Task with Model-based Force Feedback

#### 6.2.3.1 Task Definition and Requirements

The aim of this task is to apply a force on an object's surface as constant as possible while sliding the robot's tool across the surface. Figure 6.13 shows the teleoperator side in this experiment. The tool of the teleoperator was positioned away from the object's surface with a consistent offset in the vertical direction (z-axis of the world coordinates system).

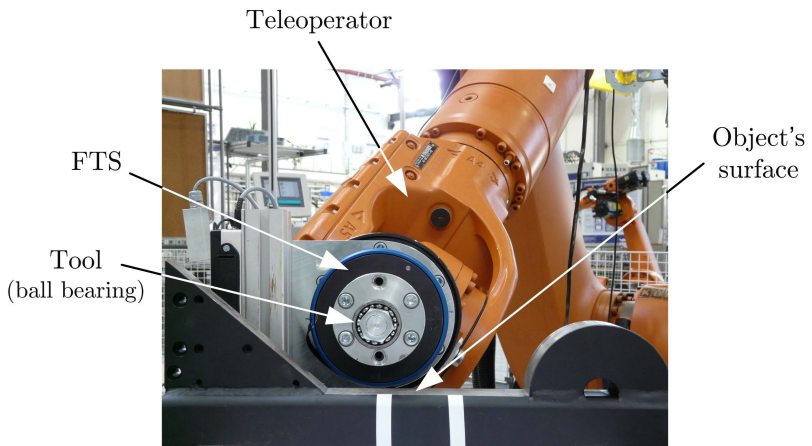


Figure 6.13: The teleoperator configuration for experiment B

Typically, the complete task entails the following four phases (cf. Figure 6.14):

1. unconstrained motion phase: the human operator moves the teleoperator in free space from the home position towards the object to be machined.
2. transition phase: the human operator brings the robot's tool in contact with the object's surface, i.e. transition from unconstrained to constrained motion.
3. constrained motion phase: the human operator slides the robot's tool over the surface of the machined object while maintaining smooth continuous contact, i.e. the applied forces in the direction normal to the constraint surface should be as constant as possible.

- releasing phase: the human operator moves the teleoperator away from the object's surface.

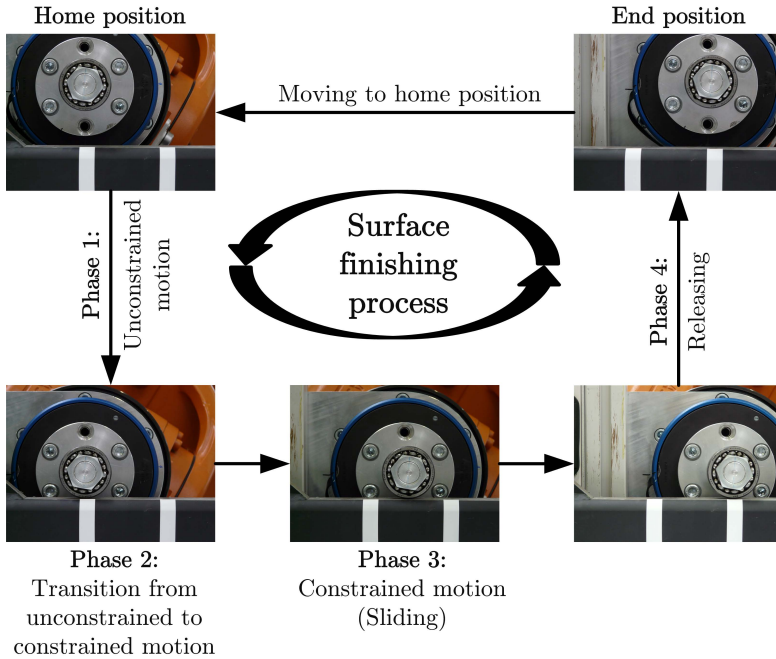


Figure 6.14: The four phases of the surface finishing task (experiment B)

During the task execution, three kinds of feedback are provided to the human operator; visual feedback of the process field, visualization of the applied force and the model-based force feedback. It was ascertained whether the model-based force feedback would provide additional assistance over and above that offered by the visualization of applied forces during task execution.

### 6.2.3.2 Industrial Relevance

In surface finishing processes such as grinding, the feed-rate and cutting depth are the critical parameters that affect the quality of the finished surface. These parameters are determined by the tangential velocity and the force  $F_n$  normal to the contact surface (YU 2000). Therefore, during a surface finishing process it is important to maintain a constant normal force while following a tangential

trajectory. As seen in Figure 6.15, the other force acting on the tool is  $F_t$  tangential to the contact surface (CAI & GOLDENBERG 1989). Both forces,  $F_n$  and  $F_t$ , are linearly related by a coefficient, called the friction coefficient (KING & HAHN 1986). If the tool motor-drive torque is available,  $F_t$  can be found by dividing the torque by the tool radius. Using the friction coefficient,  $F_n$  can be then approximately determined. By doing so,  $F_n$  can be controlled independently.

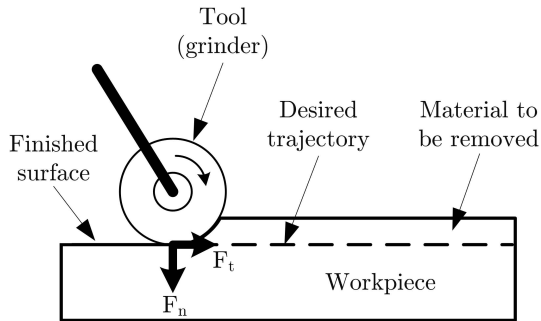


Figure 6.15: Forces acting on the tool during grinding process

As the objective of this experiment is to find out whether the model-based force feedback would provide additional assistance to help human operators regulate the normal forces, it was decided to minimize the effect of the frictional forces between the object and the robot's tool during sliding the tool over the surface. Therefore, a ball bearing is here applied. A ball bearing is a type of rolling-element bearing which consists of two races and balls in between. The using of this bearing allows having the contact forces measured at the tool to be perpendicular to the object surface. The force direction is then used to generate the model-based force signals.

### 6.2.3.3 Experimental Design

A repeated measures within-subject design was applied with model-based force feedback as independent variable, manipulated on two levels (on/off). Half of all participants started with the model-based force feedback and the other half started without. Participants were seated in a sound attenuated room to shield them from distractions.

The following performance measures were considered:

- **Task completion time (TCT):** by this measure it can be found whether the provision of the model-based force feedback would accelerate the task execution.
- **Average applied forces ( $F_{mean}$ ):** the desired applied force during the task execution is predefined to be in the range of 300 to 500 N. The overall mean forces indicate the fulfillment of this requirement.
- **Maximum applied forces ( $F_{max}$ ):** usually the maximum applied forces are used to identify the process quality; hence the reduction of this maximum value indicates lower pressure applied on the manipulated materials, which in turn reduces the possibility of material damages. This also reduces the mechanical stress applied on the robot.
- **Usability:** based on a questionnaire, users rate the usability of the model-based force feedback method.

To extract these performance measures, data was captured during the experiments. This data includes the end-effector forces and positions, the position of the joystick and the task completion time. Due to safety issues and in order to avoid crash contacts, the maximum forces were limited by a software limiter.

### 6.2.3.4 Hypothesis

The following null hypothesis which concerns the model-based force feedback is proposed for this experiment

- $H_0$ : The provision of the model-based force feedback does not improve task performance.

### 6.2.3.5 Procedure

Participants were instructed to move the robot's tool from the home position towards the object, contact the object's surface and then slide the end-effector as quickly as possible towards a pre-defined target position, without losing contact with the surface (see Figure 6.14). They were also given the opportunity to familiarize themselves with the task and the effect of force feedback. This training phase ensured that all participants were approximately at the same level of experience.

The objective was to apply a force in the range of 300 to 500 N during the task execution. The measured applied forces onto the surface were visualized using a colored bar graph (Yellow: below the desired force range, Green: within the desired range, Red: above the desired range). Each trial was repeated three

times with model-based force feedback and three times without. Prior to the start of each trial, the teleoperator was moved to a consistent start position above the left side of the object's surface, as viewed by the operator (see Figure 6.13). During the experiments, the operator had control of two axes of the teleoperator, namely y- and z-axis. After finishing the task, participants completed a survey with various questions regarding their impressions of the quality of the force feedback and the intuitiveness.

### 6.2.3.6 Data Analysis and Results

The data were screened for outliers and data with z-scores of  $z > \pm 3.29$  ( $N = 7$ ) were removed and replaced with variable group means. Based on the central limit theorem, the data were assumed to be normally distributed. Assumptions of parametric data have been met. Therefore parametric tests have been applied for further data analysis. In this experiment, there was two independent variables, the trial's number (trial 1, trial 2 and trial 3) and the force feedback type (with force feedback (FF) vs. no force feedback (NF)). Therefore, a two way repeated-measures analysis of variance (ANOVA) had been conducted with these two independent variables. The results of this experiment are introduced in the following.

#### Task Completion Time

Having the TCT as a dependent variable, there was a significant main effect of trial's number on TCT,  $F(2, 66) = 15.44, p < .001$ , regardless of the force feedback type. As shown in Figure 6.16, it was found that the mean value of TCT for the second trial ( $M = 13.04sec., SD = 5.90sec.$ ) is significantly higher than that for the first one ( $M = 8.98sec., SD = 4.79sec.$ ), but there was no significant change in the TCT between the second and third trial ( $M = 12.50sec., SD = 1.12sec.$ ). This can be argued that participants were more careful after finishing the first trial, making them to slower their performance in order to fulfill the force requirements. It was also found that a significant main effect of force feedback type on TCT exists,  $F(1, 33) = 10.51, p < .01$ , and there was no significant interaction effect between trial's number and force feedback type,  $F(2, 66) = 2.03, p = .14$ . This indicates that participants completed their task significantly faster with force feedback ( $M = 9.94sec., SD = 5.06sec.$ ) than without ( $M = 13.07sec., SD = 6.56sec.$ ), regardless of the trial's number (see Figure 6.17). Hence, the time reduction was found to be 24%. Ignoring the effect of trial's number on TCT, it can be said that the hypothesis  $H_0$  is rejected with regard to task completion time.

## 6 Experimental Evaluation

---

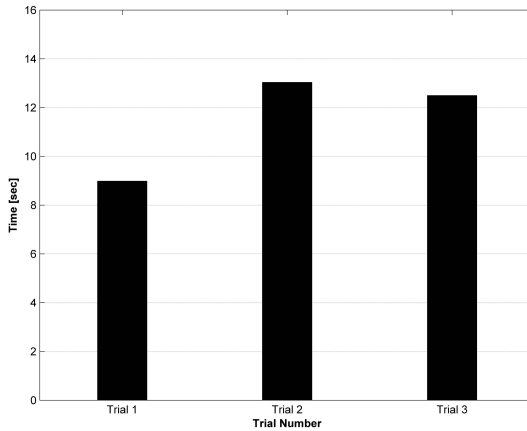


Figure 6.16: Mean task completion time for each trial irrespective of force feedback type

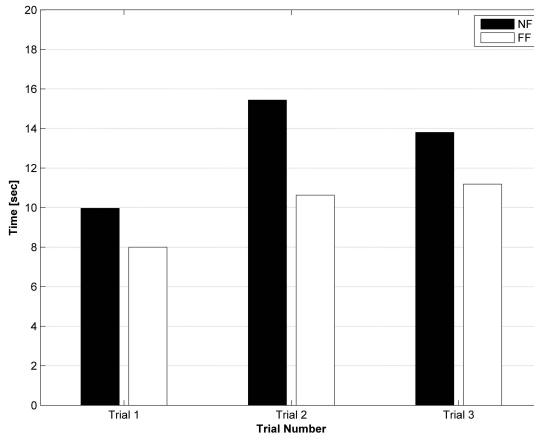


Figure 6.17: Mean task completion time for each trial by force feedback type

### Average Applied Forces

This performance measure reflects the ability of the participants to keep the applied forces onto the object's surface within the desired range during task execution. Conducting a two-way ANOVA with the trial's number and force feedback

type as independent variables and the average forces ( $F_{mean}$ ) as dependent variable revealed a significant effect of the trial's number,  $F(2, 66) = 25.31, p < .001$ . The participants applied on average significantly less forces in the second trial than in the first one,  $F(1, 33) = 50.17, p < .001$ , while the difference between the second and third trials was insignificant,  $F(1, 33) = 3.74, p = .06$ . There was no significant effect of the force feedback type on the average forces,  $F(1, 33) = 0.16, p = .69$ . It seems that participants relied on the visual display of the applied forces to stay within the desired range, rather than using the model-based force feedback. Therefore, it can be here said that the hypothesis  $H_0$  is accepted with regard to average applied forces, i.e. the model-based force feedback does not assist the human operator keep the applied forces within a desired force range. In addition, there was also no significant interaction effect between trial's number and force feedback type,  $F(2, 66) = 2.91, p = .06$ . Figure 6.18 shows the mean values of the average applied forces for each trial by feedback type.

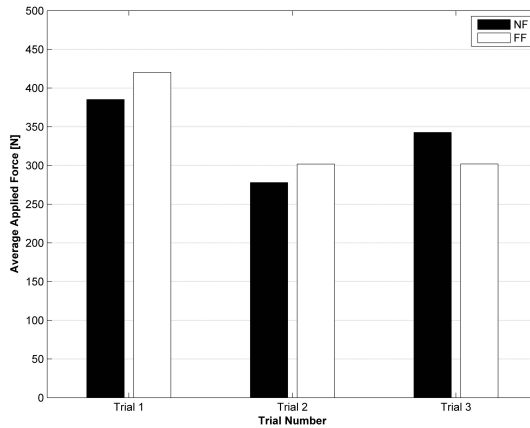


Figure 6.18: Mean values of the average forces applied onto the object's surface for each trial by feedback type

### Maximum Applied Forces

The maximum forces ( $F_{max}$ ) were taken as dependent variable in a two-way ANOVA. There was no significant effect of trial's number on these forces,  $F(2, 66) = 1.34, p = .27$ . Hence, the maximum forces applied onto the object's surface were not affected through consecutive trials, irrespective of the force feedback type. However, it was found that the force feedback type has a significant effect on the maximum forces,  $F(1, 33) = 8.80, p < .01$ . Comparing

## 6 Experimental Evaluation

---

the mean values of the maximum forces indicated that the maximum forces were significantly reduced in the case of model-based force feedback (see Figure 6.19). Furthermore, there was no significant interaction effect between the trial's number and the feedback type,  $F(2, 66) = 0.87, p = .43$ . Therefore, the hypothesis  $H_0$  is here rejected with regard to the effect on the maximum applied forces, i.e. the model-based force feedback assists the human operator reduce the maximum forces, which in turn reduces the possibility of material and teleoperator damages, hence increasing the quality of product.

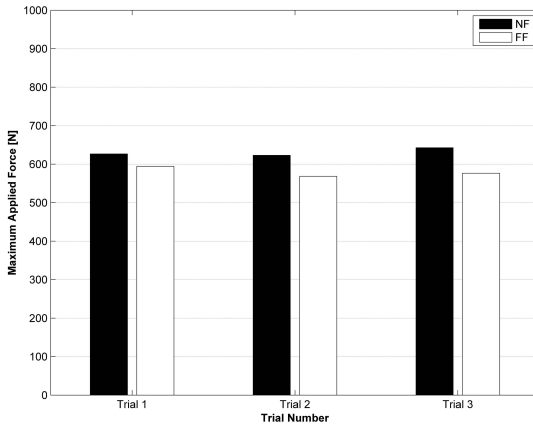


Figure 6.19: Mean values of the maximum forces applied onto the object's surface for each trial by force feedback type

### Usability

Participants were asked to complete a usability questionnaire with the following questions after finishing the entire task:

1. *In your opinion, was the force feedback: rather stable/continuous...rather unstable/discontinuous?*
2. *Did the surface feel smooth or rough to you?*
3. *Did you feel friction from the remote environment as you performed the task?*
4. *Do you think the control of the robot along the z-axis (arm up/down) was rather intuitive or not really intuitive?*

The following is the summary of the participants' responses:

- **88.24%** of the participants (30 out of 34) found the model-based force feedback stable and continuous.
- **100%** of the participants (34 out of 34) stated that they felt a smooth object's surface.
- **91.18%** of the participants (31 out of 34) did not feel friction during the task execution.

### 6.2.3.7 Summary of Experiment B

In general, the statistical analysis indicated that the developed model-based force feedback allowed participants to perform the surface finishing task significantly faster than when only a visual display of the measured applied forces is provided. It was found that the task completion time was reduced by a factor of 24%.

In contrary, it was found that the model-based force feedback does not help the human operator keep the applied forces within a desired force range. It seems that the participants used the visualization of the applied forces to fulfill this requirement. Further investigation without force visualization is suggested to find out the effect of having only haptic feedback on the average applied forces.

In addition to these findings, receiving the model-based force feedback reduced significantly the maximum forces applied to the object's surface. This aligns with the results of other studies (e.g. WAGNER ET AL. (2007) and RADI ET AL. (2010a), among others), all of which indicate that haptic feedback assists the human operator in reducing the maximum forces applied onto objects within the teleoperator environment. This influences not only the quality of products but also increases the durability of the teleoperator.

## 6.3 Conclusion

In this chapter, two user experiments are presented. The first experiment aimed at the evaluation of the three developed scaling techniques, namely position control with indexing, rate control and human intention-based control. The experimental task was to track a standardized trajectory (Schmidt trajectory). The performance of the control methods was measured for different selected segments as well as the whole trajectory with regard to speed, position accuracy and usability. It has been found that the developed human intention-based control seems to offer a valid compromise between indexing and rate control, showing comparable performance to rate control on all accuracy measures and most speed measures, whilst showing significant improvement to position

## 6 Experimental Evaluation

---

control with indexing in tracking accuracy of slope and line segments as well as task completion time of curve segment.

The aim of the second experiment was to find out the benefits of having the developed model-based force feedback in a teleoperated surface finishing/machining task, by which a constant force should be applied on an object's surface during sliding the teleoperator's tool across the surface. It has been statistically found that the model-based force feedback assists the human operator in performing the task significantly faster than when only the visual display of the applied forces is provided. This leads to a 24% reduction of the time needed to complete the task. Furthermore, it has been found that by the provision of the model-based force feedback the applied forces were more stable and the maximum forces were significantly reduced, which in turn reduces the risk of product as well as teleoperator damages attributed to excessive forces.

## 7 Operational and Economic Feasibility

*“The true measure of your worth includes all the benefits others have gained from your success.”*

---

*Cullen Hightower*

In this chapter, the operational and economic feasibility of the developed TPTA-system are assessed. For the operational feasibility, the system has been compared with conventional teleoperation systems lacking the implemented features such as the haptic feedback and scaling techniques. For the economic feasibility, the developed model-based force feedback provided quantitatively performance benefits (as seen in chapter 6), e.g. reduced execution time and improved process quality. This is representatively used to prove the economic benefits of this system.

### 7.1 Operational Feasibility

In order to assess the operational feasibility, the following basic questions need to be addressed:

- Does the developed TPTA-system with its features enhance the remote manipulation tasks regarding **time** and **quality**?
- Is there any resistance from the human operator to use the new developed system? Does the user **accept** the new features of the system?
- Is the developed system **flexibly** applicable to different production processes? Is it **expandable** to new manufacturing operations?
- Is the system **reliable** to perform teleoperated manufacturing tasks?

Answers to these questions are presented in the following:

#### **Time**

As described in the previous chapter, the developed techniques reduce the time required to accomplish the teleoperated tasks. For example, the model-based force feedback reduces the task completion time by a factor of 24% during teleoperated surface finishing tasks. Furthermore, using an adequate scaling

technique to move the teleoperator along a specific shape of trajectory speeds up the operation.

### **Quality**

Regarding quality, the teleoperator position deviations from a specific trajectory are reduced if an appropriate scaling method is applied for different trajectory shapes. Moreover, the provision of the model-based force feedback in the case of heavy-duty teleoperators decreases the risk of product and teleoperator damages attributed to excessive forces, hence enhancing the production quality.

### **Acceptance**

The survey results presented in chapter 6 leave positive marks for novice user acceptance regarding the scaling techniques and the model-based force feedback. For experienced users, some features were not accepted, which is to be expected with new technologies. This can be overcome by prolonged training of experts to become familiar with new features, e.g. human intention-based control. In general, by making the operators work more efficiently and faster, the improved system will be accepted not only at the operating personnel level but also at other levels such as the management and developers.

### **Flexibility**

In contrast to standard automation systems, which require time-consuming reprogramming, the developed TPTA-system takes just as long as the manually controlled teleoperated task and exploits the superior human abilities. The possibility to use this system as a semi-automated manufacturing system makes it more flexible in terms of reprogramming times. The teleoperated task can be flexibly programmed by the human operator and afterward the recorded motions and actions can be replayed for several times. This makes sense when considering production of small batch sizes. However, actions to adapt the system to new manufacturing process are needed, for example, changing teleoperator tools. Adding a tool changing system would increase the flexibility of the system.

### **Extensibility**

The integration of the developed techniques into any robotics system that has the minimum technical requirements is ensured as the designed system architecture is independent of any restrictions dictated by components manufacturers. This makes the system and the developed techniques extendable.

### **Reliability**

If the manufacturing tasks are to be carried out in dangerous and/or highly inaccessible areas, the deployment of the TPTA-system is solely needed. Though this will introduce some barriers between the operator and teleoperator, the

performance can be enhanced and supported as computerized control strategies are used. Therefore, the TPTA-technology can increase the reliability of the system because

- the teleoperator is controlled by a human operator whose intelligence is far superior in terms of reasoning, vision, and ingenuity, among others,
- the interaction forces between the teleoperator and objects are manually controllable by human operator, which helps to avoid component damages, and
- the performance is improved by the provision of different feedback signals (visual and haptic).

Figure 7.1 summarizes this operational feasibility assessment, by qualitatively comparing a conventional teleoperation system and the developed TPTA-system.

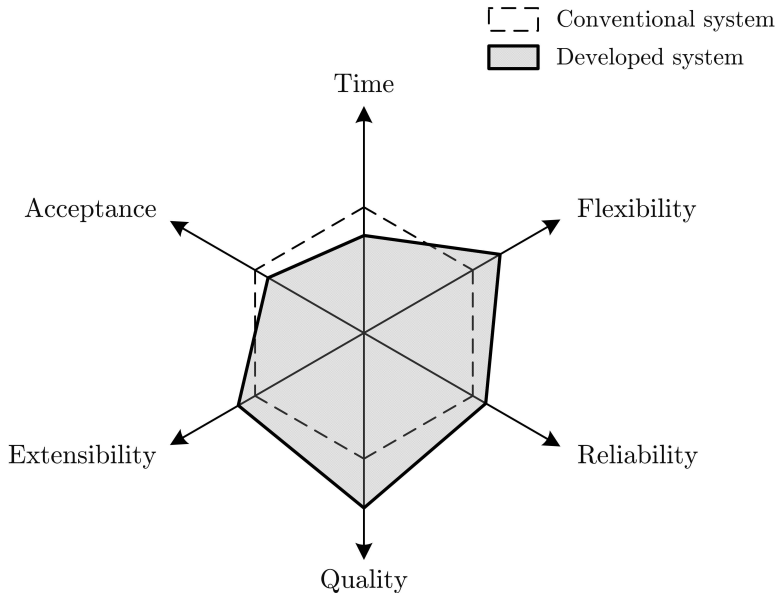


Figure 7.1: Qualitative comparison between the developed TPTA-system and a conventional teleoperation system

### 7.2 Economic Feasibility

In general, any technical system should be only used when the benefits outweigh the costs. Therefore, a cost-benefit analysis should be performed to find out whether the developed TPTA-system is economically feasible. This analysis helps in having a clear insight into the costs, benefits and risks of deployment of such system in a manufacturing facility.

Benefits can be divided into two categories: qualitative and quantitative. Beside the qualitatively derived operational benefits mentioned in the aforementioned section, the experimental evaluation (cf. chapter 6) provided quantitative performance benefits under experimental conditions (reduced execution time, improved quality, etc.). To obtain a quantitative estimate of the potential economic benefits, an example of a cost-benefit analysis is introduced in the following.

#### 7.2.1 Cost-Benefit Analysis

In this section, a cost-benefit analysis is performed to determine the economic benefits and savings that are expected from the provision of model-based haptic feedback into an industrial teleoperation system and compare them with the expected costs. This is one way to study the economic feasibility of new technologies and features (GÖTZE 2006). For illustration purpose, the following costs and benefit effects are assumed:

- The investment costs ( $\Delta I$ ) needed to integrate the model-based force feedback are 30,000 €. This includes equipment, software and development costs.
- The system lifetime ( $L$ ) is set to six years with an interest rate ( $R$ ) of 10%.
- The annual maintenance costs are expected to be 2,500 € and the annual training costs are set to 1,000 €.
- By using the model-based force feedback the human operator can perform the given task faster. The time saved depends essentially on the characteristics of the teleoperated tasks. Particularly, for the execution of a surface finishing task the average time saved as determined in this work is 24% (cf. section 6.2.3). Thus one operational hour using a conventional teleoperation system without haptic feedback is equivalent to only  $(1 - 0.24) \times 60 = 45.6$  minutes by using the developed TPTA-system with model-based force feedback. By other words, one operational hour of the developed TPTA-system is equivalent to 1.316 hour by conventional systems. This can be considered as the  $\Delta$ benefits of the provision of model-based force feedback. Thus the factor of time saved ( $SV$ ) is  $\frac{1}{1-0.24} - 1 = 0.316$ .

- With an annual usage ( $U$ ) of the developed TPTA-system in the range of 1,500 hours/year (250 days/year  $\times$  6 hours/day), about 474 hours/year can consequently be saved. Having a labor cost ( $LC$ ) of 60€/hour, an annual saving of 28,440€ can be made.

$\Delta$ Investment Costs			
Item	Formula	Cost	Unit
Haptic joystick		3,000	€
Joystick interface		500	€
RT-platform		2,500	€
Software		8,000	€
FTS		3,500	€
RSI package		2,500	€
Development Costs		10,000	€
<b>Total <math>\Delta</math> investment costs</b>	$\Delta I$	30,000	€

$\Delta$ Annual Costs			
Lifetime	$L$	6	years
Depreciation (linear)	$D = \Delta I / L$	5,000	€/year
Interest	$K = \Delta I \times R / 2$	1,500	€/year
Maintenance	$M$	2,500	€/year
Training	$T$	1,000	€/year
<b>Total <math>\Delta</math> annual costs</b>	$\Delta C = D + K + M + T$	11,000	€/year

$\Delta$ Annual Benefits			
Annual usage	$U$	1,500	hours/year
Time saved	$TS = U \times SV$	474	hours/year
Labor cost	$LC$	60	€/hour
Annual saving	$LC \times TS$	28,440	€/year
<b>Total <math>\Delta</math> annual benefits</b>	$\Delta B$	28,440	€/year

<b>Payback period</b>	$PK = \Delta I / (\Delta B - \Delta C + D)$	1.34	year
-----------------------	---	------	------

Table 7.1: Cost-Benefit Analysis

Table 7.1 shows the calculations of this example. Here, it should be mentioned that the minimum annual usage of the system which makes this investment profitable is  $\Delta C / (LC \times SV) = 580.2$  hours/year. This means that the provision of

the model-based force feedback is economic feasible if the annual usage of the system exceeds this limit.

Nevertheless, several cost saving effects are not included in this illustrative example. For instance, the quality effect of the model-based force feedback can increase the lifetime of the system by reducing the maximum forces applied to the teleoperator during the execution of constrained tasks. Furthermore, shorter operating times lead to saving in the energy used to operate the system, which, in turn, leads to reduction in the annual energy costs. These and other factors influence the cost-benefit analysis significantly. However, the aforementioned example is considered enough to express the economic potential of the provision of the model-based force feedback into existing teleoperation systems with heavy-duty teleoperators.

### 7.3 Conclusion

After determining the effectiveness of the developed techniques experimentally, this chapter highlights the technical and economic benefits gained by implementing these techniques in a TPTA-system. Comparing the developed TPTA-system with a conventional one, the task completion time is reduced and the quality of processes is increased. This is attributed to (a) the different scaling techniques that suitable for different trajectory shapes and (b) to the model-based force feedback in the case of heavy-duty teleoperators, where the direct force feedback is impracticable because of stability issues. Moreover, the economic benefits by the reduction of task completion time is explained by an illustrative example.

However, some of the developed techniques were not acceptable by certain groups of users. For example, expert users found the human intention-based control method less desirable than rate and position control. This may affect the total user-acceptance of the developed system, but this is normally expected with new technologies and could be overcome by prolonged training.

In addition to the explained benefits of the developed TPTA-system, the deployment of TPTA-technology has a special safety potential in the case of manufacturing and handling processes in dangerous and/or inaccessible environments and it is difficult to find out the exact monetary benefit of such factor. In this case, the use of TPTA-systems can be considered mandatory from a safety point of view.

## 8 General Conclusion and Future Work

*“The end crowneth the work.”*

---

*Elizabeth I*

Meanwhile, telepresence and teleaction technology receives a higher value and importance, especially after the Gulf of Mexico deepwater crisis in 2010 and Japan’s Fukushima nuclear disaster in 2011. Several remotely operated vehicles were sent to conduct measurement and maintenance tasks, since sending humans to such places is very dangerous. These teleoperated vehicles were able to stop the oil leak in the Gulf of Mexico and others are still working on the Fukushima nuclear power plants. In the wake of the Fukushima disaster, several countries decided to phaseout nuclear power. In Germany, all nuclear power plants will go offline by 2022. This means that the deployment of telepresence and teleaction technology will still be required not only to response to disasters and crisis situations, but also for decommissioning and dismantling the nuclear power plants which are planed to go offline.

In this work, the main focus was on the deployment of telepresence and teleaction technology for handling and manipulating heavy parts. For this purpose, commercial off-the-shelf components were utilized in this work to enhance the industrial usability of telepresence and teleaction systems. This reduces, in general, the overall design, construction and maintenance costs of industrial systems. However, this poses several challenges and problems, two of which were considered in this thesis.

The first challenge appears when the haptic device and the industrial robot are kinematically different. Several kinematic mapping and workspace scaling techniques were developed and implemented. In the case of insufficient number of degrees of freedom of the utilized haptic device, a mapping strategy is performed by projecting the available degrees of freedom onto a motion plane within the workspace of the teleoperator. Using homogeneous transformations the motion commands on the motion plane can be transformed into motion commands in a stationary coordinate frame of the teleoperator. However, the simultaneous control of all degrees of freedom of the teleoperator is difficult using this method. Nevertheless, it is possible to successively control different degrees of freedom by moving the motion plane to different locations within the workspace of the teleoperator.

## 8 General Conclusion and Future Work

---

Different scaling techniques, namely position control with indexing, rate control and human intention-based control, have been also developed and successfully implemented in this work. It has been found that each method incorporates advantages and disadvantages, which were presented in detail. In order to evaluate the performance of these techniques, a psychophysical experiment has been designed and conducted. The task was to track a standardized trajectory using different control methods. The performance of these methods was measured for different selected segments of this trajectory with regard to speed, position accuracy and usability. It has been found that the developed human intention-based control seems to offer a valid compromise between position control and rate control. Regarding usability, rate control received the highest scores from users. However, if the user experience is taken into account, inexperienced users found the human intention-based control more favourable than rate control, whilst experienced participants judged it unfavourable.

The second challenge, which was also considered in this work, was the provision of haptic feedback in a telepresence system with heavy-duty teleoperator. It has been shown that the stability of such a system can be achieved by intensively scaling down the interaction forces between the teleoperator and the manipulated objects before displaying them through the haptic device. This, however, affects the transparency and the performance of the system negatively. To increase the transparency of the system, a model-based force feedback has been developed to ensure stability of the system with high levels of transparency. Instead of scaling down the measured forces, model-based force signals are generated by a model located at the operator side and triggered using sensor-based signals from the teleoperator side. In a second psychophysical study, the developed model-based force feedback technique was evaluated in a teleoperated surface finishing/machining task. The objective of this study was to find out the benefits of having this model-based force feedback. Specifically, it was investigated whether model-based force feedback would provide additional assistance over that offered by the visualization of applied forces during such tasks. It has been statistically found that the model-based force feedback leads to a 24% reduction of the time needed to complete the task. Furthermore, it has been found that the applied forces were more stable and the maximum forces were significantly reduced, which in turn reduces the risks of damaging the product as well as the teleoperator.

Two main research directions are suggested for future work. The first direction involves the extension of the industrial telepresence and teleaction system by incorporating intelligence algorithms, which will help converting a fully manual operated system into a semi-automated one. As such, the system can decide whether the task should be conducted automatically or manually. By the automatic mode, the intelligence algorithms should assist the system predict

---

unexpected circumstances and react accordingly. This leads to higher system reliability.

The second direction is to investigate the potential of new technologies with regards to the other modalities, namely visual and auditory feedback. The integration of new vision technologies, such as 3D-vision and augmented reality, and 3D auditory feedback would enhance navigational capabilities in unstructured environments and in turn increase the immersion experienced by human operators.



## Bibliography

[ALL & NOURBAKHSI 2001]

All, S.; Nourbakhsh, I.: Insect Telepresence: Using Robotic Tele-Embodiment to Bring Insects Face-to-Face with Humans. *Autonomous Robots* 10 (2001), pp. 149–161.

[ARTIGAS ET AL. 2006]

Artigas, J.; Vilanova, J.; Preusche, C.; Hirzinger, G.: Time Domain Passivity Control-based Telepresence with Time Delay. In: *IEEE/RSJ International Conference on Intelligent Robots and Systems, IROS 2006, Beijing 2006*. pp. 4205–4210.

[BBC.NEWS 2010]

BBC.News: BP says oil has stopped leaking from Gulf well, online: 15th July - BBC.co.uk, 2010.

[BERESTESKY ET AL. 2004]

Berestesty, P.; Chopra, N.; Spong, M.: Discrete time passivity in bilateral teleoperation over the Internet. In: *Robotics and Automation, 2004. Proceedings. ICRA '04. 2004 IEEE International Conference on, 2004, vol. 5*. pp. 4557–4564.

[BRECHER ET AL. 2010]

Brecher, C.; Roßmann, J.; Schlette, C.; Herfs, W.; Ruf, H.; Göbel, M.: Intuitive Roboterprogrammierung in der automatisierten Montage. *wt Werkstattstechnik online* 100 (2010) 9, pp. 681–686.

[CAI & GOLDENBERG 1989]

Cai, L.; Goldenberg, A.: Position and force control approach to automatic deburring by a robot manipulator. In: *IEEE International Conference on Systems, Man and Cybernetics, 1989. Conference Proceedings, 1989, vol. 2*. pp. 784–789.

[CHIN ET AL. 1993]

Chin, K.; Dahleh, M.; Verghese, G.; Sheridan, T.: Stable Teleoperation with Scaled Feedback. *LIDS Technical Reports Series LIDS-P ; 2206*, Massachusetts Institute of Technology, Laboratory for Information and Decision Systems, U.S., 1993.

[CHOPRA ET AL. 2003]

Chopra, N.; Spong, M.; Hirche, S.; Buss, M.: Bilateral teleoperation over the

## Bibliography

---

internet: the time varying delay problem. In: American Control Conference, 2003, 2003, vol. 1. pp. 155–160.

[CLARKE 2006]

Clarke, S.: Overcoming Network Delays in Telepresence Systems with Prediction and Inertia. Phd thesis, Technische Universität München, 2006.

[COLGATE 1993]

Colgate, J.: Robust Impedance Shaping Telemanipulation. IEEE Trans. Robotics and Automation 9 (1993) 4, pp. 374 – 384.

[COLGATE ET AL. 1996]

Colgate, J.; Wannasuphprasit, W.; Peshkin, M.: COBOTS : Robots for Collaboration with Human Operators. In: Proceedings of the International Mechanical Engineering Congress and Exhibition, Atlanta, GA 1996, vol. 58. pp. 433–439.

[CONTI & KHATIB 2005]

Conti, F.; Khatib, O.: Spanning Large Workspaces Using Small Haptic Devices. In: Proceedings of the First Joint Eurohaptics Conference and Symposium on Haptic Interfaces for Virtual Environment and Teleoperator Systems. IEEE Computer Society 2005. pp. 183–188.

[CORKER & BEJCZY 1985]

Corker, K.; Bejczy, A.: Recent Advances in Telepresence Technology Development. In: Proc. of 22nd Space Congress, 1985.

[DANIEL & MCAREE 1998]

Daniel, R. W.; McAree, P. R.: Fundamental Limits of Performance for Force Reflecting Teleoperation. The International Journal of Robotics Research 17 (1998) 8, pp. 811–830.

[DEML 2007]

Deml, B.: Human Factors Issues on the Design of Telepresence Systems. Presence: Teleoperators and Virtual Environments 16 (2007) 5, pp. 471–487.

[DENNERLEIN ET AL. 2000]

Dennerlein, J. T.; Martin, D. B.; Hasser, C.: Force-feedback improves performance for steering and combined steering-targeting tasks. In: SIGCHI conference on Human factors in computing systems. New York, NY, USA: ACM Press 2000. pp. 423–429.

[DLR 2011]

DLR: German Aerospace Center - Institute of Robotics and Mechatronics, [http://www.dlr.de/rm/en/desktopdefault.aspx/tabid-5014/8373\\_read-14285/](http://www.dlr.de/rm/en/desktopdefault.aspx/tabid-5014/8373_read-14285/), 2011.

[DRAPER ET AL. 1987]

Draper, J.; Moore, W.; Herndon, J.; Weil, B.: Effects of force reflection on servomanipulator task performance. In: International topical meeting on remote systems and robotics in hostile environments, 1987.

[DUBEY ET AL. 2001]

Dubey, R.; Everett, S.; Pernalet, N.; Manocha, K.: Teleoperation assistance through variable velocity mapping. IEEE Transactions on Robotics and Automation 17 (2001) 5, pp. 761–766.

[DUCHAINED & GOSSELIN 2007]

Duchaine, V.; Gosselin, C. M.: General Model of Human-Robot Cooperation Using a Novel Velocity Based Variable Impedance Control. In: EuroHaptics Conference, 2007 and Symposium on Haptic Interfaces for Virtual Environment and Teleoperator Systems. World Haptics 2007. Second Joint, 2007. pp. 446–451.

[EPSTEIN 1985]

Epstein, H.: Multimodality , Crossmodality , and Dyslexia. Annals of Dyslexia 35 (1985) 1, pp. 35–49.

[FARKHATDINOV & RYU 2008]

Farkhatdinov, I.; Ryu, J.-H.: A Study on the Role of Force Feedback for Teleoperation of Industrial Overhead Crane. In: Proceedings of the 6th international conference on Haptics: Perception, Devices and Scenarios. Berlin, Heidelberg: Springer-Verlag 2008. EuroHaptics 2008, pp. 796–805.

[FERRELL 1964]

Ferrell, W. R.: Remote manipulation with transmission delay. Phd thesis, Massachusetts Institute of Technology. Department of Mechanical Engineering, 1964.

[FERRELL & SHERIDAN 1967]

Ferrell, W. R.; Sheridan, T. B.: Supervisory control of remote manipulation. IEEE Spectrum 4 (1967) 10, pp. 81–88.

[GOODRICH & SCHULTZ 2007]

Goodrich, M. A.; Schultz, A. C.: Human-Robot Interaction: A Survey. Foundations and Trends in Human-Computer Interaction 1 (2007) 3, pp. 203–275.

[GROEGER ET AL. 2008]

Groeger, M.; Arbter, K.; Hirzinger, G.: Motion Tracking for Minimally Invasive Robotic Surgery. Surger (2008), pp. 117–148.

[GROSS & DIRKS 2004]

Gross, M.; Dirks, V.: Mikro-Manufaktur. Mikroproduktion 2 (2004) 1, pp. 50–52.

## Bibliography

---

[GÖTZE 2006]

Götze, U.: Investitionsrechnung. Springer-Lehrbuch. Berlin/Heidelberg: Springer-Verlag 2006.

[HANNAFORD & OKAMURA 2008]

Hannaford, B.; Okamura, A. M.: Haptics, Berlin, Heidelberg: Springer Berlin Heidelberg 2008, Chapter 30. pp. 719–739.

[HANNAFORD & RYU 2001]

Hannaford, B.; Ryu, J.-H.: Time domain passivity control of haptic interfaces. In: IEEE International Conference on Robotics and Automation, ICRA 2001, 2001, vol. 2. pp. 1863–1869.

[HANNAFORD & WOODS 1989]

Hannaford, B.; Woods, L.: Performance evaluation of a 6-axis high fidelity generalized force reflecting teleoperator. In: the NASA Conference on Space Telerobotics, 1989.

[HARTENBERG & DENAVIT 1964]

Hartenberg, R.; Denavit, J.: Kinematic Synthesis of Linkages. New York: McGraw-Hill 1964.

[HASHTRUDI-ZAAD & SALCUDEAN 2002]

Hashtrudi-Zaad, K.; Salcudean, S.: Transparency in time-delayed systems and the effect of local force feedback for transparent teleoperation. IEEE Transactions on Robotics and Automation 18 (2002) 1, pp. 108–114.

[HASSENZAHL ET AL. 2003]

Hassenzahl, M.; Burmester, M.; Koller, F.: AttrakDiff : ein Fragebogen zur Messung wahrgenommener hedonischer und pragmatischer Qualität. Stuttgart: B. G. Teubner 2003. Mensch & Computer 2003 : Interaktion in Bewegung, pp. 187–196.

[HEINZMANN & ZELINSKY 1999]

Heinzmann, J.; Zelinsky, A.: Building Human-Friendly Robot Systems. In: International Symposium of Robotics Research, 1999. pp. 305–312.

[HELMS 2006]

Helms, E.: Roboterbasierte Bahnführungsunterstützung von Industriellen Handhabungs- und Bearbeitungsprozessen. Dissertation, Stuttgart University, 2006.

[HELMS ET AL. 2002]

Helms, E.; Schraft, R. D.; Hägele, M.: rob@work: Robot Assistant in Industrial Environments. In: In Proceedings of ROMAN-2002, 2002. pp. 399–404.

[HIRZINGER 1994]

Hirzinger, G.: ROTEX - The first space robot technology experiment. In: Yoshikawa, T.; Miyazaki, F. (Editors): Experimental Robotics III. Springer Berlin / Heidelberg 1994, Lecture Notes in Control and Information Sciences, vol. 200, pp. 579–598.

[HOKAYEM & SPONG 2006]

Hokayem, P. F.; Spong, M. W.: Bilateral Teleoperation: An Historical Survey. *Automatica* 42 (2006) 12, pp. 2035–2057.

[HOLLIS & SALCUDEAN 1993]

Hollis, R. L.; Salcudean, S. E.: Lorentz levitation technology: a new approach to fine motion robotics, teleoperation, haptic interfaces, and vibration isolation. In: 6th International Symposium on Robotics Research, Hidden Valley, Pennsylvania 1993.

[IFR 2009]

IFR: World robotics 2009. Technical Report, International Federation of Robotics (IFR) - Statistical Department, 2009, ISBN 978-3-8163-0577-4.

[INTUITIVE SURGICAL 2011]

Intuitive Surgical, I.: Intuitive Surgical, Inc., <http://www.intuitivesurgical.com>, 2011.

[IOSSIFIDIS ET AL. 2002]

Iossifidis, I.; Bruckhoff, C.; Theis, C.; Grote, C.; Faubel, C.; Schöner, G.: CORA: An anthropomorphic robot assistant for human environment. In: 11th IEEE International Workshop on Robot and Human Interactive Communication, 2002. pp. 392–398.

[ISO 10218-1 2006]

ISO 10218-1: Robots for industrial environments - Safety requirements - Part 1: Robot. Technical Report, ISO, Geneva, 2006.

[ISO 10218-2 2011]

ISO 10218-2: Robots and robotic devices - Safety requirements - Part 2: Industrial robot systems and integration. Technical Report, ISO, Geneva, 2011.

[ISO 11228 2003]

ISO 11228: Ergonomics - Manual handling - Part 1: Lifting and carrying. Technical Report, ISO, Geneva, 2003.

[ISO 11228 2007a]

ISO 11228: Ergonomics - Manual handling - Part 2: Pushing and pulling. Technical Report, ISO, Geneva, 2007a.

## Bibliography

---

[ISO 11228 2007b]

ISO 11228: Ergonomics - Manual handling - Part 3: Handling of low loads at high frequency. Technical Report, ISO, Geneva, 2007b.

[JACOBS ET AL. 2007]

Jacobs, S.; Holzhey, D.; Strauss, G.; Burgert, O.; Falk, V.: The impact of haptic learning in telemanipulator-assisted surgery. *Surgical laparoscopy, endoscopy & percutaneous techniques* 17 (2007) 5, pp. 402–406.

[JOHNSEN & CORLISS 1971]

Johnsen, E.; Corliss, W.: *Human Factors Applications in Teleoperator Design and Operation*. Wiley series in Human Factors, NY. 1971.

[KAZEROONI & GUO 1993]

Kazerooni, H.; Guo, J.: Human Extenders. *Journal of Dynamic Systems, Measurement, and Control* 115 (1993) 2B, pp. 281.

[KÜBLER ET AL. 2005]

Kübler, B.; Seibold, U.; Hirzinger, G.: Development of acutated and sensor integrated forceps for minimally invasive robotic surgery. *International Journal of Medical Robotics and Computer Assisted Surgery* 1 (2005) 3, pp. 96–107.

[KERN 2009]

Kern, T. A.: *Entwicklung Haptischer Geräte*. Berlin, Heidelberg: Springer Berlin Heidelberg 2009.

[KEYROUZ & DIEPOLD 2007]

Keyrouz, F.; Diepold, K.: Binaural Source Localization and Spatial Audio Reproduction for Telepresence Applications. *Presence: Teleoperators and Virtual Environments* 16 (2007) 5, pp. 509–522.

[KIM 1992]

Kim, W.: Developments of new force reflecting control schemes and an application to a teleoperation training simulator. *IEEE Comput. Soc. Press* 1992. pp. 1412–1419.

[KING & HAHN 1986]

King, R. I.; Hahn, R. S.: *Handbook of Modern Grinding Technology*. New York: Chapman and Hall 1986.

[KONTARINIS & HOWE 1996]

Kontarinis, D. A.; Howe, R. D.: Tactile Display of Vibratory Information in Teleoperation and Virtual Environments. *Presence: Teleoperators and Virtual Environments* 4 (1996) 4, pp. 387–402.

[KRÜGER ET AL. 2006]

Krüger, J.; Bernhardt, R.; Surdilovic, D.; Spur, G.: Intelligent Assist Systems for Flexible Assembly. *CIRP Annals - Manufacturing Technology* 55 (2006) 1, pp. 29–32.

[KRÜGER ET AL. 2009]

Krüger, J.; Lien, T. K.; Verl, A.: Cooperation of Human and Machines in Assembly Lines. *CIRP Annals - Manufacturing Technology* 58 (2009) 2, pp. 628 – 646.

[LANDZETTEL ET AL. 1999]

Landzettel, K.; Brunner, B.; Deutrich, K.; Hirzinger, G.; Schreiber, G.; Steinmetz, B.: DLR's Experiments on the ETS VII Space Robot Mission. In: 9th International Conference on Advanced Robotics (ICAR'99), Tokyo 1999.

[LAWRENCE 1993]

Lawrence, D.: Stability and transparency in bilateral teleoperation. *IEEE Transactions on Robotics and Automation* 9 (1993) 5, pp. 624–637.

[LAY ET AL. 2001]

Lay, K.; Prassler, E.; Dillmann, R.; Grundwald, G.; Hägele, M.; Lawitzky, G.; Stopp, A.; Seelen, W. v.: MORPHA: Communication and Interaction with Intelligent, Anthropomorphic Robot Assistants. In: International Status Conference Lead Projects Human-Computer Interaction, 2001.

[LIU ET AL. 2003]

Liu, A.; Tendick, F.; Cleary, K.; Kaufmann, C.: A Survey of Surgical Simulation: Applications, Technology, and Education. *Presence: Teleoperators and Virtual Environments* 12 (2003) 6, pp. 599–614.

[MACK 2001]

Mack, M. J.: Minimally Invasive and Robotic Surgery. *Jama The Journal Of The American Medical Association* 285 (2001) 5, pp. 568–572.

[MALLET ET AL. 2004]

Mallett, J.; Chang, D.; Rosenberg, L.; Braun, A.; Martin, K.; Beamer, J.: Enhanced Cursor Control Using Interface Devices. U.S. Patent 6816148 2004.

[MANOCHA ET AL. 2001]

Manocha, K.; Pernaletе, N.; Dubey, R.: Variable position mapping based assistance in teleoperation for nuclear cleanup. In: IEEE International Conference on Robotics and Automation, ICRA 2001, Seoul, Korea 2001, vol. 1. pp. 374–379.

[MASSIMINO & SHERIDAN 1989]

Massimino, M.; Sheridan, T.: Variable Force and Visual Feedback Effects on

## Bibliography

---

Teleoperator Man/Machine Performance. In: the NASA Conference on Space Telerobotics, 1989.

[MAYER ET AL. 2007]

Mayer, H.; Nagy, I.; Knoll, A.; Braun, E. U.; Bauernschmitt, R.; Lange, R.: Haptic Feedback in a Telepresence System for Endoscopic Heart Surgery. *Presence: Teleoperators and Virtual Environments* 16 (2007) 5, pp. 459–470.

[MCAREE & DANIEL 2000]

McAree, P. R.; Daniel, R. W.: Stabilizing Impacts in Force-Reflecting Teleoperation Using Distance-to-Impact Estimates. *The International Journal of Robotics Research* 19 (2000) 4, pp. 349–364.

[MÜNZ 2007]

Münz, R.: Aging and Demographic Change in European Societies: Main Trends and Alternative Policy Options. In: SP Discussion Paper No. 2310. Washington, DC: World Bank 2007.

[MUNIR & BOOK 2002]

Munir, S.; Book, W.: Internet-based teleoperation using wave variables with prediction. *IEEE/ASME Transactions on Mechatronics* 7 (2002) 2, pp. 124–133.

[NIEMEYER & SLOTINE 1997]

Niemeyer, G.; Slotine, J.-J.: Designing force reflecting teleoperators with large time delays to appear as virtual tools. In: *Robotics and Automation, 1997. Proceedings., 1997 IEEE International Conference on, 1997*, vol. 3. pp. 2212–2218.

[OAKLEY ET AL. 2000]

Oakley, I.; McGee, M. R.; Brewster, S.; Gray, P.: Putting the feel in 'Look and Feel'. In: *SIGCHI conference on Human factors in computing systems*. New York, NY, USA: ACM Press 2000. pp. 415–422.

[OBERER-TREITZ ET AL. 2011]

Oberer-Treitz, S.; Puzik, A.; Verl, A.: Sicherheitsbewertung der Mensch-Roboter-Kooperation. *wt Werkstattstechnik online* 101 (2011) 9, pp. 629–632.

[ORTMAIER 2003]

Ortmaier, T. J.: Motion Compensation in Minimally Invasive Robotic Surgery. Dissertation, Technische Universität München, 2003.

[OSAKI ET AL. 2008]

Osaki, A.; Kaneko, T.; Miwa, Y.: Embodied navigation for mobile robot by using direct 3D drawing in the air. In: *The 17th IEEE International Symposium on Robot and Human Interactive Communication, 2008. RO-MAN 2008, 2008*. pp. 671–676.

[OTTENSMEYER ET AL. 2000]

Ottensmeyer, M. P.; Hu, J.; Thompson, J. M.; Ren, J.; Sheridan, T. B.: Investigations into Performance of Minimally Invasive Telesurgery with Feedback Time Delays. Presence: Teleoperators and Virtual Environments 9 (2000), pp. 369–382.

[PARKER ET AL. 1993]

Parker, N. R.; Salcudean, S. E.; Lawrence, P. D.: Application of Force Feedback to Heavy Duty Hydraulic Machines. In: IEEE International Conference on Robotics and Automation. Atlanta: IEEE Comput. Soc. Press 1993. pp. 375–381.

[PAUL 1981]

Paul, R. P.: Robot Manipulators: Mathematics, Programming and Control. The MIT Press 1981.

[PENNESTRI ET AL. 2005]

Pennestri, E.; Cavacece, M.; Vita, L.: On the Computation of Degrees-of-Freedom: A Didactic Perspective. In: 5th International Conference on Multibody Systems, Nonlinear Dynamics, and Control, Parts A, B, and C. ASME 2005, vol. 6. pp. 1733–1741.

[PESHKIN & COLGATE 1999]

Peshkin, M.; Colgate, J. E.: Cobots. Industrial Robot 26 (1999) 5, pp. 335–341.

[PETZOLD 2007]

Petzold, B.: Entwicklung eines Operatorarbeitsplatzes für die telepräsen- te Inhaltsverzeichnis. Phd thesis, Technische Universität München, 2007.

[RADI & REINHART 2009]

Radi, M.; Reinhart, G.: Industrial Haptic Robot Guidance System for Assembly Processes. In: 2009 IEEE International Workshop on Haptic Audio visual Environments and Games. Lecco: IEEE 2009. pp. 69–74.

[RADI ET AL. 2010a]

Radi, M.; Reiter, A.; Zaidan, S.; Nitsch, V.; Färber, B.; Reinhart, G.: Telepresence in Industrial Applications: Implementation Issues for Assembly Tasks. Presence: Teleoperators and Virtual Environments 19 (2010a) 5, pp. 415–429.

[RADI ET AL. 2010b]

Radi, M.; Reiter, A.; Zäh, M. F.; Müller, T.; Knoll, A.: Telepresence Technology for Production: From Manual to Automated Assembly. In: Erp, J. V.; Noma, H. (Editors): EuroHaptic 2010, Amsterdam 2010b.

[RAJU ET AL. 1989]

Raju, G.; Verghese, G.; Sheridan, T.: Design issues in 2-port network models

## Bibliography

---

of bilateral remote manipulation. In: International Conference on Robotics and Automation. IEEE Comput. Soc. Press 1989. pp. 1316–1321.

[REINHART & RADI 2009]

Reinhart, G.; Radi, M.: Some Issues on Integrating Telepresence Technology into Industrial Robotic Assembly. In: WORLD ACADEMY OF SCIENCE, ENGINEERING AND TECHNOLOGY, Dubai, United Arab Emirates 2009, vol. 49. pp. 843–848.

[REINHART & SPILLNER 2010]

Reinhart, G.; Spillner, R.: Assistenzroboter in der Produktion. In: für Mechatronische Systeme, Z. I. (Editor): Internationales Forum Mechatronik 2010. Winterthur: Peter Gehring AG 2010.

[REINHART & ZAIDAN 2009]

Reinhart, G.; Zaidan, S.: A Generic Framework for Workpiece-based Programming of Cooperating Industrial Robots. In: Mechatronics and Automation 2009, Changchun, China 2009. pp. 37–42.

[REINHART ET AL. 2008]

Reinhart, G.; Zaidan, S.; Radi, M.; Wittmann, W.: On The Feasibility of a PBD Approach for a Force Controlled Robot Production Cell. In: 2nd CIRP Conference on Assembly Technologies Systems, Toronto, Canada 2008, vol. 49.

[REINHART ET AL. 2010a]

Reinhart, G.; Radi, M.; Zaidan, S.: Workspace Scaling Techniques for Haptic Robot Guidance Systems. In: Lien, T. K. (Editor): 3rd CIRP Conference on Assembly Technologies and Systems (CATS2010), Trondheim 2010a. pp. 127–132.

[REINHART ET AL. 2010b]

Reinhart, G.; Zaidan, S.; Hubele, J.: Is Force Monitoring in Cooperating Industrial Robots Necessary? In: ISR/ROBOTIK 2010 - ISR 2010 (41st International Symposium on Robotics) and ROBOTIK 2010 (6th German Conference on Robotics), Munich, Germany 2010b.

[REINTSEMA ET AL. 2007]

Reintsema, D.; Landzettel, K.; Hirzinger, G.: DLR's Advanced Telerobotic Concepts and Experiments for On-Orbit Servicing. In: Ferre, M.; Buss, M.; Aracil, R.; Melchiorri, C.; Balaguer, C. (Editors): Advances in Telerobotics. Springer Berlin / Heidelberg 2007, Springer Tracts in Advanced Robotics, vol. 31, pp. 323–345.

[RICE ET AL. 1986]

Rice, J. R.; Yorchak, J. P.; Hartley, C. S.: Capture of satellites having rotational motion. In: Proc. Human Factors Society 30th Annual Meeting, 1986.

[ROB@WORK 2010]

rob@work: rob@work, <http://www.care-o-bot.de/RobAtWork.php>, 2010.

[ROSENBERG 1993]

Rosenberg, L. B.: Virtual fixtures: Perceptual tools for telerobotic manipulation. In: Proceedings of IEEE Virtual Reality Annual International Symposium. IEEE 1993. pp. 76–82.

[RYU & PREUSCHE 2007]

Ryu, J.-H.; Preusche, C.: Stable Bilateral Control of Teleoperators Under Time-varying Communication Delay: Time Domain Passivity Approach. In: IEEE International Conference on Robotics and Automation, ICRA 2007, 2007. pp. 3508–3513.

[RYU ET AL. 2010]

Ryu, J.-H.; Artigas, J.; Preusche, C.: A passive bilateral control scheme for a teleoperator with time-varying communication delay. *Mechatronics* 20 (2010) 7, pp. 812–823, special Issue on Design and Control Methodologies in Telerobotics.

[SALLNÄS 2001]

Sallnäs, E.-L.: Improved precision in mediated collaborative manipulation of objects by haptic force feedback. In: Brewster, S.; Murray-Smith, R. (Editors): *Haptic Human-Computer Interaction*. Springer Berlin / Heidelberg 2001, Lecture Notes in Computer Science, pp. 69–75.

[SATAVA 1995]

Satava, R. M.: Virtual reality and telepresence for military medicine. *Computers in Biology and Medicine* 25 (1995) 2, pp. 229–236.

[SATO ET AL. 1992]

Sato, K.; Kimura, M.; Abe, A.: Intelligent manipulator system with nonsymmetric and redundant master-slave. *Journal of Robotic Systems* 9 (1992) 2, pp. 281–290.

[SAYERS 1999]

Sayers, C.: *Remote Control Robotics*. Secaucus, NJ, USA: Springer-Verlag New York, Inc. 1999.

[SCHRAFT ET AL. 2005]

Schraft, R. D.; Meyer, C.; Parlitzer, C.; Helms, E.: PowerMate - A Safe and Intuitive Robot Assistant for Handling and Assembly Tasks. In: IEEE International Conference on Robotics and Automation ICRA. Barcelona, Spain: IEEE 2005, vol. 4. pp. 4074–4079.

## Bibliography

---

[SCHULENBURG ET AL. 2007]

Schulenburg, E.; Elkmann, N.; Fritzsche, M.; Teutsch, C.: A Mobile Service Robot for Life Science Laboratories. In: Brauer, W.; Berns, K.; Luksch, T. (Editors): *Autonome Mobile Systeme 2007*. Springer Berlin Heidelberg 2007, Informatik aktuell, pp. 315–318.

[SECCHI ET AL. 2003]

Secchi, C.; Stramigioli, S.; Fantuzzi, C.: Digital passive geometric telemanipulation. In: *IEEE International Conference on Robotics and Automation, ICRA 2003*, 2003, vol. 3. pp. 3290–3295.

[SHERIDAN 1993]

Sheridan, T.: Space teleoperation through time delay: review and prognosis. *IEEE Transactions on Robotics and Automation* 9 (1993) 5, pp. 592–606.

[SHERIDAN 1989]

Sheridan, T. B.: Telerobotics. *Automatica* 25 (1989), pp. 487–507.

[SHERIDAN 1992]

Sheridan, T. B.: *Telerobotics, Automation, and Human Supervisory Control*. MIT Press, Cambridge 1992.

[SHULL & NIEMEYER 2007]

Shull, P.; Niemeyer, G.: Experiments in Local Force Feedback for High-Inertia, High-Friction Telerobotic Systems. In: *ASME 2007 International Mechanical Engineering Congress and Exposition (IMECE2007)*. Seattle, Washington, USA: ASME 2007. pp. 1241–1246.

[SHULL & NIEMEYER 2008]

Shull, P.; Niemeyer, G.: Force and Position Scaling Limits for Stability in Force Reflecting Teleoperation. In: *ASME Dynamic Systems and Control Conference (DSCC2008)*, Parts A and B. Ann Arbor, Michigan, USA: ASME 2008. pp. 607–614.

[SMEROBOT 2010]

SMErobot: SMErobot<sup>TM</sup> - The European Robot Initiative for Strengthening the Competitiveness of SMEs in Manufacturing, <http://www.smerobot.org/>, 2010.

[SNYDER & KAZEROONI 1996]

Snyder, T.; Kazerooni, H.: A novel material handling system. In: *Proceedings of IEEE International Conference on Robotics and Automation*. IEEE 1996. pp. 1147–1152.

[STEUER 1992]

Steuer, J.: Defining Virtual Reality: Dimensions Determining Telepresence. *Journal of Communication* 42 (1992) 4, pp. 73–93.

[STOLL 2009]

Stoll, E.: Ground Verification of Telepresence for On-Orbit Servicing. Dissertation, Technische Universität München, 2009.

[STOPP ET AL. 2003]

Stopp, A.; Horstmann, S.; Kristensen, S.; Lohnert, F.: Toward interactive learning for manufacturing assistants. *IEEE Transactions on Industrial Electronics* 50 (2003) 4, pp. 705 – 707.

[SUZUKI ET AL. 2005]

Suzuki, S.; Suzuki, N.; Hayashibe, M.; Hattori, A.; Konishi, K.; Kakeji, Y.; Hashizume, M.: Tele-surgery simulation to perform surgical training of abdominal da Vinci surgery. *International Congress Series 1281* (2005), pp. 531 – 536, cARS 2005: Computer Assisted Radiology and Surgery.

[TENDICK & CAVUSOGLU 1997]

Tendick, F.; Cavusoglu, M.: Human-machine interfaces for minimally invasive surgery. In: *Engineering in Medicine and Biology Society, 1997. Proceedings of the 19th Annual International Conference of the IEEE, 1997.*

[THIEMERMANN 2003]

Thiemermann, S.: team@work - Mensch-Roboter-Kooperation in der Montage. In: Schraft, R. D. (Editor): *Workshop für OTS-Systeme in der Robotik. Stuttgart: FpF - Verein zur Förderung der produktionstechnischen Forschung 2003.* pp. 149–159.

[TRAHANIAS ET AL. 2005]

Trahanias, P.; Burgard, W.; Argyros, A.; Hahnel, D.; Baltzakis, H.; Pfaff, P.; Stachniss, C.: TOURBOT and WebFAIR: Web-operated mobile robots for telepresence in populated exhibitions. *IEEE Robotics Automation Magazine* 12 (2005) 2, pp. 77–89.

[VOGL 2008]

Vogl, W.: Eine interaktive räumliche Benutzerschnittstelle für die Programmierung von Industrierobotern. Dissertation, Technische Universität München, 2008.

[VUKOBRATOVIC ET AL. 2009]

Vukobratovic, M.; Surdilovic, D.; Ekalo, Y.; Katic, D.: *Dynamics and Robust Control of Robot-environment Interaction.* River Edge, NJ, USA: World Scientific Publishing Co., Inc. 2009.

[WAGNER ET AL. 2007]

Wagner, C. R.; Stylopoulos, N.; Jackson, P. G.; Howe, R. D.: *The Benefit of Force*

## Bibliography

---

Feedback in Surgery: Examination of Blunt Dissection. Presence: Teleoperators and Virtual Environments 16 (2007) 3, pp. 252–262.

[WALL ET AL. 2002]

Wall, S.; Paynter, K.; Shillito, M.; Wright, M.; Scali, S.: The Effect of Haptic Feedback and Stereo Graphics in a 3D Target Acquisition Task. In: Proceedings of Eurohaptics 2002, 2002.

[YANCO & DRURY 2004]

Yanco, H. A.; Drury, J.: Classifying Human-Robot Interaction: An Updated Taxonomy. IEEE International Conference on Systems, Man and Cybernetics 3 (2004), pp. 2841–2846.

[YOKOKOHI & YOSHIKAWA 1994]

Yokokohji, Y.; Yoshikawa, T.: Bilateral Control of Master-Slave Manipulators for Ideal Kinesthetic Coupling - Formulation and Experiment. IEEE Transactions on Robotics and Automation 10 (1994) 5, pp. 605 – 620.

[YOKOKOHI ET AL. 1999]

Yokokohji, Y.; Imaida, T.; Yoshikawa, T.: Bilateral teleoperation under time-varying communication delay. In: IEEE/RSJ International Conference on Intelligent Robots and Systems, IROS 1999, 1999, vol. 3. pp. 1854–1859.

[YU 2000]

Yu, B.: Modeling, control design and mechatronic implementation of constrained robots for surface finishing applications. PhD Dissertation, Stillwater, OK, USA, 2000.

[ZÄH ET AL. 2006]

Zäh, M. F.; Reiter, A.; Clarke, S.: Design, Construction and Analysis of a Telepresent Microassembly System. In: International Workshop on Human-Centered Robotic Systems (HCRS'06), Munich, Germany 2006.

[ZHAI 1995]

Zhai, S.: Human Performance in Six Degrees of Freedom Input Control. Dissertation, University of Toronto, Canada, 1995.

[ZHAI & MILGRAM 1998]

Zhai, S.; Milgram, P.: Quantifying coordination in multiple DOF movement and its application to evaluating 6 DOF input devices. In: Proceedings of the SIGCHI conference on Human factors in computing systems. New York, NY, USA: ACM Press/Addison-Wesley Publishing Co. 1998. CHI '98, pp. 320–327.